Gluon-Induced Off-Shell Z-Boson Pair Production at the LHC

Diplomarbeit
von
Philipp Mertsch

vorgelegt bei
Professor Dr. R. Rückl

am Institut für Theoretische Physik und Astrophysik
der Bayerischen Julius-Maximilians-Universität
Würzburg

28. November 2006

Zusammenfassung

In dieser Arbeit berechne ich die schleifen-induzierte Produktion von vier geladenen Leptonen in Gluon-Fusion via zwei off-shell Z Bosonen, $gg \to Z^*Z^* \to (l\bar{l})(l'\bar{l}')$. Zusätzlich zur Quark-Antiquark-Annihilation, $q\bar{q} \to Z^*Z^*$, stellt dieser Prozess einen wichtigen Beitrag zur Z-Bosonen-Kontinuumsproduktion im Untergund des „Goldenen Higgs-Kanals", $gg \to H \to Z^*Z^*$, dar. Die Quark-Antiquark-Annihilation berechne ich in führender Ordnung. Für die Einschleifen-Helizitäts-Amplitude des Gluon-Fusions-Untergrunds wende ich eine analytische Zerlegung in Tensorstrukturen und Skalarintegrale an. Diese Darstellung verhindert größtenteils das Auftreten inverser Gram-Determinanten, die die numerische Stabilität der Lösung gefährden. Ich erkläre die Berechnung und Vereinfachung der Koeffizientenfunktionen und führe eine geeignete Phasenraum-Parametrisierung durch. Das Ergebnis stellt das Programm `GG2ZZ` dar, mit dem ich schließlich den totalen Wirkungsquerschnitt sowie verschiedene Verteilungen berechne.

Contents

1. Introduction

The Standard Model of particle physics has been extremely successful since its foundation in the early 70s extremely successful. Not only the heavy quarks, but also the gauge bosons of electroweak interactions, W and Z, have been postulated theoretically before being detected experimentally at LEP. The only missing stone which has not yet been discovered is the Higgs boson, which could explain spontaneous breaking of electroweak symmetry. Finding the Higgs boson is therefore one of the major challenges both from the experimental and theoretical side. Although one hopes to find signatures of physics beyond the Standard Model at the LHC, the major task of its experiments ATLAS and CMS is the detection of the Higgs particle.

After a short review of the Standard Model of electroweak interactions and the Higgs mechanism, I will discuss the search for the Higgs particle as postulated in the Standard Model at the Large Hadron Collider.

1.1. The Higgs mechanism

1.1.1. The Standard Model of electroweak interactions

This short review of the Standard Model of electroweak interactions [1, 2, 3] is not meant as a complete presentation of Standard Model physics but only as a motivation for the symmetry breaking via Higgs mechanism[1]. I will therefore restrict the fermions to a single family of leptons, i.e. an electron and the corresponding electron neutrino. As there is no evidence for a right-handed neutrino so far, the lepton field can be described by a left-handed doublet

$$\mathbf{L} = \begin{pmatrix} \nu_L \\ e_L \end{pmatrix} \text{ with } \nu_L = \frac{1}{2}(1-\gamma_5)\psi_\nu \text{ and } e_L = \frac{1}{2}(1-\gamma_5)\psi_e \tag{1.1}$$

and a right-handed singlet

$$e_R = \frac{1}{2}(1+\gamma_5)\psi_e. \tag{1.2}$$

Both transform as follows:

[1] QCD is therefore omitted.

$$\text{under } SU(2): \quad \mathbf{L}' = e^{-i\alpha(x)\tau/2}\mathbf{L}, \tag{1.3}$$

$$e'_R = e_R, \tag{1.4}$$

$$\text{under } U(1): \quad \mathbf{L}' = e^{-iY_L\beta(x)/2}\mathbf{L}, \tag{1.5}$$

$$e'_R = e^{-iY_R\beta(x)/2}e_R, \tag{1.6}$$

where Y_L and Y_R are the hypercharges of the left-handed doublet and the right-handed singlet, respectively.

For setting up a Lagrangian invariant under this transformation one must replace the ordinary derivative ∂_μ with the covariant derivative D_μ:

$$\partial_\mu \to D_\mu = \begin{cases} \partial_\mu + \frac{1}{2}ig'Y_L B_\mu(x) + \frac{1}{2}g\tau\mathbf{W}_\mu(x) & \text{for } \mathbf{L} \\ \partial_\mu + \frac{1}{2}ig'Y_R B_\mu(x) & \text{for } e_R \end{cases} . \tag{1.7}$$

$B_\mu(x)$ and $\mathbf{W}_\mu(x)$ are the gauge fields of the $U(1)$ and $SU(2)$ transformations, respectively. These fields themselves transform according to

$$B'_\mu(x) = B_\mu(x) + \frac{1}{g'}\partial_\mu\beta(x), \tag{1.8}$$

$$\mathbf{W}'_\mu(x) = \mathbf{W}_\mu(x) + \frac{1}{g}\partial_\mu\alpha(x) - \mathbf{W}_\mu(x) \times \alpha(x). \tag{1.9}$$

The set of transformations for the fermion fields, eqs. 1.3 - 1.6, and for the bosons, eqs. 1.8 - 1.9, is called the gauge transformation. As I will show in the next section, neither can the field $B_\mu(x)$ be identified with the photon field nor can the fields $\mathbf{W}_\mu(x)$ be identified only with the weak interactions.

Finally, the Lagrange density $\mathcal{L}$ of the electroweak theory is:

$$\begin{aligned} \mathcal{L} = & i\bar{\mathbf{L}}\gamma^\mu\left(\partial_\mu + \frac{1}{2}ig'Y_L B_\mu(x) + \frac{1}{2}g\tau\mathbf{W}_\mu(x)\right)\mathbf{L} \\ & + i\bar{e}_R\gamma^\mu\left(\partial_\mu + \frac{1}{2}ig'Y_R B_\mu(x)\right)e_R \\ & - \frac{1}{4}B_{\mu\nu}B^{\mu\nu} - \frac{1}{4}\mathbf{W}_{\mu\nu}\mathbf{W}^{\mu\nu}, \end{aligned} \tag{1.10}$$

where the field strength tensors are $B_{\mu\nu} = \partial_\mu B_\nu - \partial_\nu B_\mu$ and $\mathbf{W}_{\mu\nu} = \partial_\mu \mathbf{W}_\nu - \partial_\nu \mathbf{W}_\mu$.

The equations of motion for the fermion fields can then be derived via the Euler-Lagrange equations and one finds

$$i\gamma^\mu\left(\partial_\mu + \frac{1}{2}ig'Y_L B_\mu(x) + \frac{1}{2}g\tau\mathbf{W}_\mu(x)\right)\mathbf{L}(x) = i\gamma^\mu D_\mu\mathbf{L}(x) = 0, \tag{1.11}$$

$$i\gamma^\mu\left(\partial_\mu + \frac{1}{2}ig'Y_R B_\mu(x)\right)e_R(x) = i\gamma^\mu D_\mu e_R(x) = 0. \tag{1.12}$$

Note that there are no mass terms in the Lagrange density and the equations of motion. If there were, neither the Lagrange density nor the equations of motion would be invariant under the gauge transformation since the mass term would produce an additional term under transformation. Furthermore, a mass term would destroy the helicity as a good quantum number while the dynamical term D_μ preserves it. This again reflects the fact that only massless particles posses a definite helicity. A $SU(2)_L$ gauge theory is thus only possible with massless fermions.

Similarly, the boson fields must also be massless. A massterm in its equation of motion would not be invariant under gauge transformations and would therefore violate the gauge invariance.

Both assumptions are obviously not true in nature: Both the electrons and the gauge bosons of electroweak interactions, W and Z that will be defined in the next section, posses a mass. Therefore, the $SU(2)_L \times U(1)$ gauge symmetry must be broken to generate masses for the fermions and gauge bosons.

1.1.2. Spontaneous symmetry breaking

The Higgs field

One can conserve the gauge invariance of the Lagrange density (eq. 1.10) and thereby preserve the weak interactions mediated by the fields $B_\mu(x)$ and $\mathbf{W}_\mu(x)$, but break the invariance of the vacuum. Conserving the symmetry of the Lagrangian but breaking the symmetry of the vacuum is called spontaneous symmetry breaking.

In order to obtain a vacuum with such a property, one must introduce additional fields whose minimum does not correspond to a vanishing expectation value (as usual for other fields) but to a finite expectation value. Fields which posses this property are called Higgs fields [4, 5]. A possible implementation which breaks the $SU(2)_L \times U(1)$ symmetry and modifies the equations of motion such that the $B_\mu(x)$ and $\mathbf{W}_\mu(x)$ fields acquire mass is a doublet of complex scalar fields

$$\mathbf{\Phi}(x) = \begin{pmatrix} \Phi^+(x) \\ \Phi^0(x) \end{pmatrix} = \frac{1}{\sqrt{2}} \begin{pmatrix} \Phi_1^+(x) + i\Phi_2^+(x) \\ \Phi_1^0(x) + i\Phi_2^0(x) \end{pmatrix} \tag{1.13}$$

with $\Phi_1^+(x)$ and $\Phi_2^+(x)$ with positive electric charge and $\Phi_1^0(x)$ and $\Phi_2^0(x)$ neutral. Note that this is not the only possible but the minimal configuration that leads to a symmetry breaking.

The Lagrange density corresponding to this field is

$$\mathcal{L} = \frac{1}{2}(D_\mu \mathbf{\Phi}(x))^\dagger (D^\mu \mathbf{\Phi}(x)) - V\left(\mathbf{\Phi}(x)^\dagger \mathbf{\Phi}(x)\right) \tag{1.14}$$

$$\text{with } V(\mathbf{\Phi}(x)^\dagger \mathbf{\Phi}(x)) = -\mu^2 \mathbf{\Phi}(x)^\dagger \mathbf{\Phi}(x) + \lambda \left(\mathbf{\Phi}(x)^\dagger \mathbf{\Phi}(x)\right)^2, \quad \mu^2, \lambda > 0. \tag{1.15}$$

Note that the first expansion coefficient of $V(\mathbf{\Phi}(x)^\dagger \mathbf{\Phi}(x))$, $-\mu^2$, is negative and cannot simply be interpreted as the mass of the Higgs field. The minimum of $V(\mathbf{\Phi}(x)^\dagger \mathbf{\Phi}(x))$ is

not at $\langle \mathbf{\Phi} \rangle = 0$ but at a finite value $\mathbf{\Phi}_{min}$. The physical Higgs particle then corresponds to excitations around this minimum and its equations of motions can be gained by expanding around it.

For calculating the minimum of $V(\mathbf{\Phi}(x)^\dagger \mathbf{\Phi}(x))$, the field $\mathbf{\Phi}$ is treated like a doublet of classical fields. Minimizing its energy leads to

$$\Phi_{min} = \frac{1}{\sqrt{2}} \begin{pmatrix} 0 \\ v \end{pmatrix} \quad \text{with} \quad v = \sqrt{\frac{\mu^2}{\lambda}} \tag{1.16}$$

and for the quantum field $\mathbf{\Phi}$ this corresponds to a vacuum expectation value of

$$\langle \mathbf{\Phi} \rangle = \Phi_{min} = \frac{1}{\sqrt{2}} \begin{pmatrix} 0 \\ v \end{pmatrix}. \tag{1.17}$$

Excitations of the Higgs field around this minimum can now be parametrized by two fields, $\xi(x)$ and $H(x)$ with four degrees of freedom

$$\mathbf{\Phi} = e^{i\xi(x)\tau} \frac{1}{\sqrt{2}} \begin{pmatrix} 0 \\ v + H(x) \end{pmatrix}, \tag{1.18}$$

where the field $\xi(x)$ can be removed by a gauge transformation

$$\mathbf{\Phi}' = e^{-i\xi(x)\tau} \mathbf{\Phi} = e^{-i\xi(x)\tau} e^{i\xi(x)\tau} \frac{1}{\sqrt{2}} \begin{pmatrix} 0 \\ v + H(x) \end{pmatrix} = \frac{1}{\sqrt{2}} \begin{pmatrix} 0 \\ v + H(x) \end{pmatrix}. \tag{1.19}$$

The field $\xi(x)$ is thus not physical and only $H(x)$ corresponds to a physical particle, the famous Higgs particle. The three degrees of freedom that seem to be lost, will again show up in the W bosons when they acquire mass. Massless W bosons posses only two degrees of freedom (two transverse polarizations, like photons) whereas massive W bosons posses a third degree of freedom (longitudinal polarization).

Expanding the potential $V(\mathbf{\Phi}(x)^\dagger \mathbf{\Phi}(x))$ around the minimum,

$$V(H) \approx -\frac{1}{4}\mu^2 v^2 + \mu^2 H^2 + \lambda v H^3 + \frac{1}{4}\lambda H^4, \tag{1.20}$$

one reads of a Higgs mass of

$$m_H = \sqrt{2\mu^2}. \tag{1.21}$$

Boson masses

I will now show how the introduction of the Higgs field generates effective masses for the gauge bosons. The interaction between the Higgs field and the vector boson fields originates from the kinetic term of the Higgs field in the Lagrangian:

$$\begin{aligned}
(D_\mu \mathbf{\Phi}(x))^\dagger (D^\mu \mathbf{\Phi}(x)) &= \left\{ \left(\partial_\mu + \frac{ig}{2} \tau \mathbf{W}_\mu \right) \mathbf{\Phi}(x) \right\}^\dagger \left(\partial^\mu + \frac{ig}{2} \tau \mathbf{W}^\mu \right) \mathbf{\Phi}(x) \\
&= \frac{g^2}{4} \mathbf{\Phi}^\dagger \left(\tau \mathbf{W}_\mu \right)^\dagger \left(\tau \mathbf{W}^\mu \right) \mathbf{\Phi} + \dots \\
&= \frac{g^2}{4} \sum_{ij} W_\mu^i W^{j\mu} \Phi^\dagger \underbrace{\tau_i \tau_j}_{= \begin{cases} -\tau_j \tau_i & \text{for} \quad i \neq j \\ 1 & \text{for} \quad i = j \end{cases}} \Phi + \dots \\
&= \frac{g^2}{4} \sum_i W_\mu^i W^{i\mu} \Phi^\dagger \Phi + \dots \\
&= \frac{g^2}{8} \mathbf{W}_\mu \mathbf{W}^\mu (0, v+H) \begin{pmatrix} 0 \\ v+H \end{pmatrix} + \dots \\
&= \frac{g^2 v^2}{8} \mathbf{W}_\mu \mathbf{W}^\mu + \frac{g^2 v}{8} 2H \mathbf{W}_\mu \mathbf{W}^\mu + \dots
\end{aligned} \tag{1.22}$$

The field B_μ in the covariant derivative is suppressed here since it has no effect on how the physical W bosons acquire mass. Varying the second last term with respect to W_μ^i generates the equation of motion for the W bosons

$$\left(\Box + \frac{g^2 v^2}{4} \right) W_\mu^i = J_\mu^w, \tag{1.23}$$

where J_μ^w contains all currents except for that generated by the constant vacuum expectation value of the Higgs field. One can read off the mass of the W boson

$$M_W = \frac{gv}{2}. \tag{1.24}$$

Comparison between decay processes in the electroweak theory and in Fermi theory leads to a relation between g, M_W and G_F, the Fermi coupling between two currents:

$$\frac{G_F}{\sqrt{2}} = \frac{g^2}{8 M_W^2}. \tag{1.25}$$

Two of the W fields, W_μ^1 and W_μ^2, can be allocated to physical particles, the W^+ and W^- bosons

$$W_\mu^\pm = \frac{1}{\sqrt{2}} \left(W_\mu^1 \pm i W_\mu^2 \right). \tag{1.26}$$

It remains to explain how the fields W_μ^3 and B_μ correspond to physical particles. The interaction between these neutral gauge fields and the Higgs doublet is given by

$$\mathcal{L} = \frac{1}{4} \left(\left[g W_\mu^3 \tau_3 + g' B_\mu \right] \Phi \right)^\dagger \left[g W^{3\mu} \tau_3 + g' B^\mu \right] \Phi. \tag{1.27}$$

If one considers the vacuum expectation value $\langle \Phi \rangle$ instead of the full field Φ, one finds:

$$\begin{aligned} \mathcal{L} &= \frac{1}{4} \frac{v^2}{2} \left(-g W_\mu^{3\dagger} + g' B_\mu^\dagger \right) \left(-g W^{3\mu} + g' B^\mu \right) \\ &= \frac{1}{4} \frac{v^2}{2} \left[g^2 W_\mu^{3\dagger} W^{3\mu} + g'^2 B_\mu^\dagger B^\mu - g g' \left(W_\mu^{3\dagger} B^\mu + B_\mu^\dagger W^{3\mu} \right) \right] \\ &= \frac{1}{2} \frac{v^2}{2} \left(W_\mu^{3\dagger}, B_\mu^\dagger \right) \begin{pmatrix} g^2 & -g g' \\ -g g' & g'^2 \end{pmatrix} \begin{pmatrix} W^{3\mu} \\ B^\mu \end{pmatrix}. \end{aligned} \tag{1.28}$$

Since the mass matrix

$$\mathbf{M} = \frac{v^2}{4} \begin{pmatrix} g^2 & -g g' \\ -g g' & g'^2 \end{pmatrix} \tag{1.29}$$

is not diagonal, the fields W_μ^3 and B_μ cannot be interpreted as physical fields. But with a unitary transformation U the mass matrix can be diagonalized:

$$\mathbf{M}_D = U M U^{-1} = \frac{v^2}{4} \begin{pmatrix} 0 & 0 \\ 0 & \frac{v^2}{4}(g^2 + g'^2) \end{pmatrix}. \tag{1.30}$$

The fact that one eigenvalue is exactly zero allows for the interpretation of one of the transformed fields as the photon field. The other particle is then the neutral Z boson.

The unitary transformation is

$$U = \frac{1}{\sqrt{g'^2 + g^2}} \begin{pmatrix} g' & g \\ -g & g' \end{pmatrix} \tag{1.31}$$

and hence the photon field is

$$\begin{aligned} A_\mu &= \frac{g}{\sqrt{g'^2 + g^2}} B_\mu + \frac{g'}{\sqrt{g'^2 + g^2}} W_\mu^3 \\ &= \cos\theta_W B_\mu + \sin\theta_W W_\mu^3 \end{aligned} \tag{1.32}$$

with the abbreviations

$$\cos\theta_W := \frac{g}{\sqrt{g'^2+g^2}}; \quad \sin\theta_W := \frac{g'}{\sqrt{g'^2+g^2}}, \tag{1.33}$$

where θ_w is called the Weinberg angle or weak mixing angle.

The remaining field is identified with the Z boson

$$Z_\mu = -\sin\theta_W B_\mu + \cos\theta_W W_\mu^3. \tag{1.34}$$

To see whether these assignments really correspond to physical reality, one must check whether A_μ couples to the fields e_R and e_L with the coupling $-e$ and whether it does not couple to ν_L. These couplings can be found in the kinetic terms of the leptons:

$$\begin{aligned}\mathcal{L} &= -\bar{\mathbf{L}}\gamma^\mu\left(\frac{1}{2}g'Y_L B_\mu + \frac{1}{2}gW_\mu^3\tau_3\right)\mathbf{L} - \frac{1}{2}g'\bar{e}_R\gamma^\mu Y_R B_\mu e_R \qquad (1.35)\\ &= -\frac{1}{2}\bar{\nu}_L\gamma^\mu\left(g'Y_L B_\mu + gW_\mu^3\right)\nu_L - \frac{1}{2}\bar{e}_L\gamma^\mu\left(g'Y_L B_\mu - gW_\mu^3\right)e_L - \frac{1}{2}g'\bar{e}_R\gamma^\mu Y_R B_\mu e_R.\end{aligned}$$

Substituting the inverse transformation to eqs. 1.32 and 1.34,

$$B_\mu = A_\mu\cos\theta_W - Z_\mu\sin\theta_W \tag{1.36}$$

$$W_\mu^3 = A_\mu\sin\theta_W + Z_\mu\cos\theta_W, \tag{1.37}$$

the Lagrange density is given by

$$\begin{aligned}\mathcal{L}_k = &-\frac{1}{2}\bar{\nu}_L\gamma^\mu\left(g'Y_L\cos\theta_W + g\sin\theta_W\right)A_\mu\nu_L + \frac{1}{2}\bar{\nu}_L\gamma^\mu\left(g'Y_L\sin\theta_W - g\cos\theta_W\right)Z_\mu\nu_L\\ &-\frac{1}{2}\bar{e}_L\gamma^\mu\left(g'Y_L\cos\theta_W - g\sin\theta_W\right)A_\mu e_L + \frac{1}{2}\bar{e}_L\gamma^\mu\left(g'Y_L\sin\theta_W + g\cos\theta_W\right)Z_\mu e_L\\ &-\frac{1}{2}g'\bar{e}_R\gamma^\mu g'Y_R\cos\theta_W A_\mu e_R + \frac{1}{2}g'\bar{e}_R\gamma^\mu g'Y_R\sin\theta_W Z_\mu e_R\\ = &\frac{1}{\sqrt{g^2+g'^2}}\left[-gg'(Y_L+1)\bar{\nu}_L\gamma^\mu A_\mu\nu_L + (g'^2Y_L - g^2)\bar{\nu}_L\gamma^\mu Z_\mu\nu_L\right.\\ &-gg'(Y_L-1)\bar{e}_L\gamma^\mu A_\mu e_L + (g'^2Y_L + g^2)\bar{e}_L\gamma^\mu Z_\mu e_L\\ &\left.-gg'Y_R\bar{e}_R\gamma^\mu A_\mu e_R + g'^2Y_R\bar{e}_R\gamma^\mu Z_\mu e_R\right].\end{aligned} \tag{1.38}$$

Requiring that

1. A_μ does not couple to ν_L.
2. A_μ couples with the same strength to e_L and e_R.

implies

$$Y_L = -1 \quad \text{and} \quad Y_R = Y_L - 1 = -2 \tag{1.39}$$

Demanding furthermore that the coupling between A_μ and $e_{L,R}$ is e, one finds

$$e = \frac{gg'}{\sqrt{g^2 + g'^2}} = g \sin\theta_w. \tag{1.40}$$

The mass of the Z boson can be read off the mass matrix

$$M_Z = \frac{v}{2}\sqrt{g^2 + g'^2} = \frac{M_W}{\cos\theta_W}. \tag{1.41}$$

Since one knows e and G_F, one can determine the W and Z mass (cf. eq. 1.25):

$$\frac{G_F}{\sqrt{2}} = \frac{g^2}{8M_W^2} \Leftrightarrow M_W = \frac{g}{2}\sqrt{\frac{\sqrt{2}}{2G_F}} = \frac{e}{2\sin\theta_W}\sqrt{\frac{\sqrt{2}}{2G_F}} \approx 80\,\text{GeV} \tag{1.42}$$

$$\Rightarrow M_Z = \frac{M_W}{\cos\theta_W} \approx 90\,\text{GeV}. \tag{1.43}$$

Both the W and the Z boson were found in the UA1 and UA2 experiments at CERN's $Sp\bar{p}S$ collider in 1983 with masses of 80.4 and 91.2 GeV, respectively.

Fermion masses

The fermion masses are also generated by interactions with the Higgs field, but the couplings, so called Yukawa couplings, are free parameters of the theory and have to be introduced ad hoc whereas the W, Z and photon couplings and masses followed from the covariant derivative in the Lagrangian.

To generate the fermion masses one postulates an interaction of the form

$$\mathcal{L}_{\phi-F} = -g_e \left[\bar{L}\Phi e_R + \bar{e}_R\Phi^\dagger L\right]. \tag{1.44}$$

With the constant vacuum expectation value $\langle\Phi\rangle$ one finds the electron mass term

$$\frac{-g_e}{\sqrt{2}}\left[(\bar{\nu}_L, \bar{e}_L)\begin{pmatrix} 0 \\ v \end{pmatrix} e_R + \bar{e}_R(0, v)\begin{pmatrix} \nu_L \\ e_L \end{pmatrix}\right] = -\frac{g_e v}{\sqrt{2}}(\bar{e}_L e_R + \bar{e}_R e_L) = -\frac{g_e v}{\sqrt{2}}\bar{e}e \tag{1.45}$$

with $e = e_L + e_R$. The free parameter g_e has to be adjusted to fulfill the relation

$$m_e = \frac{g_e v}{\sqrt{2}}. \tag{1.46}$$

One thus has no prediction for the electron mass but a proportionality between the electron mass and the electron Higgs coupling. Hence, generalizing to other fermions, like quarks, the coupling of heavier fermions to the Higgs should be larger and thus the production easier.

1.2. Higgs boson searches at hadron colliders

1.2.1. Constraints on the Higgs mass

Although the Standard Model of electroweak interactions and the Higgs mechanism of spontaneous symmetry breaking explain the interactions of W bosons, Z bosons and photons as well as their masses, there is no statement on m_H. The mass of the Higgs boson remains (besides the fermion masses or its Yukawa couplings) a free parameter of the theory (cf. eq. 1.21) and has to be determined by experiment.

Which processes might contribute to evidence for a Higgs particle depends thereby strongly on its mass, but previous experiments as well as fundamental considerations allow for constraints on the possible Higgs mass. Direct searches at LEP, an electron positron collider which was operating until 2000 at the location of the LHC, have yielded a lower bound of $m_H = 114.4\,\text{GeV}$ [6]. An estimation of $m_H = 114^{+69}_{-45}\,\text{GeV}$ can be gained indirectly from electroweak precision measurements if presuming the validity of the Standard model and performing a global fit to all electroweak data [7]. Unitarity sets an upper limit on the Higgs mass of $\sim 1\,\text{TeV}$ [8, 9, 10]. It shall be noted that it is also possible to derive a mass range from a cut-off scale from which on one expects new physics [11, 12, 13]. For a cut-off of the order of the Planck scale, $10^{19}\,\text{GeV}$, the Higgs mass is constrained to a range of $130 < m_H < 190\,\text{GeV}$. For lower cut-offs, the range becomes wider.

1.2.2. Main Higgs production and decay modes

In hadronic reactions there are four main production modes for Higgs boson masses from 100 to some hundreds of GeV:

- gluon fusion by a heavy quark loop: $gg \to H$;
- vector boson fusion: $qq' \to qq'VV \to qq'H$, where the bosons V ($V + W, Z$) are emitted by quarks and scatter off each other;
- associated production with weak gauge bosons: $qq' \to WH, ZH$;
- associated production with heavy quarks: $q\bar{q}, gg \to t\bar{t}H, b\bar{b}H$, $qq, gg \to bH$.

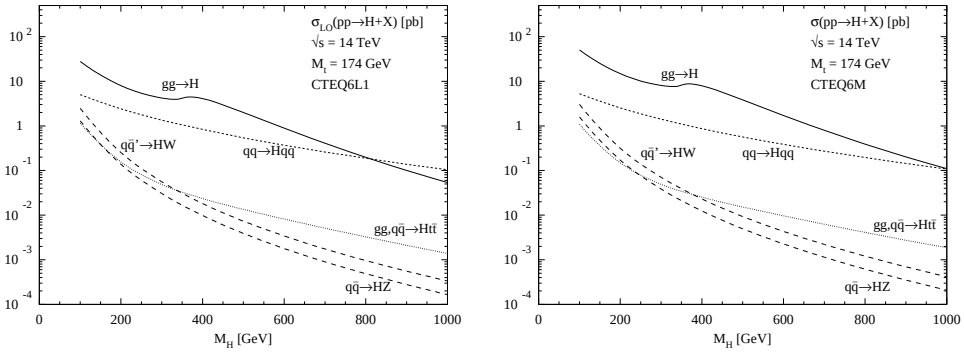

Figure 1.1.: Higgs boson production cross section as a function of the Higgs mass M_H for the LHC collider at LO (left) and NLO (right) [14]

Typical production cross sections as function of the Higgs mass are shown in fig. 1.1. While the gluon fusion process is the dominant one for small and intermediate Higgs masses, at higher masses vector boson fusion $qq' \to qqH$ reaches comparable values. At the LHC, associated production is not important except for small Higgs masses in contrast to the Tevatron where it presents an important production mode.

The branching fractions for Higgs decay depend even stronger on its mass (cf. fig. 1.2). The most important modes are:

- decay to weak gauge bosons $H \to W^+W^-, ZZ$;
- decay to heavy quarks: $H \to t\bar{t}, b\bar{b}$;
- other decays: $H \to \tau^+\tau^-, c\bar{c}, gg, \gamma\gamma$;

For masses over 140 GeV, decay into W^+W^- or ZZ bosons is the predominant decay mode. For even larger masses, $t\bar{t}$ decay can reach up to 20% of this ratio. For light Higgs bosons, decay into $b\bar{b}$ is most important followed by decays to leptons ($\tau\bar{\tau}$) and strongly interacting particles ($c\bar{c}$, gg). Decays into photons are very rare and appear only in sizable fraction for intermediate masses, but are very interesting due to their clean experimental signature.

1.2.3. The Tevatron

The Tevatron is a $p\bar{p}$ collider currently operating in Run II with a center of mass energy of 1.96 TeV. Two Higgs boson channels are most promising: associated production with W or Z and decay to $b\bar{b}$ as well as gluon fusion with decay to WW.

For a light Higgs boson, decay to $b\bar{b}$ is favored. The associated vector boson decays via $W \to l\nu$, $Z \to \nu\bar{\nu}$ or $Z \to l\bar{l}$. Backgrounds after b tagging are mainly from $Wb\bar{b}$, $Zb\bar{b}$, WZ and $t\bar{t}$ production as well as from QCD backgrounds for $ZH \to \nu\bar{\nu}b\bar{b}$. Thus, knowledge of backgrounds is important. A Higgs decay would then be visible as an excess

in the $b\bar{b}$ invariant mass spectrum. A sensitivity at the 95% confidence level is expected for a Higgs mass of $m_H = 120\,\text{GeV}$ if combining all channels and both experiments. A 5σ discovery would require an integrated luminosity of $10\,\text{fb}^{-1}$ [14] and is thus most likely not possible.

For masses above 140 GeV, the decay to two W bosons is the dominant one for which a relatively clean signature can be found in the gluon fusion channel. Although the production from gluon fusion is higher than associated production, this channel is suppressed due to the small branching ratio of $W \to l\bar{\nu}$. The background from W^+W^- continuum production is known and can be controlled by several cuts. Expectations of Higgs cross sections are an order of magnitude higher than estimations from the Standard Model and can thus be excluded to 95% C.L. 3σ sensitivity to Higgs boson masses between 160 and 170 GeV would require an integrated luminosity of about $10\,\text{fb}^{-1}$ [14]. The corresponding mode from ZZ production is about an order of magnitude smaller but contributes in combined searches.

1.2.4. The Large Hadron Collider

The Large Hadron Collider (LHC) is a proton-proton collider with a center of mass energy of 14 TeV situated at CERN and expected to start operation in 2007. There are two experiments with general purpose detectors, ATLAS and CMS, running at a luminosity of $\mathcal{L} = 10^{34}\,\text{cm}^{-2}\,\text{s}^{-2}$ after two to three years of operation. For experimental details, I refer the interested reader to the technical design reports [16, 17].

The predominant signal process

The by far dominant production mode for LHC energies is, as already stated, gluon fusion. For heavier Higgs bosons, decay to vector bosons is most important. Although the $H \to WW$ mode

$$gg \to \text{quark loop} \to H \to W^+W^- \to (l\bar{\nu})(\bar{l}'\nu')$$

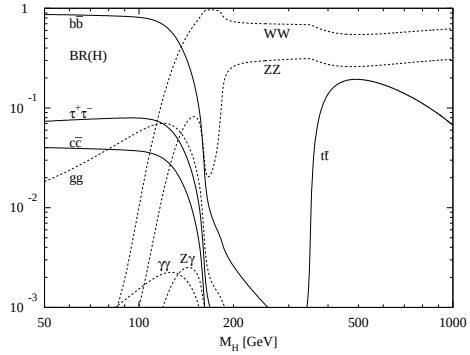

Figure 1.2.: Higgs branching ratios as a function of the Higgs mass M_H [15]

outweighs the $H \to ZZ$ mode, it is not favorable for mass measurements. Since the W bosons decay to fermion-neutrino pairs and the neutrino's momentum cannot be determined by the detector, it is not possible to reconstruct the W momenta. Thus, the Higgs mass cannot be reconstructed.

In contrast, the ZZ mode

$$pp \to H \to Z^*Z^* \to (l\bar{l})(l'\bar{l}')$$

allows for such a determination, since all four leptons can be detected. This channel is therefore called the "Golden Higgs Channel". The sensitivity for the discovery of a Standard Model Higgs boson in both experiments, Atlas and CMS, is shown in fig. 1.3.

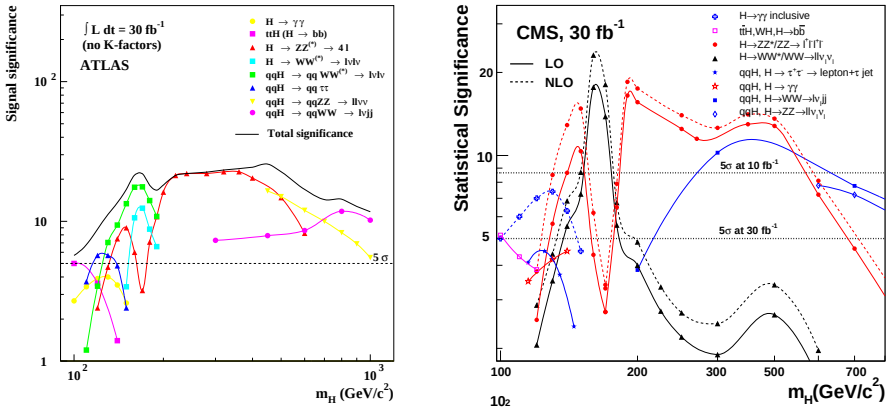

Figure 1.3.: Sensitivity for the discovery of a Standard Model Higgs boson in the Atlas (left) and CMS (right) experiments for an integrated luminosity of $30\,\mathrm{fb}^{-1}$. Systematic uncertainties have been included for the $H \to W^+W^- \to (l\bar{\nu})(\bar{l}'\nu')$ ($\pm 5\%$, left and right) and for the vector boson fusion channels ($\pm 10\%$, left only)

The gluon fusion Higgs production has been known for quite a while at leading order [18, 19]. NLO corrections have been shown to be large [20, 21]. Recently NNLO corrections have been calculated and are in good agreement within scale uncertainties from NLO.

Background processes

Although the $H \to Z^*Z^*$ mode provides experimentally quite clean signatures, it is clear that ZZ continuum production background processes should be taken into account for a precise determination of its mass. In the following, I will present the main contributions to ZZ continuum production.

$\mathbf{q\bar{q} \to Z^*Z^*}$

Quark annihilation to two Z bosons,

$$q\bar{q} \to Z^*Z^* \to (l\bar{l})(l'\bar{l}'),$$

does not pose any calculational problems as a tree level process at LO [22]. In the next chapter, I will present a LO calculation of on-shell Z pair production. Calculations of NLO corrections to this process have been performed in [23, 24, 25, 26].

$\mathbf{gg \to Z^*Z^*}$

The Z bosons are produced via a quark loop

$$gg \to \text{quark loop} \to Z^*Z^* \to (l\bar{l})(l'\bar{l}').$$

When comparing the contributions from different quark generations, the light quarks contribute most due to the propagators in the loop. The fact that this process is of NNLO in α_s is compensated by the higher luminosity of gluons in comparison to quark luminosities at the LHC.

The first full on-shell calculation of $gg \to ZZ$ and its contribution to $pp \to ZZ + X$ has been calculated by Duane A. Dicus, Chung Kao and W. W. Repko [27]. E. W. N. Glover and J. J. van der Bij have taken into account interferences with the signal $gg \to H \to ZZ$, but still for on-shell Z bosons and without subsequent decay of the vector bosons [28]. Later, the decays of the Z bosons have been incorporated [29]. There is one off-shell calculation for Z^*Z^* pair production from gluon fusion with the decays [30], but unfortunately there is no code available that could be used for predictions and only a very limited number of distributions are shown in the existing literature.

I note that in these calculations technical cuts on p_{TZ}, y_Z and $\sqrt{\hat{s}}$ have been applied to exclude the phase space region of Z boson emission in the extreme forward region where the applied calculational methods lead to numerical instabilities.

First of all, the off-shell computation presented here allows for access of the below-threshold region. Furthermore, it employs a new method that minimizes the impact of inverse Gram determinants that jeopardize the numerical stability. A stable amplitude evaluation in the entire phase space can be achieved with quadruple precision. While experimental cuts can be applied to eliminate the critical regions, with my program this is not necessary for accurate theoretical predictions. These improvements will be implemented in the `GG2ZZ` program that I will provide.

2. LO $q\bar{q} \to ZZ$ cross-section

Before calculating the loop-induced background process $gg \to Z^*Z^* \to (l\bar{l})(l'\bar{l'})$ (where l denotes the leptons e, μ (,τ)) to gluonic Higgs production I will show how to calculate another background process: the annihilation of a quark-antiquark pair into two Z bosons at LO. This is a quite simple tree-level process and has been calculated by R. W. Brown and K. O. Mikaelian [22] quite a while ago. Here, I am rather interested in demonstrating some basic quantum field theoretical techniques and in introducing the typical process for the computation of hadronic cross sections.

In hadron collider experiments, the particles which are brought to collision—in the case of the LHC two protons—are not elementary particles but posses a substructure. In the parton model, the hadrons are made up of the strongly interacting quarks and gluons. The quarks of the proton (two up quarks and one anti-down quark), called the valence quarks, interact with each other by the exchange of virtual gluons. In higher order of perturbation theory, the gluons themselves form loops of virtual quarks, called sea quarks. The momentum transfer of these interactions is low and therefore is a long-range interaction which cannot be calculated perturbatively.

When two protons are now brought two collision, single partons of the protons may interact. These interactions appear at high energies with high momentum transfer. This hard scattering is a short-distance interaction and can be calculated perturbatively due to asymptotic freedom. The interactions of the partons long before the hard scattering are absorbed into the description of the dynamics in the hadron since they appear on completely different timescales. One can thus assume that the dynamics of these interactions of single partons are approximately independent of the dynamics inside the hadron. One says, that the two dynamics factorize. This factorization depends on a scale, called the factorization scale μ. It is not evident which value to assume for the factorization scale whereby uncertainties are introduced in every calculation. Usually, one chooses a characteristic scale of the process, for electroweak processes the Z mass, for instance.

In section 2.1, I will show how to calculate the partonic cross section of the hard process, i.e. the annihilation of a quark-antiquark pair into two Z bosons at LO. In section 2.2, I will then take into account that the initial state particles of the hard process, the quarks, are partons and finally calculate the hadronic cross section.

2.1. Hard scattering process: $q\bar{q} \to ZZ$

As there exist neither a vertex coupling three Z bosons nor a vertex coupling two Z bosons and a photon, there is no s-channel diagram but only the t- and u-channel diagrams. At order e^2, there are only two diagrams (fig. 2.1).

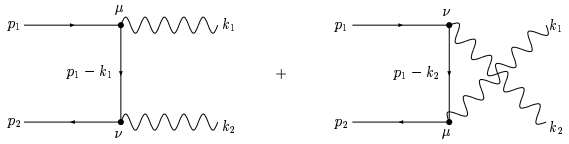

Figure 2.1.: The two diagrams contributing to $q\bar{q} \to ZZ$ in LO

The Feynman amplitude $\mathcal{M}$ is then

$$\begin{aligned}\mathcal{M} &= -i\bar{v}(p_2)\gamma^\nu(g_V^f - g_A^f\gamma_5)\frac{1}{\not{l}_1}\gamma^\mu(g_V^f - g_A^f\gamma_5)u(p_1)\epsilon_\nu^*(k_2)\epsilon_\mu^*(k_1) \\ &\quad -i\bar{v}(p_2)\gamma^\mu(g_V^f - g_A^f\gamma_5)\frac{1}{\not{l}_2}\gamma^\nu(g_V^f - g_A^f\gamma_5)u(p_1)\epsilon_\nu^*(k_2)\epsilon_\mu^*(k_1) \\ &= -i\bar{v}(p_2)T^{\mu\nu}u(p_1)\epsilon_\nu^*(k_2)\epsilon_\mu^*(k_1). \end{aligned} \tag{2.1}$$

where $T^{\mu\nu} = T_1^{\mu\nu} + T_2^{\mu\nu}$ with

$$T_1^{\mu\nu} = \gamma^\nu(g_V^f - g_A^f\gamma_5)\frac{1}{\not{l}_1}\gamma^\mu(g_V^f - g_A^f\gamma_5) \tag{2.2}$$

$$T_2^{\mu\nu} = \gamma^\mu(g_V^f - g_A^f\gamma_5)\frac{1}{\not{l}_2}\gamma^\nu(g_V^f - g_A^f\gamma_5). \tag{2.3}$$

g_V^f and g_A^f denote the vector and axialvector part of the coupling of a fermion-anti fermion pair to a Z boson, respectively:

$$g_V^f = \frac{e}{\sin\theta_W\cos\theta_W}\left(\frac{1}{2}T_3^f - \sin^2\theta_W Q_f\right) \tag{2.4}$$

$$g_A^f = -\frac{e}{\sin\theta_W\cos\theta_W}\frac{1}{2}T_3^f. \tag{2.5}$$

T_3^f is the third component of the weak isopsin and Q_f is the electric charge. The notation of slashed momenta in the denominator, for instance $\frac{1}{\not{l}_1}$, is defined by the inverse of the Feynman slash: $\frac{1}{\not{l}_1} := (\not{l}_1)^{-1}$.

The expressions for $T_1^{\mu\nu}$ and $T_2^{\mu\nu}$ can be simplified by exploiting $(\gamma_5)^2 = 1$ and the anticommutation relations $\{\gamma^\mu, \gamma_5\} = 0$,

$$\begin{aligned} T_1^{\mu\nu} &= {g_V^f}^2\gamma^\nu\frac{1}{\not{l}_1}\gamma^\mu + 2g_V^f g_A^f\gamma^5\gamma^\nu\frac{1}{\not{l}_1}\gamma^\mu + {g_A^f}^2\gamma^\nu\frac{1}{\not{l}_1}\gamma^\mu \\ &= ({g_V^f}^2 + {g_A^f}^2 + 2g_V^f g_A^f\gamma^5)\gamma^\nu\frac{1}{\not{l}_1}\gamma^\mu \quad \text{and} \quad T_2^{\mu\nu} \quad \text{analogously} \end{aligned} \tag{2.6}$$

$$\Rightarrow T^{\mu\nu} = T_1^{\mu\nu} + T_2^{\mu\nu} = ({g_V^f}^2 + {g_A^f}^2 + 2g_V^f g_A^f\gamma^5)\left(\gamma^\nu\frac{1}{\not{l}_1}\gamma^\mu + \gamma^\mu\frac{1}{\not{l}_2}\gamma^\nu\right) \tag{2.7}$$

in agreement with [22].

The complex conjugate of the Feynman amplitude, $\mathcal{M}^*$ is

$$\mathcal{M}^* = u^\dagger(p_1)T^{\dagger\rho\sigma}\bar{v}^\dagger(p_2)\epsilon_\rho(k_1)\epsilon_\sigma(k_2) = \bar{u}(p_1)\gamma_0 T^{\dagger\rho\sigma}\gamma_0 v(p_2)\epsilon_\rho(k_1)\epsilon_\sigma(k_2), \tag{2.8}$$

where

$$T^{\dagger\rho\sigma} = T_1^{\dagger\rho\sigma} + T_2^{\dagger\rho\sigma} = \left(\gamma^\sigma \frac{1}{\not{l}_1}\gamma^\rho + \gamma^\rho \frac{1}{\not{l}_2}\gamma^\sigma\right)^\dagger ({g_V^f}^2 + {g_A^f}^2 + 2g_V^f g_A^f \gamma^5)^\dagger. \tag{2.9}$$

Exploiting that $\gamma_5^\dagger = -\gamma_0\gamma_5\gamma_0$, $\gamma^{\dagger\rho} = \gamma_0\gamma^\rho\gamma_0$ and $(\gamma_0)^2 = 1$, one can rewrite $\gamma_0 T^{\dagger\rho\sigma}\gamma_0$ as $\tau^{\rho\sigma}$:

$$\gamma_0 T^{\dagger\rho\sigma}\gamma_0 = \tau^{\rho\sigma} = \left(\gamma^\rho \frac{1}{\not{l}_1}\gamma^\sigma + \gamma^\sigma \frac{1}{\not{l}_2}\gamma^\rho\right)({g_V^f}^2 + {g_A^f}^2 - 2g_V^f g_A^f \gamma^5). \tag{2.10}$$

Putting everything together yields the Feynman amplitude square

$$|\mathcal{M}|^2 = -\bar{v}(p_2)T^{\mu\nu}u(p_1)\bar{u}(p_1)\tau^{\rho\sigma}v(p_2)\epsilon_\mu^*(k_1)\epsilon_\nu^*(k_2)\epsilon_\rho(k_1)\epsilon_\sigma(k_2). \tag{2.11}$$

In a hadron collider experiment, one cannot control the spins s of the particles which enter the hard process. Hence one averages over these spins, i.e. one sums over the spin states of the initial state particles (in this case, the quarks) and divides by 4 for the 4 combinations of spin states. Furthermore, one cannot control the color states of the quarks and must thus also average over these states. As the electroweak vertices do not change the color of the quark and antiquark, c_1 and c_2, respectively, there are only contributions from the same color states. Summing over the three color states then contributes a factor $\sum_{c_1,c_2}\delta_{c_1,c_2} = 3$ and dividing by all combinations yields $\frac{1}{9}$, together $\frac{1}{3}$. Finally, the Z bosons which constitute the final state of the hard process, are of course not the final states of the physical process. Their life-time is much too short so that they do not reach the detector, but decay before. For the sake of simplicity, I will neither take into account the different decay modes of the Z bosons, nor will I distinguish their polarizations λ. Therefore, one must sum over these polarizations.

The spin and color averaged and polarization summed amplitude then reads

$$\overline{\sum}|\mathcal{M}|^2 = \frac{1}{4}\frac{1}{3}\sum_{c,s,\lambda}|\mathcal{M}|^2 = \frac{1}{12}\mathrm{Tr}\left[\not{p}_1\tau^{\rho\sigma}\not{p}_2 T^{\mu\nu}\right]\left(-g_{\mu\rho} + \frac{k_{1\mu}k_{1\rho}}{M^2}\right)\left(-g_{\nu\sigma} + \frac{k_{2\nu}k_{2\sigma}}{M^2}\right). \tag{2.12}$$

Expanding the parenthesis leads to four traces:

$$A = \mathrm{Tr}\left[\not{p}_1 \tau^{\rho\sigma} \not{p}_2 T^{\mu\nu}\right] g_{\mu\rho} g_{\nu\sigma} = \sum_{ij} \mathrm{Tr}\left[\not{p}_1 \tau_{i\mu\nu} \not{p}_2 T_j^{\mu\nu}\right] = \sum_{ij} A_{ij}, \tag{2.13}$$

$$B = \mathrm{Tr}\left[\not{p}_1 \tau^{\rho\sigma} \not{p}_2 T^{\mu\nu}\right] g_{\mu\rho} \frac{k_{2\nu} k_{2\sigma}}{M^2} = \sum_{ij} \mathrm{Tr}\left[\not{p}_1 \tau_{i\mu}^{\sigma} \not{p}_2 T_j^{\mu\nu}\right] \frac{k_{2\nu} k_{2\sigma}}{M^2} = \sum_{ij} B_{ij}, \tag{2.14}$$

$$C = \mathrm{Tr}\left[\not{p}_1 \tau^{\rho\sigma} \not{p}_2 T^{\mu\nu}\right] g_{\nu\sigma} \frac{k_{1\mu} k_{1\rho}}{M^2} = \sum_{ij} \mathrm{Tr}\left[\not{p}_1 \tau_{i\nu}^{\rho} \not{p}_2 T_j^{\mu\nu}\right] \frac{k_{1\mu} k_{1\rho}}{M^2} = \sum_{ij} C_{ij}, \tag{2.15}$$

$$D = \mathrm{Tr}\left[\not{p}_1 \tau^{\rho\sigma} \not{p}_2 T^{\mu\nu}\right] \frac{k_{1\mu} k_{1\rho}}{M^2} \frac{k_{2\nu} k_{2\sigma}}{M^2} = \sum_{ij} \mathrm{Tr}\left[\not{p}_1 \tau_i^{\rho\sigma} \not{p}_2 T_j^{\mu\nu}\right] \frac{k_{1\mu} k_{1\rho}}{M^2} \frac{k_{2\nu} k_{2\sigma}}{M^2} = \sum_{ij} D_{ij} \tag{2.16}$$

$$\tag{2.17}$$

Looking more closely at the terms inside τ and T,

$$\begin{aligned} & (g_V^{f\,2} + g_A^{f\,2} - 2 g_V^f g_A^f \gamma^5) \not{p}_2 (g_V^{f\,2} + g_A^{f\,2} + 2 g_V^f g_A^f \gamma^5) \\ &= [(g_V^{f\,2} + g_A^{f\,2})^2 + 4 g_V^{f\,2} g_A^{f\,2})] \not{p}_2 - 4 g_V^f g_A^f (g_V^{f\,2} + g_A^{f\,2}) \gamma^5 \not{p}_2 \\ &= \underbrace{[g_V^{f\,4} + g_A^{f\,4} + 6 g_V^{f\,2} g_A^{f\,2}]}_{f^1} \not{p}_2 + \underbrace{4 g_V^f g_A^f (g_V^{f\,2} + g_A^{f\,2})}_{f^5} \not{p}_2 \gamma^5, \end{aligned} \tag{2.18}$$

one notices that each trace X_{ij} can be split into two terms:

$$X_{ij} = f^1 X_{ij}^1 + f^5 X_{ij}^5. \tag{2.19}$$

What remains to compute is then

$$A = \mathrm{Tr}\left[\not{p}_1 \left(\gamma_\mu \frac{1}{\not{l}_1} \gamma_\nu + \gamma_\nu \frac{1}{\not{l}_2} \gamma_\mu\right) (f_1 \not{p}_2 + f_5 \not{p}_2 \gamma_5) \left(\gamma^\nu \frac{1}{\not{l}_1} \gamma^\mu + \gamma^\mu \frac{1}{\not{l}_2} \gamma^\nu\right)\right], \tag{2.20}$$

$$B = \mathrm{Tr}\left[\not{p}_1 \left(\gamma_\mu \frac{1}{\not{l}_1} \gamma^\sigma + \gamma^\sigma \frac{1}{\not{l}_2} \gamma_\mu\right) (f_1 \not{p}_2 + f_5 \not{p}_2 \gamma_5) \left(\gamma^\nu \frac{1}{\not{l}_1} \gamma^\mu + \gamma^\mu \frac{1}{\not{l}_2} \gamma^\nu\right)\right] \frac{k_{2\nu} k_{2\sigma}}{M^2}, \tag{2.21}$$

$$C = \mathrm{Tr}\left[\not{p}_1 \left(\gamma^\rho \frac{1}{\not{l}_1} \gamma_\nu + \gamma_\nu \frac{1}{\not{l}_2} \gamma^\rho\right)) (f_1 \not{p}_2 + f_5 \not{p}_2 \gamma_5) \left(\gamma^\nu \frac{1}{\not{l}_1} \gamma^\mu + \gamma^\mu \frac{1}{\not{l}_2} \gamma^\nu\right)\right] \frac{k_{1\mu} k_{1\rho}}{M^2}, \tag{2.22}$$

$$D = \mathrm{Tr}\left[\not{p}_1 \left(\gamma^\rho \frac{1}{\not{l}_1} \gamma^\sigma + \gamma^\sigma \frac{1}{\not{l}_2} \gamma^\rho\right) (f_1 \not{p}_2 + f_5 \not{p}_2 \gamma_5) \left(\gamma^\nu \frac{1}{\not{l}_1} \gamma^\mu + \gamma^\mu \frac{1}{\not{l}_2} \gamma^\nu\right)\right] \frac{k_{1\mu} k_{1\rho}}{M^2} \frac{k_{2\nu} k_{2\sigma}}{M^2} \tag{2.23}$$

Exploiting the rules of the so-called Clifford algebra to compute the traces, one finds for the first trace

$$A = 16(2 p_1 \cdot k_1 \; p_2 \cdot k_1 \; - M^2 p_1 \cdot p_2 \;) \left(\frac{1}{(l_1^2)^2} + \frac{1}{(l_2^2)^2}\right) - 64 \frac{p_1 \cdot p_2 \; l_1 \cdot l_2}{l_1^2 l_2^2}. \tag{2.24}$$

Introducing the Mandelstam variables s, t and u,

$$s = (p_1 + p_2)^2, \tag{2.25}$$
$$t = (p_1 - k_1)^2 = (p_2 - k_2)^2 = (l_1)^2, \tag{2.26}$$
$$u = (p_1 - k_2)^2 = (p_2 - k_1)^2 = (l_2)^2, \tag{2.27}$$

and expressing all relevant quantities in s, t and u,

$$p_1 \cdot p_2 = \frac{s}{2}, \quad k_1 \cdot k_2 = \frac{s}{2} - M^2, \quad p_1 \cdot k_1 = \frac{1}{2}(M^2 - t), \quad p_2 \cdot k_1 = \frac{1}{2}(M^2 - u), \tag{2.28}$$
$$l_1 \cdot l_2 = (p_1 - k_1)(p_1 - k_2) = -p_1(\underbrace{k_1 + k_2}_{p_1+p_2}) + k_1 \cdot k_2 = k_1 \cdot k_2 - p_1 \cdot p_2 = -M^2, \tag{2.29}$$

one rewrites A in terms of the Mandelstam variables

$$\begin{aligned} A &= 8\left([(M^2 - t)(M^2 - u) - M^2 s] \left(\frac{1}{t^2} + \frac{1}{u^2} \right) + 4\frac{sM^2}{tu} \right) \\ &= 8\left(\frac{u}{t} + \frac{t}{u} + 4M^2\frac{s}{tu} - M^4 \left(\frac{1}{t^2} + \frac{1}{u^2} \right) \right). \end{aligned} \tag{2.30}$$

The calculation of the other traces is straight forward when considering a simple trick: It is possible to cancel $\not{l}_1$ and $\not{l}_2$ in the denominators when appearing in combination with external momenta, for instance $\not{p}_2\not{k}_2\frac{1}{\not{l}_1}$. With four-momentum conservation $p_1 + p_2 = k_1 + k_2$

$$\not{p}_1\not{k}_{1,2} = -\not{p}_1\not{l}_{1,2}, \quad \not{k}_{1,2}\not{p}_1 = -\not{l}_{1,2}\not{p}_1, \quad \not{p}_2\not{k}_{1,2} = \not{p}_2\not{l}_{2,1}, \quad \not{k}_{1,2}\not{p}_2 = \not{l}_{2,1}\not{p}_2 \tag{2.31}$$

and thus

$$\not{p}_1\not{k}_{1,2}\frac{1}{\not{l}_{1,2}} = -\not{p}_1\not{l}_{1,2}\frac{1}{\not{l}_{1,2}} = \not{p}_1, \quad \not{p}_2\not{k}_{1,2}\frac{1}{\not{l}_{2,1}} = \not{p}_2\not{l}_{2,1}\frac{1}{\not{l}_{2,1}} = \not{p}_2 \quad \text{etc.} \tag{2.32}$$

Exploiting these relations, all the other traces, B, C and D, vanish since the subterms of every trace cancel each other. Thus, as the only non-zero trace is A, one finds for the spin and color averaged and polarization summed Feynman amplitude square:

$$\overline{\sum}|\mathcal{M}|^2 = \frac{1}{12}\sum_{c,s,\lambda}|\mathcal{M}|^2 = \frac{2}{3}({g_V^f}^4 + {g_A^f}^4 + 6{g_V^f}^2{g_A^f}^2)\left[\frac{t}{u} + \frac{u}{t} + 4M^2\frac{s}{tu} - M^4\left(\frac{1}{t^2} + \frac{1}{u^2} \right) \right] \tag{2.33}$$

2.1.1. The differential cross section

The differential cross section is defined by

$$d\sigma = \frac{1}{2E_a 2E_b |v_a - v_b|} d\Phi \overline{\sum} |\mathcal{M}|^2, \tag{2.34}$$

with the phase space $d\Phi$ for a $2 \to 2$ process

$$d\Phi = \left(\prod_{f=c,d} \frac{d^3 p_f}{(2\pi)^3} \frac{1}{2E_f} \right) (2\pi)^4 \delta^{(4)}(p_a + p_b - p_c - p_d) \quad \text{with} \quad E_i := \sqrt{\vec{p}_i^{\,2} + m_i^2}. \tag{2.35}$$

One can choose the z-axis of the laboratory frame along the colliding beams. The denominator of eq. 2.34 can then be rewritten as $2E_a 2E_b |v_a - v_b| = 4|\epsilon^{\mu 12 \nu} p_{1\mu} p_{2\nu}|$. $d\sigma$ is thus not manifestly Lorentz invariant, but invariant under boosts along the z-axis.

Exploiting the relation $\delta(g(x)) = \sum_i \frac{\delta(x - x_i)}{|g'(x_i)|}$, where x_i are the roots of $g(x)$, one can substitute the factors of $\frac{1}{2E_f}$ in eq. 2.35

$$dp_{f0} \delta(p_{f0}^2 - (\vec{p_f}^{\,2} + M_f^2)) \theta(p_{f0}) = \sum_{p_{f0} = \pm E_f} \frac{1}{2p_{f0}} \theta(p_{f0}) = \frac{1}{2E_f} \tag{2.36}$$

to show that $d\Phi$ is manifestly Lorentz invariant:

$$d\Phi = (2\pi)^4 \delta^{(4)}(p_a + p_b - p_c - p_d) \prod_{f=c,d} \frac{1}{(2\pi)^3} d^4 p_f \delta(p_f^2 - M_f^2) \theta(p_{f0}). \tag{2.37}$$

Therefore, $d\Phi$ is called the invariant phase space.

However, for calculational purposes, it is convenient to start from the non manifestly Lorentz invariant form of $d\Phi$ (eq. 2.35)

$$\begin{aligned} d\Phi &= \frac{1}{16\pi^2} \frac{1}{E_c E_d} d^3 p_c \underbrace{\delta^{(3)}(\vec{p}_a + \vec{p}_b - \vec{p}_c - \vec{p}_d) d^3 p_d}_{\vec{p}_d = \vec{p}_a + \vec{p}_b - \vec{p}_c} \delta(E - E_c - E_d) \\ &= \frac{1}{16\pi^2} \frac{1}{E_c E_d} p_c^2 dp_c d\Omega_c \delta(E - \sqrt{\vec{p}_c^{\,2} + M_c^2} - \sqrt{\vec{p}_d^{\,2} + M_d^2}), \end{aligned} \tag{2.38}$$

where the conservation of 3-momentum, $\vec{p}_d = \vec{p}_a + \vec{p}_b - \vec{p}_c$, is implicit from now on.

Exploiting the Lorentz invariance one can choose the center of mass system (CMS) of the partons, which will be denoted by hatted quantities, to evaluate $d\Phi$. This frame of reference is defined by

$$\begin{aligned}
\vec{\hat{P}} &:= \vec{\hat{p}}_a + \vec{\hat{p}}_b = \vec{\hat{p}}_c + \vec{\hat{p}}_d = 0 \\
\Rightarrow \hat{P} &:= \hat{p}_a + \hat{p}_b = \hat{p}_c + \hat{p}_d = (\hat{E}_a + \hat{E}_b, 0)^T = (\hat{E}_c + \hat{E}_d, 0)^T =: (\sqrt{\hat{s}}, 0)^T \\
\Rightarrow \hat{P} \cdot \hat{p}_{a,b} &= \sqrt{\hat{s}} \hat{E}_{a,b} \\
\Rightarrow \hat{E}_{a,b} &= \frac{\hat{s} + m_{a,b}^2 - m_{b,a}^2}{2\sqrt{\hat{s}}}.
\end{aligned} \tag{2.39}$$

One can express $|\vec{\hat{p}}_a|$ and $|\vec{\hat{p}}_b|$ also by the masses and $\hat{s}$:

$$\begin{aligned}
\vec{\hat{p}}_a^2 = \vec{\hat{p}}_b^2 &= \hat{E}_a^2 - m_a^2 = \frac{1}{4\hat{s}}(\hat{s} - (m_a + m_b)^2)(\hat{s} - (m_a - m_b)^2) =: \frac{1}{4\hat{s}}\lambda(\hat{s}, m_a^2, m_b^2) \\
\Rightarrow |\vec{\hat{p}}_a| = |\vec{\hat{p}}_b| &= \frac{1}{2\sqrt{\hat{s}}}\sqrt{\lambda(\hat{s}, m_a^2, m_b^2)}
\end{aligned} \tag{2.40}$$

and analogously for $|\vec{\hat{p}}_c|$ and $|\vec{\hat{p}}_d|$. Defining $\hat{p} := |\vec{\hat{p}}_c| = |\vec{\hat{p}}_d|$ the invariant phase space $d\Phi$ simplifies to

$$\begin{aligned}
d\Phi &= \frac{1}{16\pi^2}\frac{\hat{p}^2}{\hat{E}_c \hat{E}_d}\, d\hat{\Omega}\, d\hat{p}\, \delta\left(\hat{E} - \sqrt{\hat{p}^2 + M_c^2} - \sqrt{\hat{p}^2 + M_d^2}\right) \\
&= \frac{1}{16\pi^2}\frac{\hat{p}}{\hat{E}}\, d\hat{\Omega} = \frac{1}{32\pi^2}\sqrt{1 - \frac{4M^2}{\hat{E}^2}}\, d\hat{\Omega} = \frac{1}{32\pi^2}\beta\, d\hat{\Omega}.
\end{aligned} \tag{2.41}$$

The cross section $d\sigma$ then reads

$$d\sigma = \frac{1}{32\pi^2 s}\beta\, d\hat{\Omega}\overline{\sum}|\mathcal{M}|^2. \tag{2.42}$$

As the process possesses symmetry around the z-axis, $d\sigma$ will be independent of $\hat{\phi}$ and the integration over $\hat{\phi}$ yields a factor 2π:

$$d\hat{\Omega} = d\cos\hat{\theta} d\hat{\phi} \Rightarrow d\sigma = \frac{1}{32\pi s}\beta\, d\cos\hat{\theta}\frac{1}{2}\overline{\sum}|\mathcal{M}|^2. \tag{2.43}$$

The polar angle $\hat{\theta}$ is now expressed in terms of the Mandelstam variable t:

$$\begin{aligned}
t &= M^2 - 2(\hat{p}_1\hat{k}_1) = M^2 - 2(\hat{p}_{1,0}\hat{k}_{1,0} - \vec{\hat{p}}_1\vec{\hat{k}}_1) = M^2 - \frac{\hat{s}}{2}(1 - \beta\cos\hat{\theta}) \\
\frac{dt}{d\cos\hat{\theta}} &= \frac{\hat{s}\beta}{2} \Rightarrow \frac{d\hat{\sigma}}{dt} = \frac{2}{\hat{s}\beta}\frac{d\hat{\sigma}}{d\cos\hat{\theta}}
\end{aligned} \tag{2.44}$$

and finally, the differential cross section is

$$\frac{d\sigma}{dt} = \frac{1}{3}\frac{1}{8\pi\hat{s}^2}({g_V^f}^4 + {g_A^f}^4 + 6{g_V^f}^2{g_A^f}^2)\left[\frac{t}{u} + \frac{u}{t} + 4M^2\frac{s}{tu} - M^4\left(\frac{1}{t^2} + \frac{1}{u^2}\right)\right] \tag{2.45}$$

in agreement with [22].

2.1.2. The total cross-section

The total cross section $d\sigma$ of the hard process is obtained by performing the integration over t, corresponding to an integration over the polar angle $\hat{\theta}$. The boundaries of this integration are obtained from the substitution

$$t = M^2 - \frac{\hat{s}}{2}(1 - \beta\cos\theta) \quad \text{with} \quad \theta \in [0, \pi] \tag{2.46}$$

$$\Rightarrow t_{\substack{max\\min}} = M^2 - \frac{\hat{s}}{2} \pm \frac{\hat{s}}{2}\beta = \frac{1}{4}(4m^2 - \hat{s} - \hat{s} \pm 2\hat{s}\beta) = -\frac{\hat{s}}{4}(1 \mp 2\beta + \beta^2) = -\frac{\hat{s}}{4}(1 \mp \beta)^2 \tag{2.47}$$

Figure 2.2.: Two kinematic configurations which cannot be distinguished from a quantum mechanical viewpoint. The configuration on the right is obtained from the configuration on the left by a rotation of $\pi - 2\theta$ perpendicular to the beam line and a rotation of π around the beam line. When integrating over ϕ and θ both configurations contribute, although they correspond to one single quantum state. Therefore, a factor of $\frac{1}{2}$ has to be introduced by hand in the total cross section.

One must note that the factor of $\frac{1}{2}$ is necessary to avoid double counting, as explained in figure 2.2. The total cross section of the $q\bar{q} \to ZZ$ process is then given by

$$\hat{\sigma} = \frac{1}{2}\int_{t_{min}}^{t_{max}} dt \frac{d\sigma}{dt}. \tag{2.48}$$

Substituting the dependent variable $u = 2M^2 - s - t$, the integration can be performed by partial decomposition and yields

$$\sigma = \frac{1}{3}\frac{1}{4\pi s}({g_V^f}^4 + {g_A^f}^4 + 6{g_V^f}^2{g_A^f}^2)\left[\frac{4 + (1-\beta^2)^2}{2(1-\beta^2)}\log\frac{1+\beta}{1-\beta} - \beta\right], \tag{2.49}$$

again in agreement with [22] when considering that $\frac{4\pi\alpha^2}{e^4} = \frac{4\pi}{e^4}(\frac{e^2}{4\pi})^2 = \frac{1}{4\pi}$.

2.2. Hadronic Cross Section

Having calculated the cross section of the hard process, I will now explain how to derive relevant predictions. As explained before, the initial state particles of the hard scattering

process are the partons. The probability to find the parton q, in this case a quark, in the hadron, in this case in a proton, is given by the parton density functions or structure functions.

Before calculating the hadronic cross section, I will explain the kinematics of a collider experiment. I will assume that the momenta of the colliding protons, p_A and p_B are parallel to the z-axis. Thus, in their CMS which is identical to the laboratory frame

$$p_A = \frac{\sqrt{s}}{2}\begin{pmatrix}1\\0\\0\\1\end{pmatrix} \qquad \text{and} \qquad p_B = \frac{\sqrt{s}}{2}\begin{pmatrix}1\\0\\0\\-1\end{pmatrix}. \tag{2.50}$$

The total energies of the hadrons is defined as $s := (p_A + p_B)^2 \approx 2p_A p_B$.

At high energies the transverse momenta of the partons are negligible and thus the momenta of the partons p_a and p_b are fractions of the momenta p_A and p_B of the hadrons from which they come from:

$$p_a = p_A x_a \qquad \text{and} \qquad p_b = p_B x_b \qquad \text{with} \qquad x_a, x_b \in [0,1]. \tag{2.51}$$

Since the total energy of the partons is invariant one defines τ

$$\hat{s} = (\hat{p}_a + \hat{p}_a)^2 = (p_a + p_b)^2 = 2p_a p_b = x_a x_b \underbrace{2p_A p_B}_{\approx s} \approx \underbrace{x_a x_b}_{:=\tau} s \tag{2.52}$$

as the ratio of the total hadron to the total parton energy.

The cross section of the hadronic process is now a convolution of the partonic cross section σ_{hard} which has been calculated in the previous section with the parton density functions of a quark q and an antiquark $\bar{q}$, $f_{a=q}(x_a, \mu^2)$ and $f_{b=\bar{q}}(x_b, \mu^2)$, respectively, summed over all flavors which contribute to the process:

$$\sigma = \sum_q \int_0^1 dx_a \int_0^1 dx_b \; f_{a=q}(x_a) f_{b=\bar{q}}(x_b) \; \sigma_{hard}(q\bar{q} \to ZZ) + \begin{pmatrix} a=\bar{q} \\ b=q \end{pmatrix}. \tag{2.53}$$

Substituting the integration variable x_b by $\tau = x_a x_b$ which leads to $dx_a dx_b = \frac{dx_a}{x_a} d\tau$ this expression can be rewritten as

$$\sigma = \int_0^1 d\tau \underbrace{\sum_q \int_\tau^1 \frac{dx_a}{x_a} \; f_{a=q}(x_a) f_{b=\bar{q}}(x_b) \; \hat{\sigma}(q\bar{q} \to ZZ) + \begin{pmatrix} a=\bar{q} \\ b=q \end{pmatrix}}_{=:\frac{d\sigma}{d\tau} = s\frac{d\sigma}{d\hat{s}}}. \tag{2.54}$$

2.3. Results

I have evaluated the total hadronic cross section numerically in Fortran code. As parton density functions, I used the CTEQ6M set of the Les Houches Accord (LHAPDF, [31]). Plots for both the differential cross section $\frac{d\sigma}{d\hat{s}}$ and the total cross sectionσ can be found in figure 2.3.

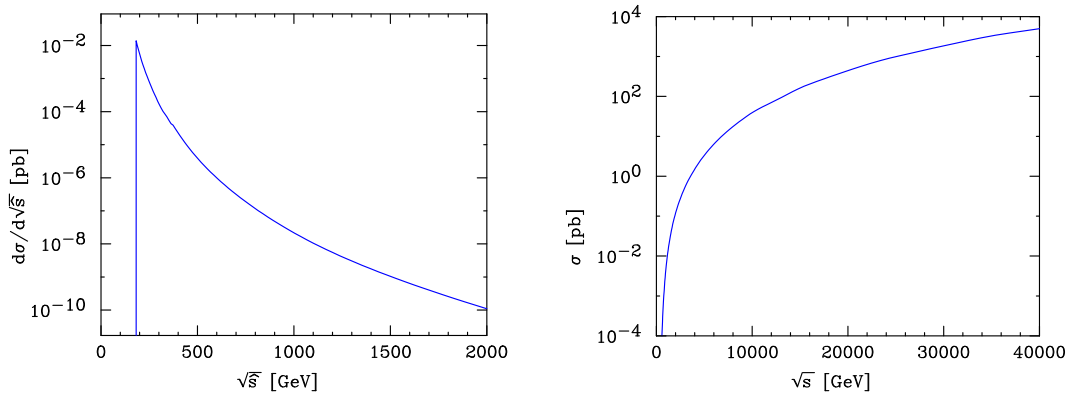

Figure 2.3.: left: $\frac{d\sigma}{d\hat{s}}(\sqrt{\hat{s}})$ for the $pp \to ZZ$ process for $\sqrt{s} = 14\,\text{TeV}$; right: $\sigma(\sqrt{s})$ for the $pp \to ZZ$ process

3. The loop induced process gg $\longrightarrow$ Z*Z*

The main goal of this work is to calculate the contribution from gluon-induced production of 4 charged leptons ($l = e, \mu(, \tau)$) via two off-shell Z bosons:

$$g(p_1) + g(p_2) \rightarrow Z^*(p_3) + Z^*(p_4) \rightarrow l(p_5)\bar{l}(p_6)l'(p_7)\bar{l}'(p_8).$$

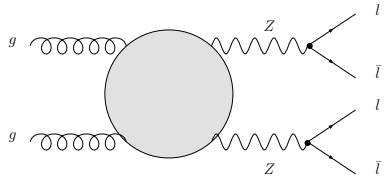

Neglecting the mass of the leptons,

$$p_5^2 = p_6^2 = p_7^2 = p_8^2 = 0,$$

leads to considerable simplifications. For this double-resonant process, there exist various topologies, loop diagrams even in leading order, either triangles or boxes (fig. 3.1), with the two intermediate Z bosons decaying each into a lepton-antilepton pair.

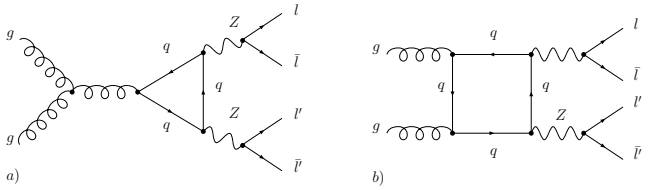

Figure 3.1.: Double-resonant contributions to $gg \rightarrow Z^*Z^* \rightarrow (l\bar{l})(l'\bar{l}')$ from a) triangle loop diagrams and b) box loop diagrams

One can directly argue that the triangle diagrams cannot contribute due to conservation of color. Let us assume that they would contribute. As gluons carry color the gluon that is exchanged in the triangle diagrams must transfer color to the triangle, but since the Z bosons are colorless objects, the conservation of color would be violated. Hence, the contributions from the triangle diagrams vanish.

There are also single resonant diagrams with the exchange of either a Z-boson or a photon (fig. 3.2), but they also vanish, mainly due to Furry's theorem, which I will demonstrate in the next section.

Figure 3.3 gives a complete list of box diagrams. The calculation of their Feynman amplitude and cross section will be presented in this chapter.

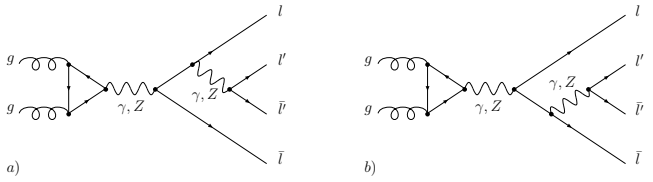

Figure 3.2.: Single-resonant contributions to $gg \to Z^*Z^* \to (l\bar{l})(l'\bar{l}')$; a) with the exchange of γ, Z

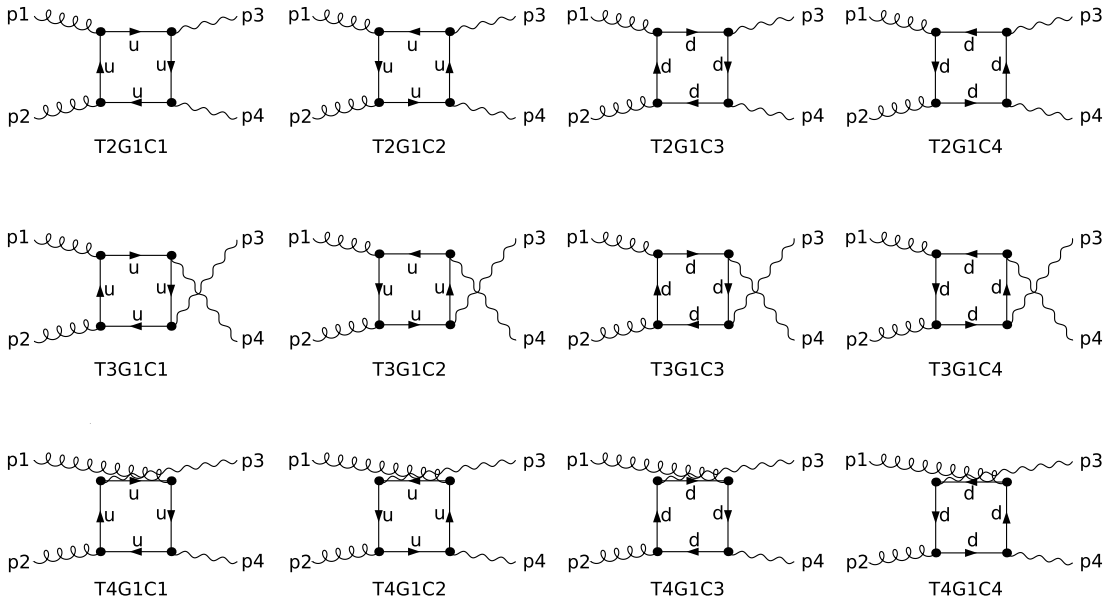

Figure 3.3.: An exhaustive list of all diagrams contributing to $gg \to Z^*Z^*$ in leading order.

3.1. Single resonant diagrams

I will now show that the single resonant diagrams from fig. 3.2 with exchange of a photon or a Z boson do not contribute to the amplitude for $gg \to (l\bar{l})(l'\bar{l}')$.

Instead of calculating the complete Feynman amplitude for the quark loop, it is sufficient to consider an effective ggZ coupling $\Gamma^{\mu_1\mu_2\mu_3}$. The tensor structure is potentially composed of all Lorentz invariants, i.e. the external momenta p_1 and p_2 as well as metric tensors and ϵ tensors. Due to Furry's theorem the contributions from the photon exchange must vanish since an odd number of gauge bosons couples to the quark loop. For the Z exchange this is only true for the contributions from the vector part of the Z coupling to the loop and thus only the axial vector part can contribute. Therefore, all tensor structures composed only of external momenta and metric tensors must vanish and only those with ϵ tensors contribute.

The effective ggZ vertex is composed of expressions where 1, 2 or 3 of the indices μ_1, μ_2 and μ_3 are carried by the ϵ tensor and the rest by external momenta or the metric tensor:

$$\begin{aligned}\Gamma^{\mu_1\mu_2\mu_3} &= A\epsilon^{\mu_1\mu_2\mu_3\sigma}\sum_{i=1,2} p_{\sigma i} \\ &+ B\left(\sum_{i=1,2} p_i^{\mu_1}\epsilon^{\mu_2\mu_3\rho\sigma} + \sum_{i=1,2} p_i^{\mu_2}\epsilon^{\mu_1\mu_3\rho\sigma} + \sum_{i=1,2} p_i^{\mu_3}\epsilon^{\mu_1\mu_2\rho\sigma}\right)\sum_{j,k=1,2} p_{\rho j}p_{\sigma k} \\ &+ C\left(\sum_{i,j=1,2} p_i^{\mu_1}p_j^{\mu_2}\epsilon^{\mu_3\nu\rho\sigma} + \sum_{i,j=1,2} p_i^{\mu_1}p_j^{\mu_3}\epsilon^{\mu_2\nu\rho\sigma} + \sum_{i,j=1,2} p_i^{\mu_2}p_j^{\mu_3}\epsilon^{\mu_1\nu\rho\sigma}\right)\sum_{k,l,m=1,2} p_{\nu k}p_{\rho l}p_{\sigma m} \\ &+ D\left(g^{\mu_1\mu_2}\epsilon^{\mu_3\nu\rho\sigma} + g^{\mu_1\mu_3}\epsilon^{\mu_2\nu\rho\sigma} + g^{\mu_2\mu_3}\epsilon^{\mu_1\nu\rho\sigma}\right)\sum_{k,l,m=1,2} p_{\nu k}p_{\rho l}p_{\sigma m}. \end{aligned} \tag{3.1}$$

This can be simplified when considering which contractions are possible in the Feynman amplitude:

The term with one contraction (first line in eq. 3.1) has a p_1 or p_2 in the superscript and when contracted with the Z momentum, $(p_1+p_2)_{\mu_3}$, one momentum appears twice in the superscript and thus the ϵ tensor vanishes. In the terms with three contractions (third and fourth line), again, at least one momentum appears twice in the superscript and thus the ϵ tensor vanishes. Only the second line survives

$$\Gamma^{\mu_1\mu_2\mu_3} = B\left(\sum_{i=1,2} p_i^{\mu_1}\epsilon^{\mu_2\mu_3\rho\sigma} + \sum_{i=1,2} p_i^{\mu_2}\epsilon^{\mu_1\mu_3\rho\sigma} + \sum_{i=1,2} p_i^{\mu_3}\epsilon^{\mu_1\mu_2\rho\sigma}\right)\sum_{j,k=1,2} p_{\rho j}p_{\sigma k},$$

but it further simplifies by transversality of the gluons

$$p_1\cdot\epsilon_1 \;= p_2\cdot\epsilon_2 \;= 0 \tag{3.2}$$

and gauge conditions

$$p_1\cdot\epsilon_2 \;= p_2\cdot\epsilon_1 \;= 0 \tag{3.3}$$

since in the first and second term there would be contractions between the external momenta p_1 and p_2 and the polarization vectors in the amplitude

$$\Gamma^{\mu_1\mu_2\mu_3} = B\sum_{i=1,2} p_i^{\mu_3}\epsilon^{\mu_1\mu_2\rho\sigma}\sum_{j,k=1,2} p_{\rho j}p_{\sigma k} = B\epsilon^{\mu_1\mu_2 p_1 p_2}(p_1^{\mu_3}+p_2^{\mu_3}).$$

This term also fulfills the Ward identity, as one can see by contracting with $p_1^{\mu_1}$ and $p_2^{\mu_2}$. The dependencies still missing are those on s, m_u^2 and m_d^2 and are contained in the function $B = B(s, m_u^2, m_d^2)$. The effective ggZ vertex is thus

$$\Gamma^{\mu} = B(s, m_u^2, m_d^2)\epsilon^{\epsilon_1\epsilon_2 p_1 p_2}(p_1^{\mu}+p_2^{\mu}). \tag{3.4}$$

Defining the momenta of the fermion propagators (cf. fig. 3.4

$$\begin{aligned} l_1 &= p_3 + k = p_3 + p_5 + p_6 = q - p_4 \\ l_2 &= -(p_4 + k) = -(p_4 + p_5 + p_6) = -q + p_3, \end{aligned}$$

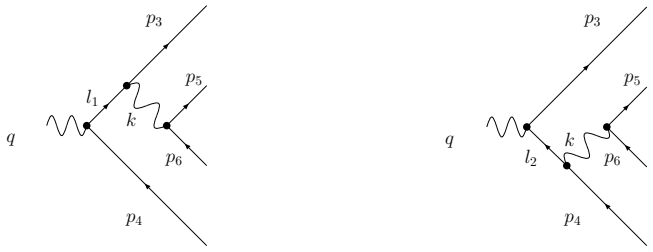

Figure 3.4.: Single resonant Z exchange diagrams

where $k = p_5 + p_6$ and $q = p_1 + p_2 = p_3 + p_4 + p_5 + p_6$, the Feynman amplitude for the sum of both diagrams is

$$\bar{u}(p_3)\not{J}_{56}\frac{\not{l}_1}{l_1^2}(-i\underbrace{\not{q}}_{\not{l}_1+\not{p}_4}(g_V - g_A\gamma_5))v(p_4)$$
$$+\bar{u}(p_3)\underbrace{\not{q}}_{-\not{l}_2+\not{p}_3}(-i(g_V - g_A\gamma_5))\frac{\not{l}_2}{l_2^2}\not{J}_{56}v(p_4),$$

where J_{56} is the leptonic current corresponding to the second γ or Z boson propagator and second fermion line. g_V^f and g_A^f denote the vector and axial vector part of the coupling of a fermion-anti fermion pair to a Z boson, respectively:

$$g_V^f = \frac{e}{\sin\theta_W\cos\theta_W}\left(\frac{1}{2}T_3^f - \sin^2\theta_W Q_f\right)$$
$$g_A^f = -\frac{e}{\sin\theta_W\cos\theta_W}\frac{1}{2}T_3^f.$$

T_3^f is the third component of the weak isopsin and Q_f is the electric charge, i.e. for charged leptons:

$$g_V = \frac{e(\sin^2\theta_W - 1)}{4\sin\theta_W\cos\theta_W}$$
$$g_A = \frac{e}{4\sin\theta_W\cos\theta_W}.$$

With $\bar{u}(p_3)\not{p}_3 = 0$ and $\not{p}_4 v(p_4) = 0$ for massless final states, the fermion propagators are canceled and one finds:

$$\bar{u}(p_3)\not{J}_{56}(-i(g_V - g_A\gamma_5))v(p_4)$$
$$-\bar{u}(p_3)\not{J}_{56}(-i(g_V - g_A\gamma_5))v(p_4)$$
$$= 0.$$

3.2. Double-resonant diagrams

For a computation of the contributions of the double-resonant diagrams it is useful to distinguish two cases: the massless and the massive case. The massless case applies approximately for the contribution of the first two generations of quarks in the loops. Compared to LHC energies which our calculation is adapted to, the masses of the up, down, charm and strange quark are negligible. We can check this by performing a calculation with massive quarks and then passing to the limit $m_q \to 0$ (cf. section 3.3.3). This assumption allows for large simplifications of the amplitude and thus improves the speed of the computation.

The massive case must be applied for the remaining bottom and top quark. Especially the top mass of 172 GeV [32] lies in the range of partonic energies $\sqrt{\hat{s}}$ and must therefore be taken into account.

Since only the box contributions survive, it is sufficient to consider off-shell production of two Z-bosons

$$g(p_1) + g(p_2) \to Z^*(p_3) + Z^*(p_4)$$

with subsequent decay of the Z's to lepton pairs

$$Z^*(p_3) \to l(p_5)\bar{l}(p_6), \quad Z^*(p_4) \to l'(p_7)\bar{l}'(p_8).$$

Here, all momenta are defined to be incoming:

$$g(p_1) + g(p_2,) + Z^*(p_3) + Z^*(p_4) \to 0.$$

The Feynman amplitude $\mathcal{M}$ for a single diagram is

$$\varepsilon_{1\mu_1}\varepsilon_{2,\mu_2}\mathcal{M}^{\mu_1\mu_2\mu_3\mu_4}P_{\mu_3\nu_3}(p_3)P_{\mu_4,\nu_4}(p_4)J_3^{\nu_3}J_4^{\nu_4},$$

where $\varepsilon_{1\mu_1}$and $\varepsilon_{2\mu_2}$ are the polarization vectors of the gluons, $P_{\mu,\nu}(p)$ is the propagator of a virtual Z boson and $J_3^{\nu_3}$ and $J_4^{\nu_4}$ are the currents of the lepton-anti lepton pairs:

$$J_3^{\nu} = \frac{1}{2}\bar{v}(p_6)\gamma^{\nu}(g_V - g_A\gamma_5)u(p_5)$$
$$J_4^{\nu} = \frac{1}{2}\bar{v}(p_8)\gamma^{\nu}(g_V - g_A\gamma_5)u(p_7).$$

where g_V and g_A denote again the vector and axial vector part of the coupling of a charged lepton-anti lepton pair to a Z boson, respectively.

One could now perform the computation of the amplitude and cross section numerically. The inconvenience is that such a computation often suffers from numerical instabilities for certain regions of phase space as will be explained later. In contrast, I opted for a analytic computation.

Such an analytic computation of the amplitude for each diagram begins by valuating the traces in $\mathcal{M}^{\mu_1\mu_2\mu_3\mu_4}$ thereby yielding a linear combination of tensor integrals. Each tensor integral will then be reduced to a linear combination of covariant tensors and coefficients which are scalar integrals. Thus, the amplitude of each diagram l consists after these reductions of a tensor structure τ_j, scalar integrals I_k and the coefficients $\mathcal{C}_{jkl}$ which are polynomials in the masses of the quarks in the loop and Mandelstam variables

$$\mathcal{M}_l = \sum_{j,k} \mathcal{C}_{jkl}(s,t,u,s_3,s_4,m_b^2,m_t^2)\,\tau_j\,I_k$$

with

$$\begin{array}{lll} s=(p_1^2+p_2)^2, & t=(p_2+p_3)^2, & u=(p_1+p_3)^2, \\ s_3=p_3^2, & s_4=p_4^2. & \end{array} \tag{3.5}$$

Reducing all the tensor structures and scalar integrals to an irreducible set of tensor structures and scalar integrals, the analytic expression simplifies enormously thereby not only improving the implementation speed but also its numerical stability. Therefore, I will show how to find such a basis of tensor structures and such a minimal set of scalar integrals

3.2.1. Tensor structures

Ingredients of the amplitude

Due to Lorentz covariance the scattering tensor $\mathcal{M}^{\mu_1\mu_2\mu_3\mu_4}$ can be decomposed to metric tensors, external momenta and ϵ tensors. Out of these elements one can construct the following structures:

- only with metric tensors: $g^{\mu_1\mu_2}g^{\mu_3\mu_4}$;
- only with external momenta: $p_{j_1}^{\mu_1}p_{j_2}^{\mu_2}p_{j_3}^{\mu_3}p_{j_4}^{\mu_4}$;
- with metric tensors and external momenta mixed: $g^{\mu_1\mu_2}p_{j_3}^{\mu_3}p_{j_4}^{\mu_4}$ etc.;
- contractions of the ϵ tensor with up to three external momenta p_j. Instead of using the ϵ tensor and contracting it with external momenta, one can introduce an orthogonal projection of the momenta p_1, p_2 and p_3,

  $$k_0^\mu = \epsilon^{\mu p_1 p_2 p_3}, \tag{3.6}$$

  where the notation of momenta in the superscript is defined by

  $$\epsilon^{abcd} := \epsilon^{\mu\nu\rho\sigma}a_\mu b_\nu c_\rho d_\sigma.$$

  As every totally antisymmetric tensor of rank n is proportional to an antisymmetrized product of n vectors, the ϵ tensor can be expressed by an antisymmetrized

product of four vectors. We choose one of these vectors to be the vector k_0^μ, as defined in eq. 3.6, and three of the vectors to be the dual vectors k_1^μ, k_2^μ and k_3^μ of the vectors p_1, p_2 and p_3, respectively, defined by

$$k_i \cdot p_j \ = \delta_{ij}. \tag{3.7}$$

With this representation of the ϵ tensor every contraction of the ϵ tensor is proportional to the vector k_0. Therefore, the ϵ tensor can be replaced by k_0 as an alternative ingredient of the decomposition. The following structures can be used:

- with one k_0 and three p_j: $k_0^{\mu_1} p_{j_2}^{\mu_2} p_{j_3}^{\mu_3} p_{j_4}^{\mu_4}$ etc.;
- with one k_0, one p_j and one $g^{\mu\nu}$: $k_0^{\mu_1} p_{j_2}^{\mu_2} g^{\mu_3\mu_4}$ etc. In this context, one should note, that

  $$k_0^\mu k_0^\nu = \alpha g^{\mu\nu} + \beta_{ij} p_i^\mu p_j^\nu, \tag{3.8}$$

  so that one can change the order of indices in products like $k_0^{\mu_1} g^{\mu_2\mu_3}$:

  $$\begin{aligned} k_0^{\mu_1} g^{\mu_2\mu_3} &= k_0^{\mu_1} k_0^{\mu_2} k_0^{\mu_3} - k_0^{\mu_1} \beta_{ij} p_i^{\mu_2} p_j^{\mu_3} \\ &= g^{\mu_1\mu_2} k_0^{\mu_3} - k_0^{\mu_1} \beta_{ij} p_i^{\mu_2} p_j^{\mu_3}. \end{aligned}$$

  This is used to always have either $g^{\mu_1\mu_2}$ or $g^{\mu_3\mu_4}$ if there is a k_0.
- with two k_0 and either two p_j or one $g^{\mu\nu}$: Exploiting eq. 3.8, one can substitute $k_0^\mu k_0^\nu$ by $g^{\mu\nu}$ and $\beta_{ij} p_i^\mu p_j^\nu$ Hence, this structure can be traced back to structures already treated above.
- with three k_0 and one p_j: This structure can again be traced back to terms like $k_0^{\mu_1} p_j^{\mu_2} g^{\mu_3\mu_4}$ and $k_0^{\mu_1} p_{j_2}^{\mu_2} p_{j_3}^{\mu_3} p_{j_4}^{\mu_4}$;
- with four k_0: This structure can be traced back to terms like $g^{\mu_1\mu_2} g^{\mu_3\mu_4}$, $g^{\mu_1\mu_2} p_{j_3}^{\mu_3} p_{j_4}^{\mu_4}$ and $p_{j_1}^{\mu_1} p_{j_2}^{\mu_2} p_{j_3}^{\mu_3} p_{j_4}^{\mu_4}$ which have already been treated above.

One can now reduce the range of occurring indices j_1, j_2, j_3, j_4 by considering that the amplitude $\mathcal{M}^{\mu_1\mu_2\mu_3\mu_4}$ will be multiplied by the polarization vectors ε_{1,μ_1}, ε_{2,μ_2} and the leptonic currents $J_{3\mu_3}$, $J_{4\mu_4}$, yielding expressions of the form $\epsilon_1 \cdot p_1$, $\epsilon_1 \cdot p_2$, $J_3 \cdot p_3$ etc. Exploiting transversality,

$$\epsilon_1 \cdot p_1 \ = \epsilon_2 \cdot p_2 \ = 0, \tag{3.9}$$

fixing the gauge by

$$\epsilon_1 \cdot p_2 \ = \epsilon_2 \cdot p_1 \ = 0 \tag{3.10}$$

and exploiting furthermore, that for massless external leptons

$$J_3 \cdot p_3 \ = J_4 \cdot p_4 \ = 0 \tag{3.11}$$

many of these terms cancel.

The Feynman amplitude consists of a linear combination:

$$\begin{aligned}
\mathcal{M}^{\mu_1\mu_2\mu_3\mu_4} &= A g^{\mu_1\mu_2} g^{\mu_3\mu_4} \\
&+ \sum_{j_1 j_2 j_3 j_4} C_{j_1 j_2 j_3 j_4} p_{j_1}^{\mu_1} p_{j_2}^{\mu_2} p_{j_3}^{\mu_3} p_{j_4}^{\mu_4} \\
&+ \sum_{j_1, j_2} B^1_{j_3 j_4} g^{\mu_1\mu_2} p_{j_3}^{\mu_3} p_{j_4}^{\mu_4} + \sum_{j_2, j_4} B^2_{j_2 j_4} g^{\mu_1\mu_3} p_{j_2}^{\mu_2} p_{j_4}^{\mu_4} + \sum_{j_2, j_3} B^3_{j_2 j_4} g^{\mu_1\mu_4} p_{j_2}^{\mu_2} p_{j_3}^{\mu_3} \\
&+ \sum_{j_1, j_4} B^4_{j_2 j_4} g^{\mu_2\mu_3} p_{j_1}^{\mu_1} p_{j_4}^{\mu_4} + \sum_{j_1, j_3} B^5_{j_1 j_3} g^{\mu_2\mu_4} p_{j_1}^{\mu_1} p_{j_3}^{\mu_3} + \sum_{j_1, j_2} B^6_{j_1 j_2} g^{\mu_3\mu_4} p_{j_1}^{\mu_1} p_{j_2}^{\mu_2} \\
&+ \sum_{j_2} E^1_{j_2 00} k_0^{\mu_1} g^{\mu_3\mu_4} p_{j_2}^{\mu_2} + \sum_{j_1} E^2_{j_1 00} k_0^{\mu_2} g^{\mu_3\mu_4} p_{j_1}^{\mu_1} \\
&+ \sum_{j_4} E^3_{00 j_4} k_0^{\mu_3} g^{\mu_1\mu_2} p_{j_4}^{\mu_4} + \sum_{j_3} E^4_{00 j_3} k_0^{\mu_4} g^{\mu_1\mu_2} p_{j_3}^{\mu_3} \\
&+ \sum_{j_2, j_3, j_4} E^1_{j_2 j_3 j_4} k_0^{\mu_1} p_{j_2}^{\mu_2} p_{j_3}^{\mu_3} p_{j_4}^{\mu_4} + \sum_{j_1, j_3, j_4} E^2_{j_1 j_3 j_4} k_0^{\mu_2} p_{j_1}^{\mu_1} p_{j_3}^{\mu_3} p_{j_4}^{\mu_4} \\
&+ \sum_{j_1, j_2, j_4} E^3_{j_1 j_2 j_4} k_0^{\mu_3} p_{j_1}^{\mu_1} p_{j_2}^{\mu_2} p_{j_4}^{\mu_4} + \sum_{j_1, j_2, j_3} E^4_{j_1 j_2 j_3} k_0^{\mu_4} p_{j_1}^{\mu_1} p_{j_2}^{\mu_2} p_{j_3}^{\mu_3},
\end{aligned} \tag{3.12}$$

where $j_1, j_2 \in \{3\}$ and $j_3, j_4 \in \{1, 2\}$.

To get the Feynman amplitude, this must be contracted with the polarization vectors, $\epsilon_{1\mu_1}^{\lambda_1}$ and $\epsilon_{2\mu_2}^{\lambda_2}$ with polarizations $\lambda_1, \lambda_2 \in \{+, -\}$, and the leptonic currents, $J_{3\mu_3}$ and $J_{4\mu_4}$:

$$\begin{aligned}
\mathcal{M}^{\lambda_1\lambda_2 J_3 J_4} &= A \epsilon_1^{\lambda_1} \cdot \epsilon_2^{\lambda_2} \ J_3 \cdot J_4 \\
&+ \sum_{j_3 j_4} C_{33 j_3 j_4} \ p_3 \cdot \epsilon_1^{\lambda_1} \ p_3 \cdot \epsilon_2^{\lambda_2} \ p_{j_3} \cdot J_3 \ p_{j_4} \cdot J_4 \\
&+ \sum_{j_3 j_4} B^1_{j_3 j_4} \epsilon_1^{\lambda_1} \cdot \epsilon_2^{\lambda_2} \ p_{j_3} \cdot J_3 \ p_{j_4} \cdot J_4 \ + \sum_{j_4} B^2_{3 j_4} \epsilon_1^{\lambda_1} \cdot J_3 \ p_3 \cdot \epsilon_2^{\lambda_2} \ p_{j_4} \cdot J_4 \\
&+ \sum_{j_3} B^3_{3 j_3} \epsilon_1^{\lambda_1} \cdot J_4 \ p_3 \cdot \epsilon_2^{\lambda_2} \ p_{j_3} \cdot J_3 \ + \sum_{j_4} B^4_{3 j_4} \epsilon_2^{\lambda_2} \cdot J_3 \ p_3 \cdot \epsilon_1^{\lambda_1} \ p_{j_4} \cdot J_4 \\
&+ \sum_{j_3} B^5_{3 j_3} \epsilon_2^{\lambda_2} \cdot J_4 \ p_3 \cdot \epsilon_1^{\lambda_1} \ p_{j_3} \cdot J_3 \ + B^6_{33} J_3 \cdot J_4 \ p_3 \cdot \epsilon_1^{\lambda_1} \ p_3 \cdot \epsilon_2^{\lambda_2} \\
&+ E^1_{300} k_0 \cdot \epsilon_1^{\lambda_1} \ J_3 \cdot J_4 \ p_3 \cdot \epsilon_2^{\lambda_2} \ + E^2_{300} k_0 \cdot \epsilon_2^{\lambda_2} \ J_3 \cdot J_4 \ p_3 \cdot \epsilon_1^{\lambda_1} \\
&+ \sum_{j_4} E^3_{00 j_4} k_0 \cdot J_3 \ \epsilon_1^{\lambda_1} \cdot \epsilon_2^{\lambda_2} \ p_{j_4} \cdot J_4 \ + \sum_{j_3} E^3_{00 j_3} k_0 \cdot J_4 \ \epsilon_1^{\lambda_1} \cdot \epsilon_2^{\lambda_2} \ p_{j_3} \cdot J_3 \\
&+ \sum_{j_3 j_4} E^1_{3 j_3 j_4} k_0 \cdot \epsilon_1^{\lambda_1} \ p_3 \cdot \epsilon_2^{\lambda_2} \ p_{j_3} \cdot J_3 \ p_{j_4} \cdot J_4 \ + E^2_{3 j_3 j_4} k_0 \cdot \epsilon_2^{\lambda_2} \ p_3 \cdot \epsilon_1^{\lambda_1} \ p_{j_3} \cdot J_3 \ p_{j_4} \cdot J_4
\end{aligned}$$

$$+\sum_{j_4} E^3_{33j_4} k_0\cdot J_3\; p_3\cdot\epsilon_2^{\lambda_2}\; p_3\cdot\epsilon_1^{\lambda_1}\; p_{j_4}\cdot J_4 \;+\sum_{j_3} E^4_{33j_3} k_0\cdot J_4\; p_3\cdot\epsilon_2^{\lambda_2}\; p_3\cdot\epsilon_1^{\lambda_1}\; p_{j_3}\cdot J_3 \quad (3.13)$$

The notation of polarization indices, $\lambda_{1,2}$ in the superscript is defined by

$$A^{\lambda_{1,2}} := A^\mu \epsilon_\mu^{\lambda_{1,2}}(p_{1,2}).$$

Transformation to gauge invariant expressions

In order to rewrite the amplitude in a manifestly gauge-invariant way, one introduces the Abelian part of the gluon field strength tensor and its dual by

$$\begin{aligned}\mathcal{F}_j^{\mu_1\mu_2} &= p_j^{\mu_1}\epsilon_j^{\mu_2} - p_j^{\mu_2}\epsilon_j^{\mu_1}\\ \tilde{\mathcal{F}}_j^{\mu_1\mu_2} &= \epsilon^{\mu_1\mu_2\mu_3\mu_4}\mathcal{F}_{j\mu_3\mu_4} = 2\epsilon^{\mu_1\mu_2 p_j\epsilon_j}.\end{aligned}$$

The transformations of expressions defined with the gauge fixing of eq. 3.10 to gauge invariant expressions are then

$$\begin{aligned}\epsilon_1^{\lambda_1}\cdot\epsilon_2^{\lambda_2} &\to -\frac{1}{s}\mathrm{tr}(\mathcal{F}_1^{\lambda_1}\mathcal{F}_2^{\lambda_2}),\\ \epsilon_1^{\lambda_1}\cdot p_3 &\to \frac{2}{s}p_2\cdot\mathcal{F}_1^{\lambda_1}\cdot p_3,\\ \epsilon_2^{\lambda_2}\cdot p_3 &\to \frac{2}{s}p_1\cdot\mathcal{F}_2^{\lambda_2}\cdot p_3,\\ \epsilon_1^{\lambda_1}\cdot J_k &\to \frac{2}{s}p_2\cdot\mathcal{F}_1^{\lambda_1}\cdot J_k,\\ \epsilon_2^{\lambda_2}\cdot J_k &\to \frac{2}{s}p_1\cdot\mathcal{F}_2^{\lambda_2}\cdot J_k,\\ k_0\cdot\epsilon_1^{\lambda_1} = \epsilon^{\lambda_1 p_1 p_2 p_3} &\to -\frac{1}{2}p_2\cdot\widetilde{\mathcal{F}}_1^{\lambda_1}\cdot p_3,\\ k_0\cdot\epsilon_2^{\lambda_2} = \epsilon^{\lambda_2 p_1 p_2 p_3} &\to \frac{1}{2}p_1\cdot\widetilde{\mathcal{F}}_2^{\lambda_2}\cdot p_3.\end{aligned}$$

Substituting these expressions into eq. 3.13,

$$\begin{aligned}&\mathcal{M}^{\lambda_1\lambda_2 J_3 J_4}\\ &= -\frac{A}{s}tr\left(\mathcal{F}_1^{\lambda_1}\mathcal{F}_2^{\lambda_2}\right)J_3\cdot J_4 \;+\sum_{j_3 j_4}\frac{4C_{33j_3j_4}}{s^2}p_2\cdot\mathcal{F}_1^{\lambda_1}\cdot p_3\; p_1\cdot\mathcal{F}_2^{\lambda_2}\cdot p_3\; p_{j_3}\cdot J_3\; p_{j_4}\cdot J_4\\ &-\sum_{j_3 j_4}\frac{B^1_{j_3j_4}}{s}tr\left(\mathcal{F}_1^{\lambda_1}\mathcal{F}_2^{\lambda_2}\right)p_{j_3}\cdot J_3\; p_{j_4}\cdot J_4 \;+\sum_{j_4}B^2_{3j_4}\frac{2}{s}p_2\cdot\mathcal{F}_1^{\lambda_1}\cdot J_3\;\frac{2}{s}p_1\cdot\mathcal{F}_2^{\lambda_2}\cdot p_3\; p_{j_4}\cdot J_4\\ &+\sum_{j_3}B^3_{3j_3}\frac{2}{s}p_2\cdot\mathcal{F}_1^{\lambda_1}\cdot J_4\;\frac{2}{s}p_1\cdot\mathcal{F}_2^{\lambda_2}\cdot p_3\; p_{j_3}\cdot J_3 \;+\sum_{j_4}B^4_{3j_4}\frac{2}{s}p_1\cdot\mathcal{F}_2^{\lambda_2}\cdot J_3\;\frac{2}{s}p_2\cdot\mathcal{F}_1^{\lambda_1}\cdot p_3\; p_{j_4}\cdot J_4\\ &+\sum_{j_3}B^5_{3j_3}\frac{2}{s}p_1\cdot\mathcal{F}_2^{\lambda_2}\cdot J_4\;\frac{2}{s}p_2\cdot\mathcal{F}_1^{\lambda_1}\cdot p_3\; p_{j_3}\cdot J_3 \;+\frac{4B^6_{33}}{s^2}J_3\cdot J_4\; p_2\cdot\mathcal{F}_1^{\lambda_1}\cdot p_3\; p_1\cdot\mathcal{F}_2^{\lambda_2}\cdot p_3\end{aligned}$$

$$
\begin{aligned}
&- \frac{E^1_{300}}{s} p_2 \cdot \widetilde{\mathcal{F}}_1^{\lambda_1} \cdot p_3 \; J_3 \cdot J_4 \; p_1 \cdot \mathcal{F}_2^{\lambda_2} \cdot p_3 \; - \frac{E^2_{300}}{s} p_1 \cdot \widetilde{\mathcal{F}}_2^{\lambda_2} \cdot p_3 \; J_3 \cdot J_4 \; p_2 \cdot \mathcal{F}_1^{\lambda_1} \cdot p_3 \\
&- \sum_{j_4} \frac{E^3_{00j_4}}{s} k_0 \cdot J_3 \; tr\left(\mathcal{F}_1^{\lambda_1} \mathcal{F}_2^{\lambda_2}\right) p_{j_4} \cdot J_4 \; - \sum_{j_3} \frac{E^4_{00j_3}}{s} k_0 \cdot J_4 \; tr\left(\mathcal{F}_1^{\lambda_1} \mathcal{F}_2^{\lambda_2}\right) p_{j_3} \cdot J_3 \\
&- \sum_{j_3 j_4} \frac{E^1_{3j_3j_4}}{s} p_2 \cdot \widetilde{\mathcal{F}}_1^{\lambda_1} \cdot p_3 \; p_1 \cdot \mathcal{F}_2^{\lambda_2} \cdot p_3 \; p_{j_3} \cdot J_3 \; p_{j_4} \cdot J_4 \\
&- \sum_{j_3 j_4} \frac{E^2_{3j_3j_4}}{s} p_1 \cdot \widetilde{\mathcal{F}}_2^{\lambda_2} \cdot p_3 \; p_2 \cdot \mathcal{F}_1^{\lambda_1} \cdot p_3 \; p_{j_3} \cdot J_3 \; p_{j_4} \cdot J_4 \\
&+ \sum_{j_4} \frac{4E^3_{33j_4}}{s^2} k_0 \cdot J_3 \; p_1 \cdot \mathcal{F}_2^{\lambda_2} \cdot p_3 \; p_2 \cdot \mathcal{F}_1^{\lambda_1} \cdot p_3 \; p_{j_4} \cdot J_4 \\
&+ \sum_{j_3} \frac{4E^4_{33j_3}}{s^2} k_0 \cdot J_4 \; p_1 \cdot \mathcal{F}_2^{\lambda_2} \cdot p_3 \; p_2 \cdot \mathcal{F}_1^{\lambda_1} \cdot p_3 \; p_{j_3} \cdot J_3 \; ,
\end{aligned}
$$

one finds a manifestly Lorentz invariant representation of the amplitude $\mathcal{M}^{\lambda_1\lambda_2 J_3 J_4}$ and furthermore, gauge invariance reflected in the Ward identities which one finds all fulfilled. Nevertheless, this representation is still reducible, i.e. not all terms are independent. This could be exploited for checks of the amplitude: Due to symmetries of the amplitude one finds relations for the coefficients which one can check explicitly.

Helicity amplitudes

The representation of the amplitude which I presented so far exhibits a problem which will become apparent later on: The coefficients A, B^i_{mn} etc. contain denominators of the form $2s(ut - s_3 s_4)$. As I will show later, these terms approach zero in the extreme forward scattering region and the amplitude diverge there. But since these divergences do not correspond to any physical singularities they are only present in this representation and can be overcome by changing to a different representation.

I will now show that by calculating the helicity amplitudes $\mathcal{M}^{+-J_3J_4}$, $\mathcal{M}^{+-J_3J_4}$, $\mathcal{M}^{-+J_3J_4}$ and $\mathcal{M}^{--J_3J_4}$, some of the dangerous denominators can be canceled and the amplitude will be expressed in terms of an irreducible tensor basis. Exploiting CP symmetry, there is no need to calculate all four helicity amplitudes since they fulfill the following relations:

$$
\begin{aligned}
\mathcal{M}^{--J_3J_4}(s,t,u,s_3,s_4) &= \mathcal{M}^{++J_4J_3}(s,u,t,s_4,s_3), \\
\mathcal{M}^{-+J_3J_4}(s,t,u,s_3,s_4) &= \mathcal{M}^{+-J_4J_3}(s,u,t,s_4,s_3).
\end{aligned}
$$

It is thus sufficient to calculate just $\mathcal{M}^{++J_3J_4}(s,t,u,s_3,s_4)$ and $\mathcal{M}^{+-J_3J_4}(s,t,u,s_3,s_4)$ which will be denoted by $++$ and $+-$ in the following.

I will now make use of the spinor helicity formalism following [33] providing a convenient representation of massless spin 1 polarization vectors which must obey

$$
\begin{aligned}
p \cdot \epsilon^\lambda(p) &= 0, \\
\epsilon^\lambda(p) \cdot \epsilon^{\lambda'}(p) &= -\delta_{\lambda,\lambda'}.
\end{aligned}
$$

In the bracket notation, the massless spinors are

$$|p_\pm\rangle := u_\pm(p) = v_\mp(p),$$
$$\langle p_\pm| := \bar{u}_\pm(p) = \bar{v}_\mp(p).$$

The polarization vectors are introduced by referring to another massless momentum q:

$$\epsilon^+_\mu(p_1) := \frac{\langle 2_-|\mu|1_-\rangle}{\sqrt{2}\langle 2_-|1_+\rangle},$$
$$\epsilon^-_\mu(p_1) := \frac{\langle 2_+|\mu|1_+\rangle}{\sqrt{2}\langle 2_+|1_-\rangle},$$
$$\epsilon^+_\mu(p_2) := \frac{\langle 1_-|\mu|2_-\rangle}{\sqrt{2}\langle 1_-|2_+\rangle},$$
$$\epsilon^-_\mu(p_2) := \frac{\langle 1_+|\mu|2_+\rangle}{\sqrt{2}\langle 1_+|2_-\rangle},$$

where $\langle pq\rangle := \langle p_-|q_+\rangle$. For details, I refer to the appendix A.1.

Using the spinor helicity formalism one obtains the following relation (cf. appendix A.1):

$$\epsilon^{+\mu}(p_1)\epsilon^{+\nu}(p_2) = -\frac{1}{s}\frac{[12]}{\langle 12\rangle}\left(p_1^\mu p_2^\nu + p_1^\nu p_2^\mu - p_1\cdot p_2 g^{\mu\nu} - i\epsilon^{p_1\nu p_2\mu}\right).$$

The constraints are therefore given by

$$\begin{aligned}
\epsilon^{+\mu}(p_1)\epsilon^{+\nu}(p_2)p_{3\mu}p_{3\nu} &= -\frac{1}{2s}\frac{[12]}{\langle 12\rangle}\left(ut - s_3 s_4\right),\\
\epsilon_1^+\cdot\epsilon_2^+ &= \frac{[12]}{\langle 12\rangle},\\
\epsilon_1^+\cdot J_k\ \epsilon_2^+\cdot p_3 &= -\frac{1}{s}\frac{[12]}{\langle 12\rangle}\left(p_1\cdot J_k\ \frac{t-s_3}{2} + p_2\cdot J_k\ \frac{u-s_3}{2} - i\epsilon^{p_1p_3p_2J_k}\right),\\
\epsilon_1^+\cdot p_3\ \epsilon_2^+\cdot J_k &= -\frac{1}{s}\frac{[12]}{\langle 12\rangle}\left(p_1\cdot J_k\ \frac{t-s_3}{2} + p_2\cdot J_k\ \frac{u-s_3}{2} + i\epsilon^{p_1p_3p_2J_k}\right),\\
\epsilon_1^+\cdot k_0\ \epsilon_2^+\cdot p_3 &= \frac{1}{s}\frac{[12]}{\langle 12\rangle}k_0^2,\\
\epsilon_1^+\cdot p_3\ \epsilon_2^+\cdot k_0 &= -\frac{1}{s}\frac{[12]}{\langle 12\rangle}k_0^2.
\end{aligned}$$

Substituting these relations into eq. 3.13 and suppressing the phase factor of $\frac{[12]}{\langle 12\rangle}$, the ++ amplitude is given by

$$\mathcal{M}^{++J_3J_4}$$

$$
\begin{aligned}
&= \left[A - B^6_{33}\frac{(tu-s_3s_4)}{2s} + E^1_{300}\frac{1}{s}k_0^2 + E^2_{300}\frac{1}{s}k_0^2\right] J_3\cdot J_4\\
&+ \left[-C_{3311}\frac{(tu-s_3s_4)}{2s} + B^1_{11} - \frac{1}{s}\frac{t-s_3}{2}[B^2_{31}+B^3_{31}+B^4_{32}+B^5_{32}] + E^1_{311}\frac{1}{s}k_0^2 + E^2_{311}\frac{1}{s}k_0^2\right] p_1\cdot J_3\; p_1\cdot J_4\\
&+ \left[-C_{3312}\frac{(tu-s_3s_4)}{2s} + B^1_{12} - \frac{1}{s}\frac{t-s_3}{2}[B^2_{32}+B^3_{31}+B^4_{31}+B^5_{32}] + E^1_{312}\frac{1}{s}k_0^2 + E^2_{312}\frac{1}{s}k_0^2\right] p_1\cdot J_3\; p_2\cdot J_4\\
&+ \left[-C_{3321}\frac{(tu-s_3s_4)}{2s} + B^1_{21} - \frac{1}{2}\frac{u-s_3}{2}[B^2_{31}+B^3_{32}+B^4_{32}+B^5_{31}] + E^1_{321}\frac{1}{s}k_0^2 + E^2_{321}\frac{1}{s}k_0^2\right] p_2\cdot J_3\; p_1\cdot J_4\\
&+ \left[-C_{3322}\frac{(tu-s_3s_4)}{2s} + B^1_{22} - \frac{1}{2}\frac{u-s_3}{2}[B^2_{32}+B^3_{32}+B^4_{31}+B^5_{31}] + E^1_{322}\frac{1}{s}k_0^2 + E^2_{322}\frac{1}{s}k_0^2\right] p_2\cdot J_3\; p_2\cdot J_4\\
&- 2\left[B^3_{31}+B^5_{32}\right] p_1\cdot J_3\; p_3\cdot J_4\\
&- 2\left[B^3_{32}+B^5_{31}\right] p_2\cdot J_3\; p_3\cdot J_4\\
&+ \left[E^3_{001} + [B^2_{31}+B^4_{31}]\frac{1}{s} - \frac{(tu-s_3s_4)}{2s}E^3_{331}\right]\epsilon^{p_1p_3p_2J_3} p_1\cdot J_4\\
&+ \left[E^4_{001} + [B^3_{31}+B^5_{31}]\frac{1}{s} - \frac{(tu-s_3s_4)}{2s}E^4_{331}\right]\epsilon^{p_1p_3p_2J_4} p_1\cdot J_3\\
&+ \left[E^3_{002} + [B^2_{32}+B^4_{32}]\frac{1}{s} - \frac{(tu-s_3s_4)}{2s}E^3_{332}\right]\epsilon^{p_1p_3p_2J_3} p_2\cdot J_4\\
&+ \left[E^4_{002} + [B^3_{32}+B^5_{32}]\frac{1}{s} - \frac{(tu-s_3s_4)}{2s}E^4_{332}\right]\epsilon^{p_1p_3p_2J_4} p_2\cdot J_3\ . \qquad (3.14)
\end{aligned}
$$

Note that the leptonic currents J_3 and J_4 appear in 11 different terms on the left hand side. Not all of these are independent as I will show later.

For the $+-$ amplitude, one applies eq. A.34,

$$
\epsilon^{+\mu}(p_1)\epsilon^{-\nu}(p_2) = \frac{\mathrm{tr}^-[\not p_1\not p_3\not p_2\gamma^\mu]\mathrm{tr}^-[\not p_1\not p_3\not p_2\gamma^\nu]}{2s(ut-s_3s_4)}\frac{\langle 2-|\not p_3|1-\rangle}{\langle 1-|\not p_3|2-\rangle},
$$

with tr^- defined as in eq. A.35 and finds that

$$
\begin{aligned}
\epsilon_1^+\cdot\epsilon_2^- &= 0,\\
\epsilon_1^+\cdot p_3\;\epsilon_2^-\cdot p_3 &= \frac{\langle 2-|\not p_3|1-\rangle}{\langle 1-|\not p_3|2-\rangle}\frac{ut-s_3s_4}{32s},\\
\epsilon_1^+\cdot J_k\;\epsilon_2^-\cdot p_3 &= \frac{\langle 2-|\not p_3|1-\rangle}{\langle 1-|\not p_3|2-\rangle}\frac{1}{8s}\left(p_1\cdot J_k\;\frac{t-s_3}{2} + p_2\cdot J_k\;\frac{u-s_3}{2} - i\epsilon^{p_1p_3p_2J_k}\right),\\
\epsilon_1^+\cdot p_3\;\epsilon_2^-\cdot J_k &= \frac{\langle 2-|\not p_3|1-\rangle}{\langle 1-|\not p_3|2-\rangle}\frac{1}{8s}\left(p_1\cdot J_k\;\frac{t-s_3}{2} + p_2\cdot J_k\;\frac{u-s_3}{2} + i\epsilon^{p_1p_3p_2J_k}\right),\\
\epsilon_1^+\cdot k_0\;\epsilon_2^-\cdot p_3 &= -\frac{\langle 2-|\not p_3|1-\rangle}{\langle 1-|\not p_3|2-\rangle}\frac{1}{16s}k_0^2,\\
\epsilon_1^+\cdot k_0\;\epsilon_2^-\cdot p_3 &= \frac{\langle 2-|\not p_3|1-\rangle}{\langle 1-|\not p_3|2-\rangle}\frac{1}{16s}k_0^2.
\end{aligned}
$$

Substituting these relations in eq. 3.13 and suppressing the phase factors of $\frac{\langle 2-|\not p_3|1-\rangle}{\langle 1-|\not p_3|2-\rangle}$, the $+-$ amplitude simplifies to

$$
\begin{aligned}
&\mathcal{M}^{+-J_3J_4}\\
&= \frac{1}{8s}\left[\frac{ut-s_3s_4}{4}B^6_{33} - \frac{k_0^2}{2}[E^1_{300}-E^2_{300}]\right] J_3\cdot J_4
\end{aligned}
$$

$$
\begin{aligned}
&+\frac{1}{8s}\left[\frac{ut-s_3s_4}{4}C_{3311}-\frac{k_0^2}{2}[E^1_{311}-E^2_{311}]+\frac{t-s_3}{2}(B^2_{31}+B^3_{31}+B^4_{31}+B^5_{31})\right]p_1\cdot J_3\;p_1\cdot J_4\\
&+\frac{1}{8s}\left[\frac{ut-s_3s_4}{4}C_{3312}-\frac{k_0^2}{2}[E^1_{312}-E^1_{312}]+\frac{t-s_3}{2}(B^3_{32}+B^4_{32})+\frac{u-s_3}{2}(B^3_{31}+B^5_{31})\right]p_1\cdot J_3\;p_2\cdot J_4\\
&+\frac{1}{8s}\left[\frac{ut-s_3s_4}{4}C_{3321}-\frac{k_0^2}{2}[E^1_{321}-E^2_{321}]+\frac{t-s_3}{2}(B^3_{32}+B^5_{32})+\frac{u-s_3}{2}(B^2_{31}+B^4_{31})\right]p_2\cdot J_3\;p_1\cdot J_4\\
&+\frac{1}{8s}\left[\frac{ut-s_3s_4}{4}C_{3322}-\frac{k_0^2}{2}[E^1_{322}-E^2_{322}]+\frac{tu-s_3}{2}(B^2_{32}+B^3_{32}+B^4_{32}+B^5_{32})\right]p_2\cdot J_3\;p_2\cdot J_4\\
&+\frac{1}{8s}\left[\frac{ut-s_3s_4}{32s}E^4_{331}\right]p_1\cdot J_3\;\epsilon^{p_1p_3p_2J_4}\\
&+\frac{1}{8s}\left[\frac{ut-s_3s_4}{32s}E^4_{332}\right]p_2\cdot J_3\;\epsilon^{p_1p_3p_2J_4}\\
&+\frac{1}{8s}\left[\frac{ut-s_3s_4}{32s}E^3_{332}\right]p_2\cdot J_4\;\epsilon^{p_1p_3p_2J_3}\\
&+\frac{1}{8s}\left[\frac{ut-s_3s_4}{32s}E^3_{331}\right]p_1\cdot J_4\;\epsilon^{p_1p_3p_2J_3}
\end{aligned}
\qquad (3.15)
$$

Here, the leptonic currents J_3 and J_4 appear in 9 different terms on the left hand side.

Auxiliary vector $\tilde{p}_3$

Although the numerators $(ut - s_3s_4)$ canceled some of the dangerous denominators, there are still some present in the amplitude. To further suppress their appearance, an auxiliary vector $\tilde{p}_3$ is introduced thereby providing more numerators $(ut - s_3s_4)$. It is defined by

$$
\begin{aligned}
p_3 &= \frac{t-s_3}{s}p_1+\frac{u-s_3}{s}p_2+\tilde{p}_3,\\
p_4 &= \frac{u-s_4}{s}p_1+\frac{t-s_4}{s}p_2-\tilde{p}_3.
\end{aligned}
$$

One can now make the following replacements in the helicity amplitudes, eqs. 3.14 and 3.15:

$$
\begin{aligned}
p_2\cdot J_3 &= -\frac{t-s_3}{u-s_3}p_1\cdot J_3-\frac{s}{u-s_3}\tilde{p}_3\cdot J_3\\
p_2\cdot J_4 &= -\frac{u-s_4}{t-s_4}p_1\cdot J_4+\frac{s}{t-s_4}\tilde{p}_3\cdot J_4\\
\tilde{p}_3\cdot J_3\;\epsilon(p_1,p_2,\tilde{p}_3,J_4) &= \tilde{p}_3\cdot J_4\;\epsilon(p_1,p_2,\tilde{p}_3,J_3)-\frac{ut-s_3s_4}{s}\;\epsilon(p_1,p_2,J_3,J_4).
\end{aligned}
$$

The tensor structures from eqs. 3.14 and 3.15 are now transformed to tensor structures in terms of $\tilde{p}_3$:

$$
\begin{aligned}
p_1\cdot J_3\;p_2\cdot J_4\;&\to -\frac{u-s_4}{t-s_4}p_1\cdot J_3\;p_1\cdot J_4\;+\frac{s}{t-s_4}p_1\cdot J_3\;\tilde{p}_3\cdot J_4\;,\\
p_2\cdot J_3\;p_1\cdot J_4\;&\to -\frac{t-s_3}{u-s_3}p_1\cdot J_3\;p_1\cdot J_4\;+\frac{s}{u-s_3}\tilde{p}_3\cdot J_3\;p_1\cdot J_4\;,
\end{aligned}
$$

$$
\begin{aligned}
p_2\cdot J_3\; p_2\cdot J_4 \;&\to \frac{(t-s_3)(u-s_4)}{(u-s_3)(t-s_4)} p_1\cdot J_3\; p_1\cdot J_4 \;-\frac{(t-s_3)s}{(u-s_3)(t-s_4)} p_1\cdot J_3\; \tilde{p}_3\cdot J_4 \\
&\quad \frac{s(u-s_4)}{(u-s_3)(t-s_4)} \tilde{p}_3\cdot J_4\; p_1\cdot J_4 \;-\frac{s2}{(u-s_3)(t-s_4)} \tilde{p}_3\cdot J_3\; \tilde{p}_3\cdot J_4\;, \\
p_1\cdot J_3\; p_3\cdot J_4 \;&\to (-1+\frac{u-s_4}{t-s_4}) p_1\cdot J_3\; p_1\cdot J_4 \;+\frac{s}{t-s_4} p_1\cdot J_3\; \tilde{p}_3\cdot J_4\;, \\
p_2\cdot J_3\; p_3\cdot J_4 \;&\to -\frac{t-s_3}{u-s_3}(-1+\frac{u-s_4}{t-s_4}) p_1\cdot J_3\; p_1\cdot J_4 \;+\frac{(t-s_3)s}{(u-s_3)(t-s_4)} p_1\cdot J_3\; \tilde{p}_3\cdot J_4\;, \\
p_1\cdot J_3\; \epsilon^{p_1p_3p_2J_4} &\to -p_1\cdot J_3\; \epsilon(p_1,p_2,\tilde{p}_3,J_4), \\
p_1\cdot J_4\; \epsilon^{p_1p_3p_2J_3} &\to -p_1\cdot J_4\; \epsilon(p_1,p_2,\tilde{p}_3,J_3), \\
p_2\cdot J_3\; \epsilon^{p_1p_3p_2J_4} &\to \frac{t-s_3}{u-s_3} p_1\cdot J_3\; \epsilon(p_1,p_2,\tilde{p}_3,J_4) + \frac{s}{u-s_3} \tilde{p}_3\cdot J_3\; \epsilon(p_1,p_2,\tilde{p}_3,J_4), \\
p_2\cdot J_4\; \epsilon^{p_1p_3p_2J_3} &\to \frac{t-s_3}{u-s_3} p_1\cdot J_4\; \epsilon(p_1,p_2,\tilde{p}_3,J_3) + \frac{s}{t-s_4} \tilde{p}_3\cdot J_4\; \epsilon(p_1,p_2,\tilde{p}_3,J_3).
\end{aligned}
$$

Note that the 9 bilinears in J_3 and J_4 on the left hand side are reduced to linear combinations of only 8 bilinears on the right hand side. Together with $J_3\cdot J_4$ 9 independent terms, all bilinear in J_3 and J_4, occur:

$$
\begin{aligned}
\tau_1 &= J_3\cdot J_4 \\
\tau_2 &= p_1\cdot J_3\; p_1\cdot J_4 \\
\tau_3 &= p_1\cdot J_3\; \tilde{p}_3\cdot J_4 \\
\tau_4 &= p_1\cdot J_3\; \epsilon(p_1,p_2,\tilde{p}_3,J_4) \\
\tau_5 &= \tilde{p}_3\cdot J_3\; p_1\cdot J_4 \\
\tau_6 &= \tilde{p}_3\cdot J_3\; \tilde{p}_3\cdot J_4 \\
\tau_7 &= \epsilon(p_1,p_2,J_3,J_4) \\
\tau_8 &= p_1\cdot J_4\; \epsilon(p_1,p_2,\tilde{p}_3,J_3) \\
\tau_9 &= \tilde{p}_3\cdot J_4\; \epsilon(p_1,p_2,\tilde{p}_3,J_3).
\end{aligned}
\tag{3.16}
$$

As they come from different contractions of the leptonic currents and external momenta with the scattering tensor these terms will be called tensor structures and the minimal set of tensor structures is the tensor basis.

Performing the same substitutions in the $++$ and the $+-$ amplitude yields an amplitude that is built out of these tensor structures τ_j:

$$
\mathcal{M} = \sum_j \mathcal{C}_j(s,t,u,s_3,s_4,m_b^2,m_t^2)\;\tau_j.
$$

The coefficients $\mathcal{C}_j(s,t,u,s_3,s_4,m_b^2,m_t^2)$ are polynomials of the quark masses and the Mandelstam variables.

3.2.2. Scalar integrals

The tensor structures which have been calculated in the previous section have arisen from the Lorentz structure of the amplitude. Contracting this tensor structure with the polarization vectors $\epsilon^{\mu_1}(p_1)$ and $\epsilon^{\mu_2}(p_2)$ and the leptonic currents $J_3^{\mu_3}$ and $J_4^{\mu_4}$, I derived helicity amplitudes and finally an irreducible set of 9 independent bilinears in J_3 and J_4, $\{\tau_j\}$. The coefficients $\mathcal{C}_j$ of this tensor structures are polynomials of the quark masses, m_b and m_t, and the Mandelstam variables, s, t, u, s_3 and s_4. I will now show how to decompose the amplitude of each diagram to a set of scalar integrals.

The scattering tensor for each diagram consists of loop integrals, for instance for the diagram $T2G1C1$ (cf. fig. 3.5)

$$\mathcal{M}^{\mu_1\mu_2\mu_3\mu_4} = \int \frac{d^4k}{(2\pi)^4} \frac{\mathrm{tr}\left[\gamma^{\mu_2}(\not{k}+\not{p}_1-\not{p}_3-\not{p}_4+m_u)\gamma^{\mu_4}(g_V-g_A\gamma_5)(\not{k}+\not{p}_1-\not{p}_3+m_u)\gamma^{\mu_3}(g_V-g_A\gamma_5)(\not{k}+\not{p}_1+m_u)\gamma^{\mu_1}(\not{k}+m_u)\right]}{((k+p_1-p_3-p_4)^2-m_u^2)((k+p_1-p_3)^2-m_u^2)((k+p_1)^2-m_u^2)(k^2-m_u^2)},$$

where couplings and constant factors are suppressed.

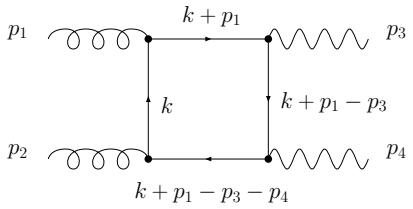

Figure 3.5.: The diagram $T2G1C1$ contributing to the process $gg \to Z^*Z^*$

Integrals of this form are logarithmically divergent since the powers of the loop momentum in the numerator and the denominator are equal. This leads to divergences when evaluating the integral. For instance, the scalar 2-point function

$$\int \frac{d^nk}{(k^2-A+i\epsilon)^2} = i\pi^{n/2}(-1)^N \frac{\Gamma(N-\frac{n}{2})}{\Gamma(N)} \frac{1}{(A-i\epsilon)^{N-n/2}}\bigg|_{N=2} \tag{3.17}$$

diverges for $n = 4$.

One thus applies dimensional regularization, i.e. generalizes the dimension of the integral from four dimensions to $n = 4 - 2\epsilon$ where n is not integer. To ensure that the natural dimension of the integral, M^0, is independent of n, the factor of μ^{4-n} has to be introduced where μ is a mass scale. When finally performing the limit $n \to 4$, the dependence on μ cancels and the divergences show up as poles in the gamma function (cf. eq. 3.17).

The dimenisonally regulated tensor integral from eq. 3.17 is then given by

$$\mathcal{M}^{\mu_1\mu_2\mu_3\mu_4} = \mu^{4-n}\int \frac{d^nk}{(2\pi)^n} \frac{1}{((k+p_1-p_3-p_4)^2-m_u^2)((k+p_1-p_3)^2-m_u^2)((k+p_1)^2-m_u^2)(k^2-m_u^2)} \mathrm{tr}\left[\gamma^{\mu_2}(\not{k}+\not{p}_1-\not{p}_3-\not{p}_4+m_u)\gamma^{\mu_4}(g_V-g_A\gamma_5)(\not{k}+\not{p}_1-\not{p}_3+m_u)\gamma^{\mu_3}(g_V-g_A\gamma_5)(\not{k}+\not{p}_1+m_u)\gamma^{\mu_1}(\not{k}+m_u)\right]$$

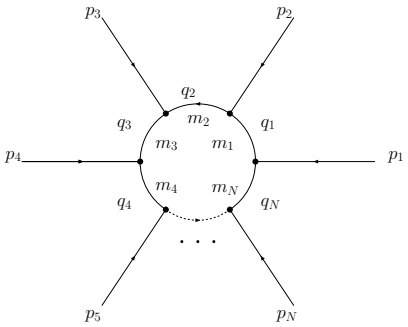

Figure 3.6.: N-point graph

.

which can be written as a linear combination of 4-, 3- and 2-point tensor integrals with the N-point tensor integral being defined in a standard form by

$$\begin{aligned} & I_{N,n}^{\mu_1\mu_2\mu_3\ldots\mu_r}(p_1,p_2,\ldots,p_N;m_1,m_2,\ldots,m_N) \\ &= \frac{(2\pi\mu)^{4-d}}{i\pi^2}\int d^nk \frac{k^{\mu_1}\ldots k^{\mu_r}}{(q_1^2-m_1^2+i\epsilon)(q_2^2-m_2^2+i\epsilon)\ldots(q_N^2-m_N^2+i\epsilon)}. \end{aligned}$$

The momenta of the propagators q_j are related to the external momenta p_j and the momentum running in the loop k (cf. fig. 3.6) by

$$q_j = k + r_j \text{ with } r_j = \sum_{i=1}^{N} p_i.$$

As I will show now, such tensor integrals can be reduced to a linear combination of tensor structures and scalar integrals, i.e. integrals of the form

$$\begin{aligned} & I_{N,n}(p_1,p_2,\ldots,p_N;m_1,m_2,\ldots,m_N) \\ &= \frac{(2\pi\mu)^{4-d}}{i\pi^2}\int d^nk \frac{1}{(q_1^2-m_1^2+i\epsilon)(q_2^2-m_2^2+i\epsilon)\ldots(q_N^2-m_N^2+i\epsilon)} \end{aligned}$$

There exist various techniques for reducing such tensor integrals to simpler ones, that is tensor integrals with less external legs and propagators. The first is from G. Passarino and M. J. G. Veltmann [34]. Their reduction scheme starts with the usual decomposition to a linear combination of tensor structures (like the Lorentz structure in eq. 3.12) and coefficients, the so-called form factors. Performing different contractions with external momenta and metric tensors then leads to a system of linear equations. The form factors can then be determined by solving the system of linear equations. Unfortunately, not only the number of terms rises by reduction, but there appear terms of $(tu-s_3s_4)^{-1}$ that

diverge for certain regions of phase space and thus deteriorate the numerical stability of the amplitude.

Here, a different approach [35, 36] is applied for tensor the reduction. In contrast to [34], there do not appear dangerous denominators in the tensor reduction due to the choice of basis integrals. Only when tracing the basis integrals back to even simpler integrals, this denominators arise. However, by grouping this denominators with linear combinations of scalar integrals vanishing for the same regions of phase space, divergences can be canceled to a certain amount. All in all, the number of such terms can be kept small. The results of this approach are cited in the following.

Definitions

I will start by setting the conventions for general N-point functions (cf. fig. 3.6). All momenta are supposed to be incoming. For conveniently governing the propagators in the integral, an ordered set of propagator labels is defined by

$$S = \{j_1, \ldots, j_N\}.$$

The momentum of the j-th propagator is $q_j = k + r_j$ where k is the momentum running in the loop and r_j is a combination of external momenta: $r_j = p_j + r_{j-1}$. Momentum conservation leads to $r_0 = r_N$ and one can choose $r_0 = r_N = 0$ such that $r_j = \sum_{i=1}^{j} p_i$.

The momentum representation of a scalar N-point function is

$$I_N^n(S) := \int \frac{d^n k}{i\pi^{n/2}} \frac{1}{\prod_{i=1}^{N}(q_i^2 - m_i^2 + i\delta)}. \tag{3.18}$$

By introducing the Feynman parameters z_i, performing the Wick rotation and executing the momentum integration, one finds the following representation in Feynman parameter space:

$$I_N^n(S) = (-1)^N \Gamma(N - \frac{n}{2}) \int \prod_{i=1}^{N} dz_i \delta(1 - \sum_{l=1}^{N} z_l)(R^2)^{\frac{n}{2}-N}$$

$$\text{with } R^2 = -\frac{1}{2} z \cdot \mathcal{S} \cdot z \; - i\delta = -\frac{1}{2} \sum_{i,j=1}^{N} z_i \mathcal{S}_{ij} z_j - i\delta,$$

where the matrix $\mathcal{S}$ contains all kinematic information on the process and is defined by

$$\mathcal{S}_{ij} = (r_i - r_j)^2 - m_i^2 - m_j^2.$$

In the reduction there will appear integrals in which one or more propagators labeled by $j_1, \ldots j_m$ are canceled. These integrals are called "pinch" integrals. The ordered set of propagator labels then reduces to

$$S \setminus \{j_1, \ldots j_m\}.$$

Such reductions can already be performed before the tensor and scalar reduction if numerators of the form $k \cdot r_i$ are present. Integrals with such numerators are called reducible, since the number of propagators and its rank can be reduced. For example, $2k \cdot r_1$ can be expressed as

$$\begin{aligned} 2k \cdot r_1 &= -k^2 + (k + r_1)^2 - r_1^2 + m_N^2 - m_1^2 - m_N^2 + m_1^2 \\ &= -(k^2 - m_N^2) + ((k + r_1)^2 - m_1^2) - (r_1^2 - m_1^2 + m_N^2), \end{aligned}$$

thus yielding a sum of three integrals. In the first one, the n-th propagator, $(k^2 - m_N^2)$, is canceled. In the second one, the first propagator, $((k - r_1)^2 - m_1^2)$, is canceled. In the last integral all propagators survive, but at least the rank is reduced by one. Thus, one rank r N-point function has been reduced to two rank $(r-1)$ $(N-1)$-point functions and one rank $(r-1)$ N-point function, each possessing a simpler structure than the original function. In these integrals loop momenta must be shifted to again match the standard form. After performing this procedure on all reducible integrals only irreducible integrals remain, thus simplifying the amplitude considerably.

The cancellation of a propagator has a graphic equivalence: A propagator which has been canceled in the integral is omitted in the diagram, too. Hence, two or more external momenta enter at the same vertex and are thus added. An example for a pinched N-point diagram is given in fig. 3.7.

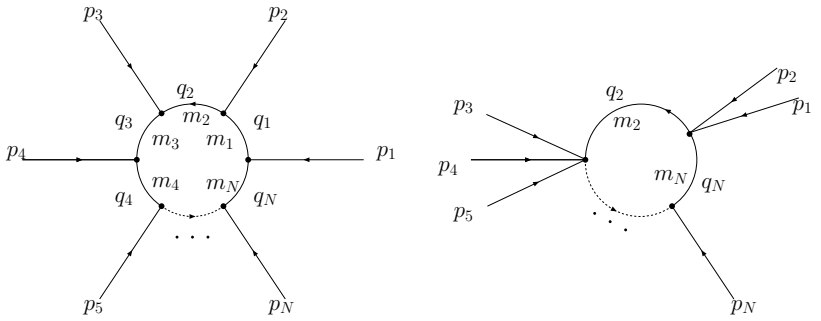

Figure 3.7.: Left: N-point diagram; right: pinched N-point diagram obtained by pinching the propagators 1, 3 and 4

The N-point rank r tensor integral is usually defined as

$$I_N^{n,\mu_1,\ldots,\mu_r}(S) := \int \frac{d^n k}{i\pi^{n/2}} \frac{k^{\mu_1} \ldots k^{\mu_r}}{\prod_{i=1}^{N} (q_i^2 - m_i^2 + i\delta)}. \tag{3.19}$$

The disadvantage of this notation is that after each reduction step with a cancellation of a propagator the loop momentum k has to be shifted to again achieve a standard representation of the tensor integrals for further reduction thereby leading to a proliferation of terms. This problem can be overcome by choosing a shift invariant representation of tensor integrals. Therefore, the N-point rank r tensor integral is defined alternatively by

$$I_N^{n,\mu_1,\ldots,\mu_r}(a_1,\ldots,a_r;S) := \int \frac{d^nk}{i\pi^{n/2}} \frac{q_{a_1}^{\mu_1}\ldots q_{a_r}^{\mu_r}}{\prod_{i=1}^N (q_i^2 - m_i^2 + i\delta)}. \tag{3.20}$$

The usual representation (eq. 3.19) can always be reproduced by setting all a_i to N. Furthermore, denominators constructed out of combinations q_i of external momenta and the loop momentum appear naturally in Feynman rules.

The starting point for the reduction algorithm is a decomposition of the tensor integral into Tensor structures and form factors. For a shift invariant definition of the tensor integrals, the tensor structures must of course be shift invariant, too. For this purpose they are defined in terms of metric tensors, $g^{\mu\nu}$ and shift invariant vectors

$$\Delta_{ij}^\mu := r_i^\mu - r_j^\mu = q_i^\mu - q_j^\mu. \tag{3.21}$$

For $N \leq 5$, one defines the form factors $A^{N,r}_{j_1\ldots j_r}(S)$, $B^{N,r}_{j_1\ldots j_r-2}(S)$ and $C^{N,r}_{j_1\ldots j_r-4}(S)$ by

$$\begin{aligned}
&I_N^{n,\mu_1,\ldots,\mu_r}(a_1,\ldots,a_r;S) \\
&= \sum_{j_1\ldots j_r\in S} \left[\dot{\Delta}_{j_1\cdot}\ldots\dot{\Delta}_{j_r\cdot}\right]^{\{\mu_1\ldots\mu_r\}}_{\{a_1\ldots a_r\}} A^{N,r}_{j_1\ldots j_r}(S) \\
&+ \sum_{j_1\ldots j_r-2\in S} \left[\ddot{g}\dot{\Delta}_{j_1\cdot}\ldots\dot{\Delta}_{j_r-2\cdot}\right]^{\{\mu_1\ldots\mu_r\}}_{\{a_1\ldots a_r\}} B^{N,r}_{j_1\ldots j_r-2}(S) \\
&+ \sum_{j_1\ldots j_r-4\in S} \left[\ddot{g}\ddot{g}\dot{\Delta}_{j_1\cdot}\ldots\dot{\Delta}_{j_r-4\cdot}\right]^{\{\mu_1\ldots\mu_r\}}_{\{a_1\ldots a_r\}} C^{N,r}_{j_1\ldots j_r-4}(S).
\end{aligned} \tag{3.22}$$

The brackets stand for the sum over all different combinations of r Lorentz indices distributed to the objects in the brackets. This is similar to the decomposition of the Lorentz structure performed in the last subsection.

This shift invariant representation can again be transformed to the standard notation in r_i:

$$\begin{aligned}
&I_N^{n,\mu_1,\ldots,\mu_r}(S) = I_N^{n,\mu_1,\ldots,\mu_r}(N,\ldots,N;S) \\
&= \sum_{j_1\ldots j_r\in S} \left[\dot{r}_{j_1}\ldots\dot{r}_{j_r}\right]^{\{\mu_1\ldots\mu_r\}} A^{N,r}_{j_1\ldots j_r}(S) \\
&+ \sum_{j_1\ldots j_r-2\in S} \left[\ddot{g}\dot{r}_{j_1}\ldots\dot{r}_{j_r-2}\right]^{\{\mu_1\ldots\mu_r\}} B^{N,r}_{j_1\ldots j_r-2}(S) \\
&+ \sum_{j_1\ldots j_r-4\in S} \left[\ddot{g}\ddot{g}\dot{r}_{j_1}\ldots\dot{r}_{j_r-4}\right]^{\{\mu_1\ldots\mu_r\}} C^{N,r}_{j_1\ldots j_r-4}(S).
\end{aligned} \tag{3.23}$$

For instance, the 4 point rank 4 tensor integral is decomposed as follows:

$$\begin{aligned}
& I_4^{n,\mu_1,\mu_2,\mu_3,\mu_4}(S) \\
= & \sum_{j_1,j_2,j_3,j_4} \left[r_{j_1}^{\mu_1} r_{j_2}^{\mu_2} r_{j_3}^{\mu_3} r_{j_4}^{\mu_4} \right] A_{j_1 j_2 j_3 j_4}^{44}(S) \\
& + \sum_{j_1,j_2} \Big[g^{\mu_1\mu_2} r_{j_1}^{\mu_3} r_{j_2}^{\mu_4} + g^{\mu_1\mu_3} r_{j_1}^{\mu_2} r_{j_2}^{\mu_4} + g^{\mu_1\mu_4} r_{j_1}^{\mu_2} r_{j_2}^{\mu_3} \\
& + g^{\mu_2\mu_3} r_{j_1}^{\mu_1} r_{j_2}^{\mu_4} + g^{\mu_2\mu_4} r_{j_1}^{\mu_1} r_{j_2}^{\mu_3} + g^{\mu_3\mu_4} r_{j_1}^{\mu_1} r_{j_2}^{\mu_2} \Big] B_{j_1 j_2}^{44}(S) \\
& + \left[g^{\mu_1\mu_2} g^{\mu_3\mu_4} + g^{\mu_1\mu_3} g^{\mu_2\mu_4} + g^{\mu_1\mu_4} g^{\mu_2\mu_4} \right] C^{44}(S)
\end{aligned}$$

with $j_i = 1, 2, 3$.

Finally, in the reduction of the tensor integrals, there will appear integrals in Feynman parameter space with Feynman parameters in the numerator. These are defined by:

$$I_N^n(l_1, \ldots, l_r) := (-1)^N \Gamma(N - \frac{n}{2}) \int \prod_{i=1}^{N} dz_i \delta(1 - \sum_{l=1}^{N} z_l) z_{l_1} \ldots z_{l_r} (R^2)^{n/2-N} \quad (3.24)$$

Scalar reduction

The scalar N-point integral

$$I_N^n(S) = \int \frac{d^n k}{i\pi^{n/2}} \frac{1}{\prod_{j=1}^{N} (q_j^2 - m_j^2 + i\delta)}$$

is decomposed into a IR finite part of higher dimension, $I_{fin}(S)$, and an algebraically simpler part, $I_{div}(S)$, carrying potential IR divergences:

$$\begin{aligned}
I_N^n(S) &= I_{div}(S) + I_{fin}(S) \\
&= \sum_{i \in S} b_i(S) \int \frac{d^n k}{i\pi^{n/2}} \frac{q_i^2 - m_i^2}{\prod_{j=1}^{N} (q_j^2 - m_j^2 + i\delta)} + \int \frac{d^n k}{i\pi^{n/2}} \frac{(1 - \sum_{i \in S} b_i(S))(q_i^2 - m_i^2)}{\prod_{j=1}^{N} (q_j^2 - m_j^2 + i\delta)}.
\end{aligned}$$

The coefficients b_i of this decomposition can be chosen conveniently. $I_{div}(S)$ is reducible and yields a sum of integrals with one propagator pinched:

$$I_{div}(S) = \sum_{i \in S} b_i(S) I_{N-1,l}^n(S \setminus \{i\}).$$

When introducing Feynman parameters z_i in $I_{fin}(S)$ and shifting the loop momentum $k = l - \sum_{i \in S} z_i r_i$ the numerator of $I_{fin}(S)$ becomes:

$$1 - \sum_{i \in S} b_i(S)(q_i^2 - m_i^2) = (-l^2 + R^2) \sum_{i \in S} b_i(S) + \sum_{j \in S} z_j \left[1 - \sum_{i \in S} \{ \mathcal{S}_{ij} + 2l \cdot \Delta_{ij} \} \right].$$

with R and $\mathcal{S}$ as defined above. The term linear in l vanishes due to symmetry and one chooses

$$1 - \sum_{i \in S} \mathcal{S}_{ij} = 0 \tag{3.25}$$

so that $I_{fin}(S)$ becomes

$$\begin{aligned} I_{fin}(S) &= -B(S)\Gamma(N) \int_0^1 \prod_{i \in S} dz_i \delta(1 - \sum_{l \in S} z_l) \int \frac{d^n l}{i\pi^{n/2}} \frac{l^2 + R^2}{(l^2 - R^2)^N} \\ &= -B(S)(N - n - 1) I_N^{n+2}(S) \end{aligned}$$

with $B(S)$ defined as

$$B(S) = \sum_{i \in S} b_i(S). \tag{3.26}$$

For non-exceptional four-dimensional kinematics (i.e. all external momenta are independent), eq. 3.25 is fulfilled with

$$b_i = \sum_{k \in S} \mathcal{S}^{-1}_{ki}$$

since $\mathcal{S}$ is invertible. For exceptional kinematics, $\mathcal{S}$ is not invertible but there exists a construction yielding the coefficients $b_i(S)$ fulfilling eq. 3.25.

Putting all pieces together, the scalar N-point integral becomes:

$$I_N^n(S) = -B(S)(N - n - 1) I_N^{n+2}(S) - \sum_{i \in S} b_i(S) I_{N-1}^n(S \setminus \{i\}). \tag{3.27}$$

This does not seem to be a simplification since now an $(n + 2)$-dimensional integral is present, but, however, the IR poles are isolated in the pinched functions. Furthermore, this relation can be used to reduce $(n + 2)$-dimensional functions which appear in the tensor reduction to lower dimensional functions.

As a simple example, the reduction of a scalar 3-point function reads

$$I_3^n(S) = -B(S)(2 - n) I_3^{n+2}(S) - \sum_{i \in S} b_i(S) I_2^n(S \setminus \{i\}). \tag{3.28}$$

Tensor reduction

The tensor integrals can be reduced by a generalization of the scalar reduction scheme: Adding and subtracting a linear combination of pinched integrals one obtains a similar decomposition

$$I_N^{n,\mu_1,\ldots,\mu_r}(a_1,\ldots,a_r;S) = \int \frac{d^nk}{i\pi^{n/2}} \frac{\left[q_{a_1}^{\mu_1} + \sum_{j\in S} \mathcal{C}_{ja_1}^{\mu_1}(q_j^2 - m_j^2)\right] q_{a_2}^{\mu_2} \ldots q_{a_r}^{\mu_r}}{\prod_{i\in S}(q_i^2 - m_i^2 + i\delta)} - \sum_{j\in S} \mathcal{C}_{ja_1}^{\mu_1} \int \frac{d^nk}{i\pi^{n/2}} \frac{(q_j^2 - m_j^2) q_{a_2}^{\mu_2} \ldots q_{a_r}^{\mu_r}}{\prod_{i\in S}(q_i^2 - m_i^2 + i\delta)},$$

where the coefficients $\mathcal{C}_{ja_1}^{\mu_1}$ can be adjusted conveniently. The potentially divergent term is again reducible and gives

$$-\sum_{j\in S} \mathcal{C}_{ja_1}^{\mu_1} I_{N-1}^{n,\mu_2,\ldots,\mu_r}(a_2,\ldots,a_r;S\setminus\{j\}). \tag{3.29}$$

The finite part can be simplified by a scheme generalized from the scalar reduction. Therefore, Feynman parameters are introduced and a shift of the loop momentum is performed to achieve a quadratic form in denominator. The momenta then become

$$q_a = l + \sum_{i\in S} z_i \Delta_{ai}. \tag{3.30}$$

Demanding the coefficients $\mathcal{C}_{ja}^{\mu_1}$ to fulfill

$$\sum_{j\in S} \mathcal{S}_{ij} \mathcal{C}_{ja}^{\mu_1} = \Delta_{ia}^{\mu}, \quad a \in S,$$

the term $A_{a1}^{\mu_1}$ in the brackets reads:

$$A_{a1}^{\mu_1} = \left[q_{a_1}^{\mu_1} + \sum_{j\in S} \mathcal{C}_{ja_1}^{\mu_1}(q_j^2 - m_j^2) \right] = l_\nu \left(\mathcal{T}_{a_1a_2}^{\mu\nu} + 2\mathcal{V}_{a_1}^{\mu} \sum_{i\in S} z_i \Delta_{a_2i}^{\nu} \right) + (l^2 + R^2)\mathcal{V}_{a_1}^{\mu},$$

where

$$\mathcal{V}_a^{\mu} = \sum_{j\in S} \mathcal{C}_{ja}^{\mu} \quad \text{and} \quad \mathcal{T}_{a_1a_2}^{\mu\nu} = g^{\mu\nu} + 2\sum_{j\in S} \mathcal{C}_{ja_1}^{\mu} \Delta_{ja_2}^{\nu}.$$

The integrand in the finite part is thus either proportional to l or to $l^2 + R^2$ and yields higher dimensional integrals with Feynman parameters in the numerator for $r > 1$ when integrated over the loop momentum.

Applying this reduction scheme iteratively, all n-dimensional tensor integrals of rank r can be reduced to integrals of rank 0, scalar integrals, partly of higher dimensions and with Feynman parameters in the numerators. The tensor structure thereby gets

decomposed as in eq. 3.23. Comparing the coefficients of this tensor structures the form factors will be expressed in terms of scalar integrals.

I will again give a very simple example by decomposing a rank 1 3-point function to its Lorentz structure and form factors. The splitting into IR finite and divergent parts is

$$I_3^{n,\mu_1}(a_1;S) = \int \frac{d^n k}{i\pi^{n/2}} \frac{\left[q_{a_1}^{\mu_1} + \sum_{j\in S} \mathcal{C}_{ja_1}^{\mu_1}(q_j^2 - m_j^2)\right]}{\prod_{i\in S}(q_i^2 - m_i^2 + i\delta)} - \sum_{j\in S} \mathcal{C}_{ja_1}^{\mu_1} \int \frac{d^n k}{i\pi^{n/2}} \frac{(q_j^2 - m_j^2)}{\prod_{i\in S}(q_i^2 - m_i^2 + i\delta)}.$$

With

$$C_{ja_1}^{\mu_1} = \sum_i \mathcal{S}_{ij}^{-1} \Delta_{ia_1}^{\mu_1} \tag{3.31}$$

the divergent part becomes

$$I_{div} = \sum_{l\in S} \sum_{j\in S} \mathcal{S}_{lj}^{-1} I_2^n(s \setminus \{j\}) \Delta_{ja_1}^{\mu_1}. \tag{3.32}$$

The finite part is also quite simple since the terms linear in l (cf. eq. 3.31) cancel due to symmetry when integrated over l. I_{fin} is then given by

$$\Gamma(N) \int_0^1 \prod_{i\in S} dz_i \delta(1 - \sum_{l\in S} z_l) \int \frac{d^n l}{i\pi^{n/2}} \frac{l^2 + R^2}{(l^2 - R^2)^N} \mathcal{V}_{a_1}^{\mu_1}\Big|_{N=3}, \tag{3.33}$$

where

$$\mathcal{V}_{a_1}^{\mu} = \sum_{j\in S} \mathcal{C}_{ja_1}^{\mu} = \sum_{k\in S} b_k \Delta_{ka_1}^{\mu}, \tag{3.34}$$

and hence

$$\sum_{k\in S} b_k \Delta_{ka_1}^{\mu_1} \underbrace{\Gamma(N) \int_0^1 \prod_{i\in S} dz_i \delta(1 - \sum_{l\in S} z_l) \int \frac{d^n l}{i\pi^{n/2}} \frac{l^2 + R^2}{(l^2 - R^2)^N} \mathcal{V}_{a_1}^{\mu_1}\Big|_{N=3}}_{(2-n) I_3^{n+2}(S)}. \tag{3.35}$$

The function $I_3^{n+2}(S)$ can be expressed by lower dimensional integrals, exploiting eq. 3.28:

$$I_3^{n+2}(S) = -\frac{1}{B(S)(2-n)} \left(I_3^n(S) + \sum_{i\in S} b_i(S) I_2^n(S \setminus \{i\}) \right). \tag{3.36}$$

One then finds

$$I_{fin} = \sum_{k\in S} \frac{b_k}{B(S)} \left(\sum_{i\in S} b_i(S) I_2^n(S\setminus\{i\}) - I_3^n(S) \right) \Delta^{\mu_1}_{ka_1}. \tag{3.37}$$

Putting together the finite and the divergent part yields

$$\begin{aligned} & I_3^{n\mu_1}(a_1;S) \\ &= \sum_{l\in S} \Delta^{\mu_1}_{la_1} A_l^{31}(S) \\ &= \sum_{l\in S} \Delta^{\mu_1}_{la_1} \left\{ \frac{b_k}{B(S)} \left(\sum_{i\in S} b_i(S) I_2^n(S\setminus\{i\}) - I_3^n(S) \right) - \sum_{j\in S} \mathcal{S}^{-1}_{lj} I_2^n(s\setminus\{j\}) \right\}. \end{aligned}$$

The form factors $A_l^{31}(S)$ can then be read off as

$$A_l^{31}(S) = \frac{b_k}{B(S)} \left(\sum_{i\in S} b_i(S) I_2^n(S\setminus\{i\}) - I_3^n(S) \right) - \sum_{j\in S} \mathcal{S}^{-1}_{lj} I_2^n(s\setminus\{j\}). \tag{3.38}$$

As mentioned above the standard representation of tensor integrals (eq. 3.19) can be obtained from the alternative representation (eq. 3.20) by setting all a_i to N:

$$\begin{aligned} & I_3^{n\mu_1}(S) \\ &= I_3^{n\mu_1}(N;S) \\ &= \sum_{l\in S} r_l^{\mu_1} A_l^{31}(S) \\ &= \sum_{l\in S} r_l^{\mu_1} \left\{ \frac{b_k}{B(S)} \left(\sum_{i\in S} b_i(S) I_2^n(S\setminus\{i\}) - I_3^n(S) \right) - \sum_{j\in S} \mathcal{S}^{-1}_{lj} I_2^n(s\setminus\{j\}) \right\}. \end{aligned}$$

In my program I used an existing implementation of the form factors.

Numerical stability

Higher dimensional scalar integrals with or without non-trivial numerators, i.e. with Feynman parameters in the numerators, can be traced back to scalar integrals with trivial numerators, cf. eq. 3.36, for instance. The problem now arises since B from eq. 3.26 is related to the determinant of another kinematic matrix G, the Gram matrix, by the relation

$$B\det\mathcal{S} = (-1)^{N+1}\det G \tag{3.39}$$

which I just cite here and where $G = G^{(N)}$ with

$$G^{(a)}_{ij} := 2\Delta_{ia}\Delta_{ja}. \tag{3.40}$$

Here, a be is one of the propagator labels which is chosen for reference.

In the case of a kinematic 4-point configuration as presented in fig. 3.5 the r_i are

$$r_1 = p_1, \quad r_2 = p_1 - p_3, \quad r_3 = p_1 - p_3 - p_4 = -p_2, \quad r_4 = r_0 = 0.$$

Defining the Mandelstam variables and virtualities of the Z bosons

$$\begin{array}{lll} s = (p_1 + p_2)^2, & t = (p_2 - p_3)^2, & u = (p_1 - p_3)^2 \\ s_3 = p_3^2, & s_4 = p_4^2 & \end{array}, \tag{3.41}$$

the Gram matrix G is given by

$$G = \begin{pmatrix} 0 & u - s_3 & -s \\ u - s_3 & 2u & u - s_4 \\ -s & u - s_4 & 0 \end{pmatrix} \tag{3.42}$$

and its determinant $\det G$ by

$$\begin{aligned} \det G &= -2s(u - s_3)(u - s_4) - 2us^2 \\ &= -2s\left(u^2 - us_4 - s_3u + s_3s_4 + 2us\right) \\ &= 2s(ut - s_3s_4). \end{aligned}$$

The expression in parenthesis, $(ut - s_3s_4)$, can now be related to the transverse momentum of one of the Z bosons: If p_1 and p_2 are parallel to the z axis,

$$p_{1,2} \cdot p_3 \ = E_{1,2}E_3 - p_{z1,2}p_{z3} = E_{1,2}E_3 - E_{1,2}p_{z3} = E_{1,2}(E_3 - p_{z3}),$$

and with

$$p_1 \cdot p_3 \ = \frac{u - s_3}{2}; \quad p_2 \cdot p_3 \ = \frac{t - s_3}{2}; \quad E_1 = E_2 = \frac{\sqrt{s}}{2}$$

one can rewrite this expression as

$$\begin{aligned} &\frac{(u - s_3)(t - s_3)}{s} = E_3^2 - p_{z3}^2 = p_3^2 + \vec{p}_{T3}^{\,2}, \\ &\Rightarrow \vec{p}_{T3}^{\,2} = \frac{1}{s}\left(tu - us_3 - ts_3 + s_3^2 - ss_3\right) = \frac{1}{s}\left(ut - s_3s_4\right). \end{aligned}$$

Hence, if the transverse momentum $\vec{p}_{T3}$ reaches zero, the Gram determinant $\det G$ becomes very small and by eq. 3.39, $B(S)$ becomes very large.

Since the amplitude is finite the divergences introduced by $B^{-1} \sim \det{}^{-1} G$ in eq. 3.38, for instance, must be compensated by suitable vanishing factors. The occurring huge cancellations can cause instabilities in numerical evaluation with finite precision.

Inverse Gram determinants can be prevented if one does not further reduce the basis integrals after tensor reduction. Then, no dangerous denominators are present but the basis integrals are either of higher dimension or have Feynman parameters in the numerators and must therefore be evaluated in a special way.

A different method was applied in the implementation of the form factors which I used: The higher dimensional integrals both with trivial and non-trivial numerators were reduced to simple scalar integrals but the expressions were grouped in such a way that cancellations of inverse Gram determinants were possible.

The irreducible set of scalar integrals

Every tensor integral appearing in the initial expression of the amplitude for one single graph (like eq. 3.18) can be expressed by a linear combination of tensor structures and form factors. The form factors can again be expressed by a linear combination of scalar integrals. This decomposition of the form factors can be calculated using the reduction technique presented in the previous subsections. Instead of calculating them myself, I used an existing implementation.

I will now show which is the irreducible set of scalar functions for a single graph. As already stated, the Feynman amplitude for a single graph is a linear combination of n-dimensional 4-, 3-, and 2-point tensor integrals (the tadpole integral vanishes):

$$I_4^{n,\mu,\nu,\rho,\sigma}, \quad I_3^{n,\mu,\nu,\rho}, \quad I_2^{n,\mu,\nu}. \tag{3.43}$$

By tensor reduction, these can be reduced to linear combinations of $(n+4)$- and $(n+2)$-dimensional scalar 4-point integrals, $(n+2)$- and n-dimensional scalar 3-point integrals and n-dimensional 2-point scalar integrals:

$$I_4^{n+4}, \quad I_4^{n+2}, \quad I_3^{n+2}, \quad I_3^n, \quad I_2^n. \tag{3.44}$$

Finally, the $(n+4)$-dimensional box can be expressed in terms of $(n+2)$ dimensional boxes and triangles and the $(n+2)$ dimensional triangles can be expressed in terms of n-dimensional triangles and bubbles. The irreducible set of scalar integrals remaining after the reductions is then

$$I_4^{n+2}, \quad I_3^n, \quad I_2^n. \tag{3.45}$$

For a single graph, $T2G1C1$, I will now exemplarily show the scalar functions. Instead of giving the momenta of the propagators $q_1, q_2 \ldots$ as arguments, I will employ a different notation using all independent scalar products of the external momenta. For a 4-point integral, one needs 6 scalar products which can be chosen, for instance,

$$(p_1+p_2)^2 = s, \quad (p_1+p_3)^2 = u, \quad p_1^2, \quad p_2^2, \quad p_3^2, \quad p_4^2.$$

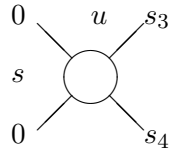

$$\texttt{BOXd6}(\texttt{u}, \texttt{s}, \texttt{0}, \texttt{s}_4, \texttt{s}_3, \texttt{0}, \texttt{m}_\texttt{t}^2, \texttt{m}_\texttt{t}^2, \texttt{m}_\texttt{t}^2, \texttt{m}_\texttt{t}^2).$$

Diagrams and scalar integrals with less external momenta and propagators are obtained either by decomposing reducible tensor integrals or by applying tensor and scalar reduction. In both cases the arguments can be obtained by the so-called pinching technique: Starting with the 4-point function (3.5), one reduces the rank of the function by pinching the propagators in all combinations. By pinching one propagator, one obtains the 3-point integrals:

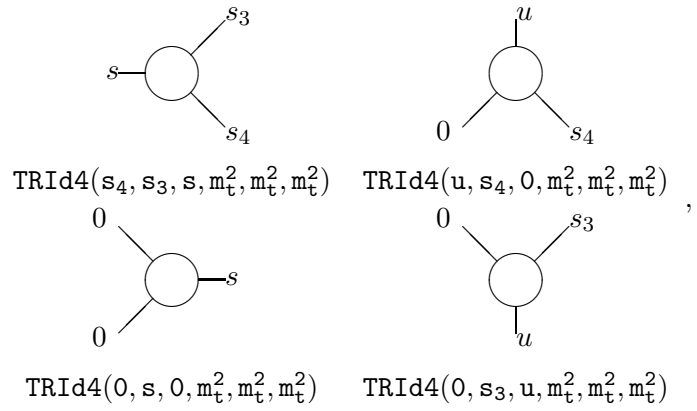

$\texttt{TRId4}(\texttt{s}_4, \texttt{s}_3, \texttt{s}, \texttt{m}_\texttt{t}^2, \texttt{m}_\texttt{t}^2, \texttt{m}_\texttt{t}^2)$ $\texttt{TRId4}(\texttt{u}, \texttt{s}_4, 0, \texttt{m}_\texttt{t}^2, \texttt{m}_\texttt{t}^2, \texttt{m}_\texttt{t}^2)$,

$\texttt{TRId4}(0, \texttt{s}, 0, \texttt{m}_\texttt{t}^2, \texttt{m}_\texttt{t}^2, \texttt{m}_\texttt{t}^2)$ $\texttt{TRId4}(0, \texttt{s}_3, \texttt{u}, \texttt{m}_\texttt{t}^2, \texttt{m}_\texttt{t}^2, \texttt{m}_\texttt{t}^2)$

and by pinching two propagators, the 2-point integrals:

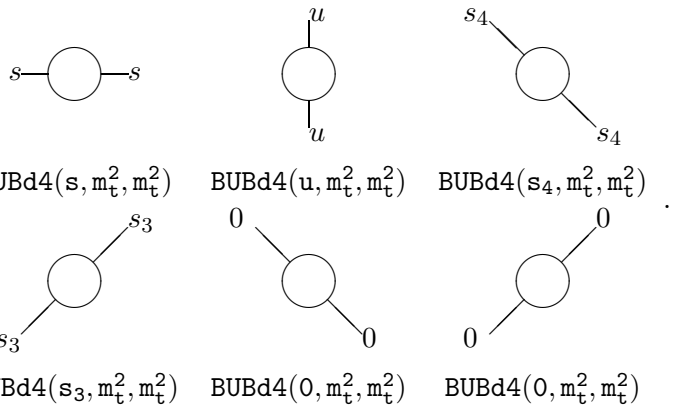

$\texttt{BUBd4}(\texttt{s}, \texttt{m}_\texttt{t}^2, \texttt{m}_\texttt{t}^2)$ $\texttt{BUBd4}(\texttt{u}, \texttt{m}_\texttt{t}^2, \texttt{m}_\texttt{t}^2)$ $\texttt{BUBd4}(\texttt{s}_4, \texttt{m}_\texttt{t}^2, \texttt{m}_\texttt{t}^2)$.

$\texttt{BUBd4}(\texttt{s}_3, \texttt{m}_\texttt{t}^2, \texttt{m}_\texttt{t}^2)$ $\texttt{BUBd4}(0, \texttt{m}_\texttt{t}^2, \texttt{m}_\texttt{t}^2)$ $\texttt{BUBd4}(0, \texttt{m}_\texttt{t}^2, \texttt{m}_\texttt{t}^2)$

For the graph $T2G1C1$ one thus finds an irreducible set of 10 scalar integrals:

$\texttt{BOXd6}(\texttt{u}, \texttt{s}, 0, \texttt{s}_4, \texttt{s}_3, 0, \texttt{m}_\texttt{t}^2, \texttt{m}_\texttt{t}^2, \texttt{m}_\texttt{t}^2, \texttt{m}_\texttt{t}^2)$
$\texttt{TRId4}(\texttt{s}_4, \texttt{s}_3, \texttt{s}, \texttt{m}_\texttt{t}^2, \texttt{m}_\texttt{t}^2, \texttt{m}_\texttt{t}^2)$
$\texttt{TRId4}(\texttt{u}, \texttt{s}_3, 0, \texttt{m}_\texttt{t}^2, \texttt{m}_\texttt{t}^2, \texttt{m}_\texttt{t}^2)$
$\texttt{TRId4}(0, \texttt{s}, 0, \texttt{m}_\texttt{t}^2, \texttt{m}_\texttt{t}^2, \texttt{m}_\texttt{t}^2)$
$\texttt{TRId4}(0, \texttt{s}_4, \texttt{u}, \texttt{m}_\texttt{t}^2, \texttt{m}_\texttt{t}^2, \texttt{m}_\texttt{t}^2)$
$\texttt{BUBd4}(\texttt{s}, \texttt{m}_\texttt{t}^2, \texttt{m}_\texttt{t}^2)$
$\texttt{BUBd4}(\texttt{u}, \texttt{m}_\texttt{t}^2, \texttt{m}_\texttt{t}^2)$
$\texttt{BUBd4}(\texttt{s}_3, \texttt{m}_\texttt{t}^2, \texttt{m}_\texttt{t}^2)$
$\texttt{BUBd4}(\texttt{s}_4, \texttt{m}_\texttt{t}^2, \texttt{m}_\texttt{t}^2)$
$\texttt{BUBd4}(0, \texttt{m}_\texttt{t}^2, \texttt{m}_\texttt{t}^2)$

.

For other diagrams there appear other sets of arguments of which some can be related to each other. For example

$$\texttt{TRId4}(\texttt{es3}, \texttt{eu}, 0, \texttt{emt2}, \texttt{emt2}, \texttt{emt2}) = \texttt{TRId4}(\texttt{eu}, \texttt{es3}, 0, \texttt{emt2}, \texttt{emt2}, \texttt{emt2})$$

since all masses in each quark loop are equal. Hence, the propagator momenta and thus the scalar products of external momenta can be exchanged. Exploiting identities like this, the set of scalar integrals form all diagrams with massive quarks consists of 30 functions. In the massless case, these can still be reduced to a set of 14 functions. These sets are also listed in appendix A.3.

3.2.3. Summary

I have shown how to decompose the amplitude of each graph l to a linear combination of tensor structures $\tilde{\tau}_j$ and basis functions I_k and have given irreducible sets of both. The sum over all diagrams then reads

$$\mathcal{M}^{\lambda_1\lambda_2 J_3 J_4} = \sum_l \sum_k \sum_{j=1}^{9} \tilde{\mathcal{C}}_{j,k,l}(s,t,u,s_3,s_4,m_b^2,m_t^2)\ \tilde{\tau}_j\ I_k. \tag{3.46}$$

3.3. Implementation

In the preceding chapter I have presented a decomposition of the amplitude into terms carrying the tensor structure, scalar integrals and functions of Lorentz scalars. Furthermore, I have shown how to suppress the occurrence of dangerous Gram determinants that may lead to numerous instabilities. In this chapter, I will explain how to analytically compute the amplitude and then numerically determine the total cross section for the process and distributions. The calculation is greatly automated, i.e. the code is in large part generated dynamically, starting with the diagrams and yielding in the end numerical results for total cross sections and distributions.

In the different stages of the calculation, I used four different programming languages to adapt the environment in the best possible way to the needs of the analytic manipulation. I applied FORM [37] to manipulate the amplitude, because FORM already disposes of the necessary structure (γ matrices, traces etc.), decomposing the amplitude to the coefficients `C[i,j]` introduced in 3.2.2. The coefficients for different diagrams are added and simplified in Maple. The calculation of the amplitude $\mathcal{M}$ is then done in Fortran for which files have been generated automatically in the Maple code. Finally, the computation of cross sections (including the whole phase space parametrization) is performed in C++ code, which allows the use of object-oriented structures, for example for conveniently implementing selection cuts.

3.3.1. Manipulating the Feynman amplitude of individual diagrams

Generation of the diagrams

I used the Mathematica package FeynArts/FormCalc [38] for generating the Feynman amplitude for all 12 double-resonant box diagrams (cf. fig. 3.3). Instead of directly piping its output to FORM, I saved it into the file `Graphs.h` which served as input file for customized manipulations.

Generation of the FORM code

For each diagram, the Maple program `BuildFormCode.map` generates a FORM file. The input consists of the Feynman amplitude for each diagram (`Graphs.h`) and a list of the tensor structures and basis functions as worked out in the previous subsection (cf. chapter 3.2) in the file `INPUT_LISTS.map`. It sequentially generates FORM files named `Graph_`*topology*`_`*helicity*`.frm` which are executed consecutively.

From now on, each diagram and its amplitude are treated separately. The subroutines which are applied to them will be explained below.

subroutine `Diracology`

The dimensional regularization prevents the amplitude from being divergent but leads to the so called γ_5 problem: All γ matrices can be generalized to n dimensions, except for the γ_5 matrix. Therefore, standard dimensional splitting rules are applied, following

[39]: All objects are replaced by their n-dimensional continuations, only the external momenta and the γ_5 matrix are kept 4-dimensional. The n-dimensional objects are then split into a 4-dimensional component, denoted by a hat, and a $(n-4)$-dimensional component, denoted by a tilde:

$$k = \hat{k} + \tilde{k}, \tag{3.47}$$

$$\gamma^\mu = \hat{\gamma}^\mu + \tilde{\gamma}^\mu. \tag{3.48}$$

The 4 dimensional γ algebra remains unchanged, i.e.

$$\{\hat{\gamma}^\mu, \gamma_5\} = 0, \tag{3.49}$$

$$\{\hat{\gamma}^\mu, \hat{\gamma}^\nu\} = 2\hat{g}^{\mu\nu} \tag{3.50}$$

and as the external momenta p_i are kept 4-dimensional, the scalar products with n dimensional quantities reduce to scalar products with the 4 dimensional components:

$$p_i^\mu \gamma_\mu = p_i^\mu \hat{\gamma}_\mu, \quad p_i^\mu k_\mu = p_i^\mu \hat{k}_\mu. \tag{3.51}$$

In n dimensions, the anticommutator is demanded to be formally the same as in 4 dimensions, namely the metric tensor:

$$\begin{aligned} 2(\hat{g}^{\mu\nu} + \tilde{g}^{\mu\nu}) = 2g^{\mu\nu} =: \{\gamma^\mu, \gamma^\nu\} \\ \Leftrightarrow \{\hat{\gamma}^\mu, \hat{\gamma}^\nu\} + \{\tilde{\gamma}^\mu, \tilde{\gamma}^\nu\} = \{\hat{\gamma}^\mu, \hat{\gamma}^\nu\} + \{\hat{\gamma}^\mu, \tilde{\gamma}^\nu\} + \{\tilde{\gamma}^\mu, \hat{\gamma}^\nu\} + \{\tilde{\gamma}^\mu, \tilde{\gamma}^\nu\} \\ \Rightarrow \{\hat{\gamma}^\mu, \tilde{\gamma}^\nu\} = 0. \end{aligned} \tag{3.52}$$

Introducing this decomposition to the code, all traces with an odd number of $\tilde{\not{k}}$ vanish similar to traces of an odd number of γ matrices vanishing in 4 dimensions. In the traces with an even number of $\tilde{\not{k}}$, the gamma matrices are commuted until two $\tilde{\not{k}}$ stand side by side and are pulled out of the trace as $\tilde{k}^2$. Now, there are no more $(n-4)$-dimensional objects in the trace and the usual Clifford algebra can be applied.

subroutines `ProjectOnPP/ProjectOnPM`

After having removed the particularities of n-dimensional γ matrix algebra, $\mathcal{M}^{\mu_1\mu_2\mu_3\mu_4}$ is contracted with the polarization vectors $\epsilon^{\lambda_1}_{1\mu_1}$ and $\epsilon^{\lambda_2}_{2\mu_2}$, thus yielding the helicity amplitudes $\mathcal{M}^{\lambda_1\lambda_2\mu_3\mu_4}$ (cf. sec. 3.2.1). Since only two of the four helicity amplitudes are independent, it suffices to calculate $\mathcal{M}^{++\mu_3\mu_4}$ and $\mathcal{M}^{+-\mu_3\mu_4}$.

Note, that the expressions for the polarization vectors in terms of external momenta can be obtained via the spinor helicity formalism (cf. A.1). The expressions are (eqs. A.32, A.34):

$$\epsilon^{+\mu}(p_1)\epsilon^{+\nu}(p_2) = -\frac{1}{s}\frac{[12]}{\langle 12\rangle}\left(p_1^\mu p_2^\nu + p_1^\nu p_2^\mu - p_1 \cdot p_2 g^{\mu\nu} - \epsilon^{p_1\nu p_2\mu}\right) \tag{3.53}$$

$$\epsilon^{+\mu}(p_1)\epsilon^{-\nu}(p_2) = \frac{\mathrm{tr}^-\left(p_1, p_3, p_2, \mu\right)\mathrm{tr}^-\left(p_1, p_3, p_2, \nu\right)}{2s(ut - s_3 s_4)}\frac{\langle 2 - |\not{p}_3|1-\rangle}{\langle 1 - |\not{p}_3|2-\rangle}. \tag{3.54}$$

Both $\frac{[12]}{\langle 12\rangle}$ and $\frac{\langle 2-|\not{p}_3|1-\rangle}{\langle 1-|\not{p}_3|2-\rangle}$ are global phase factors and can therefore be suppressed.[1]

subroutine `PtoR`

The propagator momenta of the N-point functions are currently still of the form

$$k + q_j = k + \sum_{i=1}^{j} p_i, \tag{3.55}$$

where p_i denotes the i-th external momentum. In contrast, for the formulae for decomposing the tensor integrals into tensor structures and form factors to be applicable the propagator momenta have to be of the form

$$k + r_j \tag{3.56}$$

(cf. 3.19). Thus, the replacements

$$\sum_{i=1}^{j} p_i \to r_j \tag{3.57}$$

are performed which will be revoked after the reductions.

subroutines `CancelPropInBox/CancelPropInTri`

The amplitude contains so far some reducible integrals which should be reduced thus increasing the number but considerably simplifying the complexity of the integrals. Such reductions have been explained in sec. 3.2.2.

subroutine `PROtoTI`

So far, the amplitude does not contain tensor integrals in the proper representation (cf. eq. 3.19), but a lot of tensor integrals contracted with external momenta, i.e. scalar integrals with numerators of the form $k \cdot r_j$ or contractions like $\epsilon^{k\cdots}$. These expression are rewritten to achieve the proper representation.

Furthermore, there are still remnants of the n-dimensional algebra, namely scalar integrals containing factors of $\tilde{k} \cdot \tilde{k}$. These integrals are not of the standard form for scalar reduction, but can be expressed by standard integrals:

$$\int \frac{d^n k}{i\pi^{n/2}} \frac{(\tilde{k} \cdot \tilde{k})^\alpha}{(k^2 - M^2)^N} = (-1)^\alpha \frac{\Gamma(\alpha - \epsilon)}{\Gamma(1-\epsilon)} \frac{n-4}{2} I_N^{n+2\alpha}, \tag{3.58}$$

$$\int \frac{d^n k}{i\pi^{n/2}} \frac{(\tilde{k} \cdot \tilde{k})^\alpha k^\mu k^\nu}{(k^2 - M^2)^N} = (-1)^{\alpha+1} \frac{\Gamma(\alpha - \epsilon)}{\Gamma(1-\epsilon)} g_{\mu\nu} \frac{n-4}{4} \frac{n+2\alpha}{n} I_N^{n+2+2\alpha}. \tag{3.59}$$

The amplitude now consists of a linear combination of scalar and tensor integrals in a standard form, and is prepared for reduction formulae.

[1] This, however, can lead to disagreement when comparing complex amplitudes.

subroutine `TItoFF`

The tensor reduction algorithm, presented in sec. 3.2.2, can be applied by decomposing the tensor integrals into tensor structures and form factors. The form factors are then retained symbolically to allow for simplifications before expressing the as linear combinations of scalar integrals. For example, the 4 point rank 4 tensor integral is decomposed as follows:

$$\begin{aligned}
& I_4^{n,\mu_1,\mu_2,\mu_3,\mu_4}(S) \\
= & \sum_{j_1,j_2,j_3,j_4} \left[r_{j_1}^{\mu_1} r_{j_2}^{\mu_2} r_{j_3}^{\mu_3} r_{j_4}^{\mu_4} \right] A_{j_1 j_2 j_3 j_4}^{44}(S) \\
& + \sum_{j_1,j_2} \Big[g^{\mu_1\mu_2} r_{j_1}^{\mu_3} r_{j_2}^{\mu_4} + g^{\mu_1\mu_3} r_{j_1}^{\mu_2} r_{j_2}^{\mu_4} + g^{\mu_1\mu_4} r_{j_1}^{\mu_2} r_{j_2}^{\mu_3} \\
& + g^{\mu_2\mu_3} r_{j_1}^{\mu_1} r_{j_2}^{\mu_4} + g^{\mu_2\mu_4} r_{j_1}^{\mu_1} r_{j_2}^{\mu_3} + g^{\mu_3\mu_4} r_{j_1}^{\mu_1} r_{j_2}^{\mu_2} \Big] B_{j_1 j_2}^{44}(S) \\
& + \left[g^{\mu_1\mu_2} g^{\mu_3\mu_4} + g^{\mu_1\mu_3} g^{\mu_2\mu_4} + g^{\mu_1\mu_4} g^{\mu_2\mu_4} \right] C^{44}(S)
\end{aligned} \tag{3.60}$$

with $j_1, j_2, j_3 \in 1, 2, 3$.

The amplitude is now a linear combination of Lorentz structures, form factors and scalar integrals.

subroutine `RtoP`

Since the tensor reduction for which the propagators had to be of the form $k + r_j$ has taken place, the r_j can be resubstituted in terms of external momenta p_i:

$$r_j = \sum_{i=1}^{j} p_i. \tag{3.61}$$

subroutine `SchoutenIds`

The tensor structure will now be expressed in the tensor basis derived in chapter 3.2. First of all, the ϵ tensors with different contractions must be reduced to those present in the tensor basis, eq. 3.16. To keep these substitutions simple one would like to cancel as many contractions as possible.

Therefore, Schouten Identities are exploited: Every totally antisymmetric tensor can be expressed as an antisymmetrized product of basis vectors. The ϵ tensor, a totally antisymmetric tensor of rank 4, can thus be expressed by an antisymmetrized product of four vectors.

Choosing one of these vectors to be the vector k_0^μ, as defined in eq. 3.6, and the other three to be the dual vectors k_1^ν, k_2^ρ and k_3^σ of the vectors p_1, p_2 and p_3, respectively, as defined in eq. 3.7 and antisymmetrizing the product one obtains a representation of the tensor $\epsilon^{\mu\nu\rho\sigma}$. The advantage of this representation is that its contractions with external

momenta lead to many products $k_i \cdot p_j$ with $i \neq j$ thus partly remedying the proliferation of terms due to the antisymmetrization in the implementation of the ϵ tensor.

subroutine `EpsTenBase`

Here, the representation of the ϵ tensor in the basis given in the last step is completed. Firstly, the pseudoinverse $\mathcal{H}$ of the Gram matrix G is given in terms of external momenta p_j and the inverse Gram determinant $|G|^{-1}$.

Furthermore, it is exploited that $p_3 \cdot J_3 = p_4 \cdot J_4 = 0$ for currents of massless leptons J_3 and J_4 and the auxiliary vector $\tilde{p}_3$ (cf. 3.16) is introduced by

$$p_2 \cdot J_3 = -\frac{t - s_3}{u - s_3} p_1 \cdot J_3 - \frac{s}{u - s_3} \tilde{p}_3 \cdot J_3 \,, \tag{3.62}$$

$$p_2 \cdot J_4 = -\frac{u - s_4}{t - s_4} p_1 \cdot J_4 + \frac{s}{t - s_4} \tilde{p}_3 \cdot J_4 \,, \tag{3.63}$$

$$\tilde{p}_3 \cdot J_3 \, \epsilon(p_1, p_2, \tilde{p}_3, J_4) = \tilde{p}_3 \cdot J_4 \, \epsilon(p_1, p_2, \tilde{p}_3, J_3) + \frac{ut - s_3 s_4}{s} \epsilon(p_1, p_2, J_3, J_4), \tag{3.64}$$

thus removing p_2 from the products of the form $p_i \cdot J_k$ and leading to the tensor basis (eq. 3.16). Here, Gram determinants $|G| \propto (ut - s_3 s_4)$ appear which cancel the inverse Gram determinants from the tensor reduction.

subroutine `MandelstamBasis`

To obtain Lorentz invariant quantities, all scalar products of momenta are replaced by the Mandelstam variables s, t, u, s_3, s_4.

subroutines `TC44s0230m1211 etc.`

The amplitude now consists of functions of the Mandelstam variables and the masses multiplied with basis functions and tensor structures. Its coefficients $\mathcal{C}_{j,l}$ are now treated in a loop over all tensor structures $\tilde{\tau}_j$. For each N, the full tensor reduction is applied by expressing the form factors in terms of scalar functions (cf. eq. 3.44).

subroutine `ReduceBox`

Then, the scalar reduction algorithm further simplifies the scalar integrals: All form factors which appear in the reduction of box diagrams are expressed by 4-point scalar functions, in n, $n+2$ and $n+4$ dimensions. The $n+4$-dimensional ones can again be expressed by $n+2$-dimensional 3- and 4-point scalar integrals (cf. eq. 3.45).

The same applies for the form factors and scalar integrals from reduction of 3- and 2-point functions. The corresponding routines are `TC3exp`, `TC2exp` and `ReduceTriangle`, `ReduceBubble`, respectively.

subroutine `ExpandInEpsilonNoIR`

As one does not expect IR divergences in the amplitude of any diagram, a finite expression can be obtained by taking the limit $n \to 4 \Leftrightarrow \epsilon \to 0$. For this purpose, all functions of the dimensionality n are expanded in ϵ (according to $n = 4 - 2\epsilon$) to $\mathcal{O}(\epsilon)$. The box and triangle functions are finite and thus all products of these functions with $\epsilon^n, n \geq 1$ vanish in the limit $\epsilon \to 0$. In contrast, the bubble functions posses poles $\propto \frac{1}{\epsilon}$. Thus, contributions of products of bubble functions and ϵ survive.

The Feynman amplitude for one diagram and one single tensor structure is now a linear combination of functions of Lorentz scalars, i.e. the kinematic variables s, t, u, s_3, s_4 and masses m_b^2 and m_t^2, and the scalar integrals as explained in sec. 3.2.2 and listed for all the diagrams in the appendix A.3.

Finally, the coefficients of the basis functions I_k, $\tilde{\mathcal{C}}_{j,k,l}(s, t, u, s_3, s_4, m_b^2, m_t^2)$, in the tensor coefficients $\mathcal{C}_{j,l}$ are written to files.

3.3.2. Simplifying the coefficients

Simplifying the coefficients

One now disposes of the coefficients $\mathcal{C}_{j,k,l}$ for each diagram l, written each in a single file. The Maple program `Simplify_Coefficients.map` expands these coefficients in ϵ, factorizes the coefficients of this expansion and tries to find typical functions of the kinematic variables, mostly Kaellen functions, to shorten the expressions. Then, all factors are put together again and the coefficients for all tensor structures and basis integrals appearing in the amplitude of this diagram are written to `SimRes_`*topology*`_`*helicity*`.out`.

Adding the contributions from all the diagrams

Since only the box contributions survive, the contributions from all box topologies are added, i.e. the coefficients $\mathcal{C}_{j,k,l}$ from all box diagrams are added:

$$\tilde{\mathcal{C}}_{j,k} = \sum_l \tilde{\mathcal{C}}_{j,k,l}. \tag{3.65}$$

The contributions from all diagrams are contained in `COEFFS_BOX_ggZZ_PP_MASSIVE.out` and `COEFFS_BOX_ggZZ_PM_MASSIVE.out` for $++$ and $+-$ helicities in the massive case and in `COEFFS_BOX_ggZZ_PP_MASSLESS.out` and `COEFFS_BOX_ggZZ_PM_MASSLESS.out` for the massless case.

Creating Fortran code

So far, the expressions for the coefficients $\tilde{\mathcal{C}}_{j,k}$ are in Maple format, but for the computation of the amplitude they are needed in Fortran format, each coefficient as a function of its arguments, the Mandelstam variables and the masses. The external momenta serve as input parameters from which the Mandelstam variables and finally the amplitude are

computed. The leptonic currents J_3 and J_4 appearing in the tensor structures $\tilde{\tau}_j$ must be expressed in terms of external momenta, too, which can be achieved in the spinor helicity formalism (cf. eqs. A.46 and A.47):

$$J_3^{\mu_3} = \frac{(4\sin\theta_W - 1)\mathrm{tr}[\not{p}_7\not{p}_1\not{p}_8\gamma^{\mu_3}] + \mathrm{tr}[\gamma_5\not{p}_7\not{p}_1\not{p}_8\gamma^{\mu_3}]}{4\sqrt{s_{17}s_{18}}}, \tag{3.66}$$

$$J_4^{\mu_4} = \frac{(4\sin\theta_W - 1)\mathrm{tr}[\not{p}_5\not{p}_2\not{p}_6\gamma^{\mu_4}] + \mathrm{tr}[\gamma_5\not{p}_5\not{p}_2\not{p}_6\gamma^{\mu_4}]}{4\sqrt{s_{25}s_{26}}}. \tag{3.67}$$

The ϵ tensors contracted with leptonic currents, like $\epsilon(p_1, p_2, \tilde{p}_3, J_4)$, are contractions of the external leptons and ϵ tensors. As only 5 external momenta are independent, we can choose 5 ϵ tensors contracted with external momenta as a basis:

$$\{\epsilon_k\} = \{\epsilon(p_1, p_2, p_5, \tilde{p}_3), \epsilon(p_1, p_2, p_8, \tilde{p}_3), \epsilon(p_1, p_2, p_5, p_8), \epsilon(p_1, p_5, p_8, \tilde{p}_3), \epsilon(p_2, p_5, p_8, \tilde{p}_3)\}. \tag{3.68}$$

The tensor structures $\tilde{\tau}_j$ are then computed as

$$\tilde{\tau}_j = \sum_{k=1}^{5} c_{jk}\epsilon_k. \tag{3.69}$$

After these preparations the amplitude is finally returned as

$$\mathcal{M}^{\lambda_1\lambda_2 J_3 J_4} = \sum_l \sum_k \sum_{j=1}^{9} \tilde{\mathcal{C}}_{j,k,l}(s, t, u, s_3, s_4, m_b^2, m_t^2)\ \tilde{\tau}_j\ I_k. \tag{3.70}$$

3.3.3. Checks I

Having calculated the coefficients $\mathcal{C}_{ij}$ in the amplitude

$$\mathcal{M}^{\lambda_1\lambda_2 J_3 J_4} = \sum_{\substack{\text{tensor} \\ \text{structures} \\ i}} \sum_{\substack{\text{basis} \\ \text{functions} \\ j}} \mathcal{C}_{ij}\tilde{\tau}_i I_j, \tag{3.71}$$

I have performed a first check of these coefficients, exploiting two symmetries of the amplitude, namely Bose and CP symmetry. After revealing the transformation laws of the tensor structures $\tilde{\tau}_i$ and the basis functions I_j under both transformations, I will show that demanding invariance of the amplitude leads to constraints on the coefficients which can be tested.

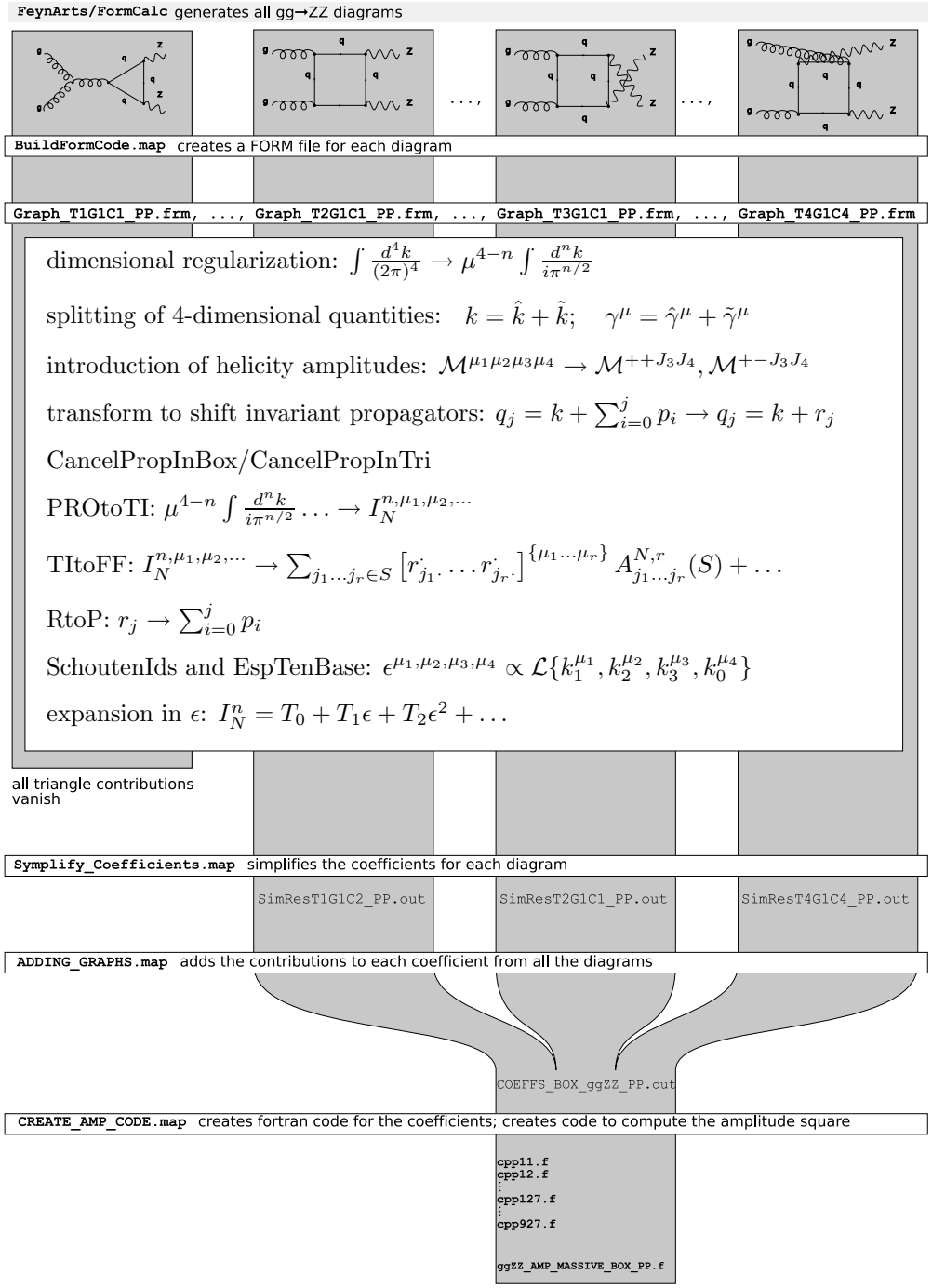

Figure 3.8.: Diagram showing the manipulation of the Feynman amplitude $\mathcal{M}^{++}$, from the diagrams to the coefficients and amplitude files; the manipulation for $\mathcal{M}^{+-}$ is completely analogous

Bose symmetry

After having extracted the color algebra for the strong interacting particles (which only leads to a color factor of $\frac{1}{32}$ as I have shown) the two gluons cannot be distinguished any more. Thus, the amplitude must be invariant under interchange of their momenta p_1 and p_2:

$$\mathcal{M}^{\lambda_1\lambda_2 J3J4}(p_1,p_2,p_3,p_4) = \mathcal{M}^{\lambda_2\lambda_1 J3J4}(p_2,p_1,p_3,p_4). \tag{3.72}$$

Interchanging the momenta affects the Mandelstam variables t and u

$$t \leftrightarrow u, \tag{3.73}$$

while s, s_3, s_4 and $\tilde{p}_3$ are invariant.

For calculating the transformation properties of the 9 tensor structures one exploits (cf. 3.16)

$$p_1 \cdot J_3 \to p_2 \cdot J_3 = -\frac{t-s_3}{u-s_3} p_1 \cdot J_3 - \frac{s}{u-s_3}\tilde{p}_3 \cdot J_3, \tag{3.74}$$

$$p_1 \cdot J_4 \to p_2 \cdot J_4 = -\frac{u-s_4}{t-s_4} p_1 \cdot J_4 + \frac{s}{t-s_4}\tilde{p}_3 \cdot J_4 \tag{3.75}$$

and

$$\begin{aligned} \epsilon(p_1,p_2,J_3,J_4) &= -\frac{s}{ut-s_3s_4}\left(\tilde{p}_3\cdot J_3\epsilon(p_1,p_2,\tilde{p}_3,J_4) - \tilde{p}_3\cdot J_4\epsilon(p_1,p_2,\tilde{p}_3,J_3)\right) \\ \Rightarrow \tilde{p}_3\cdot J_3\ \epsilon(p_1,p_2,\tilde{p}_3,J_4) &= \tilde{p}_3\cdot J_4\ \epsilon(p_1,p_2,\tilde{p}_3,J_3) - \frac{ut-s_3s_4}{s}\ \epsilon(p_1,p_2,J_3,J_4) \end{aligned} \tag{3.76}$$

The 9 tensor structures then transform under Bose transformation as follows:

$$\begin{aligned} J_3\cdot J_4 &\to J_3\cdot J_4 \\ p_1\cdot J_3\ p_1\cdot J_4 &\to \frac{(t-s_3)(u-s_4)}{(u-s_3(t-s_4)} p_1\cdot J_3\ p_1\cdot J_4 + \frac{s(u-s_4)}{(u-s_3)(t-s_4)}\tilde{p}_3\cdot J_3\ p_1\cdot J_4 \\ &\quad -\frac{(t-s_3)s}{(u-s_3)(t-s_4)} p_1\cdot J_3\ \tilde{p}_3\cdot J_4 - \frac{s^2}{(u-s_3)(t-s_4)}\tilde{p}_3\cdot J_3\ \tilde{p}_3\cdot J_4 \\ p_1\cdot J_3\ \tilde{p}_3\cdot J_4 &\to -\frac{t-s_3}{u-s_3} p_1\cdot J_3\ \tilde{p}_3\cdot J_4 - \frac{s}{u-s_3}\tilde{p}_3\cdot J_3\ \tilde{p}_3\cdot J_4 \\ p_1\cdot J_3\ \epsilon(p_1,p_2,\tilde{p}_3,J_4) &\to \frac{t-s_3}{u-s_3} p_1\cdot J_3\ \epsilon(p_1,p_2,\tilde{p}_3,J_4) + \frac{s}{u-s_3}\tilde{p}_3\cdot J_3\epsilon(p_1,p_2,\tilde{p}_3,J_4) \\ &= \frac{t-s_3}{u-s_3} p_1\cdot J_3\ \epsilon(p_1,p_2,\tilde{p}_3,J_4) + \frac{s}{u-s_3}\tilde{p}_3\cdot J_4\epsilon(p_1,p_2,\tilde{p}_3,J_3) \\ &\quad -\frac{ut-s_3s_4}{u-s_3}\epsilon(p_1,p_2,J_3,J_4) \\ \tilde{p}_3\cdot J_3\ p_1\cdot J_4 &\to -\frac{u-s_4}{t-s_4}\tilde{p}_3\cdot J_3\ p_1\cdot J_4 + \frac{s}{t-s_4}\tilde{p}_3\cdot J_3\ \tilde{p}_3\cdot J_4 \\ \tilde{p}_3\cdot J_3\ \tilde{p}_3\cdot J_4 &\to \tilde{p}_3\cdot J_3\ \tilde{p}_3\cdot J_4 \end{aligned}$$

$$\epsilon(p_1,p_2,J_3,J_4) \to -\epsilon(p_1,p_2,J_3,J_4)$$
$$p_1\cdot J_4\;\epsilon(p_1,p_2,\tilde{p}_3,J_3) \to \frac{u-s_4}{t-s_4}p_1\cdot J_4\;\epsilon(p_1,p_2,\tilde{p}_3,J_3) - \frac{s}{t-s_4}\tilde{p}_3\cdot J_4\;\epsilon(p_1,p_2,\tilde{p}_3,J_3)$$
$$\tilde{p}_3\cdot J_4\;\epsilon(p_1,p_2,\tilde{p}_3,J_3) \to -\tilde{p}_3\cdot J_4\;\epsilon(p_1,p_2,\tilde{p}_3,J_3)$$

The transformation properties of the basis functions can be easily obtained by applying the transformation rules to their arguments and then interchanging the arguments to obtain one of the basis functions. One thus finds:

$$\begin{aligned}
f(1)&=\texttt{BOXd6}(\texttt{u},\texttt{s},0,\texttt{s}_4,\texttt{s}_3,0,\texttt{m}_\texttt{t}^2,\texttt{m}_\texttt{t}^2,\texttt{m}_\texttt{t}^2,\texttt{m}_\texttt{t}^2) &&\to\texttt{BOXd6}(\texttt{t},\texttt{s},0,\texttt{s}_3,\texttt{s}_4,0,\texttt{m}_\texttt{t}^2,\texttt{m}_\texttt{t}^2,\texttt{m}_\texttt{t}^2,\texttt{m}_\texttt{t}^2)&&=f(2)\\
f(2)&=\texttt{BOXd6}(\texttt{t},\texttt{s},0,\texttt{s}_3,\texttt{s}_4,0,\texttt{m}_\texttt{t}^2,\texttt{m}_\texttt{t}^2,\texttt{m}_\texttt{t}^2,\texttt{m}_\texttt{t}^2) &&\to\texttt{BOXd6}(\texttt{u},\texttt{s},0,\texttt{s}_4,\texttt{s}_3,0,\texttt{m}_\texttt{t}^2,\texttt{m}_\texttt{t}^2,\texttt{m}_\texttt{t}^2,\texttt{m}_\texttt{t}^2)&&=f(1)\\
f(3)&=\texttt{BOXd6}(\texttt{t},\texttt{u},\texttt{s}_3,0,\texttt{s}_4,0,\texttt{m}_\texttt{t}^2,\texttt{m}_\texttt{t}^2,\texttt{m}_\texttt{t}^2,\texttt{m}_\texttt{t}^2) &&\to\texttt{BOXd6}(\texttt{t},\texttt{u},\texttt{s}_3,0,\texttt{s}_4,0,\texttt{m}_\texttt{t}^2,\texttt{m}_\texttt{t}^2,\texttt{m}_\texttt{t}^2,\texttt{m}_\texttt{t}^2)&&=f(3)\\
f(4)&=\texttt{TRId4}(\texttt{s}_4,\texttt{s}_3,\texttt{s},\texttt{m}_\texttt{t}^2,\texttt{m}_\texttt{t}^2,\texttt{m}_\texttt{t}^2) &&\to\texttt{TRId4}(\texttt{s}_4,\texttt{s}_3,\texttt{s},\texttt{m}_\texttt{t}^2,\texttt{m}_\texttt{t}^2,\texttt{m}_\texttt{t}^2)&&=f(4)\\
f(5)&=\texttt{TRId4}(\texttt{u},\texttt{s}_3,\texttt{m}_\texttt{t}^2,\texttt{m}_\texttt{t}^2,\texttt{m}_\texttt{t}^2,\texttt{m}_\texttt{t}^2) &&\to\texttt{TRId4}(0,\texttt{s}_3,\texttt{t},\texttt{m}_\texttt{t}^2,\texttt{m}_\texttt{t}^2,\texttt{m}_\texttt{t}^2)&&=f(9)\\
f(6)&=\texttt{TRId4}(0,\texttt{s},0,\texttt{m}_\texttt{t}^2,\texttt{m}_\texttt{t}^2,\texttt{m}_\texttt{t}^2) &&\to\texttt{TRId4}(0,\texttt{s},0,\texttt{m}_\texttt{t}^2,\texttt{m}_\texttt{t}^2,\texttt{m}_\texttt{t}^2)&&=f(6)\\
f(7)&=\texttt{TRId4}(0,\texttt{s}_4,\texttt{u},\texttt{m}_\texttt{t}^2,\texttt{m}_\texttt{t}^2,\texttt{m}_\texttt{t}^2) &&\to\texttt{TRId4}(\texttt{t},\texttt{s}_4,0,\texttt{m}_\texttt{t}^2,\texttt{m}_\texttt{t}^2,\texttt{m}_\texttt{t}^2)&&=f(8)\\
f(8)&=\texttt{TRId4}(\texttt{t},\texttt{s}_4,0,\texttt{m}_\texttt{t}^2,\texttt{m}_\texttt{t}^2,\texttt{m}_\texttt{t}^2) &&\to\texttt{TRId4}(0,\texttt{s}_4,\texttt{u},\texttt{m}_\texttt{t}^2,\texttt{m}_\texttt{t}^2,\texttt{m}_\texttt{t}^2)&&=f(7)\\
f(9)&=\texttt{TRId4}(0,\texttt{s}_3,\texttt{t},\texttt{m}_\texttt{t}^2,\texttt{m}_\texttt{t}^2,\texttt{m}_\texttt{t}^2) &&\to\texttt{TRId4}(\texttt{u},\texttt{s}_3,\texttt{m}_\texttt{t}^2,\texttt{m}_\texttt{t}^2,\texttt{m}_\texttt{t}^2,\texttt{m}_\texttt{t}^2)&&=f(5)\\
f(10)&=\texttt{BUBd4}(\texttt{s},\texttt{m}_\texttt{t}^2,\texttt{m}_\texttt{t}^2) &&\to\texttt{BUBd4}(\texttt{s},\texttt{m}_\texttt{t}^2,\texttt{m}_\texttt{t}^2)&&=f(10)\\
f(11)&=\texttt{BUBd4}(\texttt{u},\texttt{m}_\texttt{t}^2,\texttt{m}_\texttt{t}^2) &&\to\texttt{BUBd4}(\texttt{u},\texttt{m}_\texttt{t}^2,\texttt{m}_\texttt{t}^2)&&=f(12)\\
f(12)&=\texttt{BUBd4}(\texttt{t},\texttt{m}_\texttt{t}^2,\texttt{m}_\texttt{t}^2) &&\to\texttt{BUBd4}(\texttt{t},\texttt{m}_\texttt{t}^2,\texttt{m}_\texttt{t}^2)&&=f(11)\\
f(13)&=\texttt{BUBd4}(\texttt{s}_3,\texttt{m}_\texttt{t}^2,\texttt{m}_\texttt{t}^2) &&\to\texttt{BUBd4}(\texttt{s}_3,\texttt{m}_\texttt{t}^2,\texttt{m}_\texttt{t}^2)&&=f(13)\\
f(14)&=\texttt{BUBd4}(\texttt{s}_4,\texttt{m}_\texttt{t}^2,\texttt{m}_\texttt{t}^2) &&\to\texttt{BUBd4}(\texttt{s}_4,\texttt{m}_\texttt{t}^2,\texttt{m}_\texttt{t}^2)&&=f(14)\\
f(15)&=\texttt{BUBd4}(0,0,\texttt{m}_\texttt{t}^2) &&\to\texttt{BUBd4}(0,0,\texttt{m}_\texttt{t}^2)&&=f(15)\\
f(16)&=\texttt{BOXd6}(\texttt{u},\texttt{s},0,\texttt{s}_4,\texttt{s}_3,0,\texttt{m}_\texttt{b}^2,\texttt{m}_\texttt{b}^2,\texttt{m}_\texttt{b}^2,\texttt{m}_\texttt{b}^2) &&\to\texttt{BOXd6}(\texttt{t},\texttt{s},0,\texttt{s}_3,\texttt{s}_4,0,\texttt{m}_\texttt{b}^2,\texttt{m}_\texttt{b}^2,\texttt{m}_\texttt{b}^2,\texttt{m}_\texttt{b}^2)&&=f(17)\\
f(17)&=\texttt{BOXd6}(\texttt{t},\texttt{s},0,\texttt{s}_3,\texttt{s}_4,0,\texttt{m}_\texttt{b}^2,\texttt{m}_\texttt{b}^2,\texttt{m}_\texttt{b}^2,\texttt{m}_\texttt{b}^2) &&\to\texttt{BOXd6}(\texttt{u},\texttt{s},0,\texttt{s}_4,\texttt{s}_3,0,\texttt{m}_\texttt{b}^2,\texttt{m}_\texttt{b}^2,\texttt{m}_\texttt{b}^2,\texttt{m}_\texttt{b}^2)&&=f(16)\\
f(18)&=\texttt{BOXd6}(\texttt{t},\texttt{u},\texttt{s}_3,0,\texttt{s}_4,0,\texttt{m}_\texttt{b}^2,\texttt{m}_\texttt{b}^2,\texttt{m}_\texttt{b}^2,\texttt{m}_\texttt{b}^2) &&\to\texttt{BOXd6}(\texttt{t},\texttt{u},\texttt{s}_3,0,\texttt{s}_4,0,\texttt{m}_\texttt{b}^2,\texttt{m}_\texttt{b}^2,\texttt{m}_\texttt{b}^2,\texttt{m}_\texttt{b}^2)&&=f(18)\\
f(19)&=\texttt{TRId4}(\texttt{s}_4,\texttt{s}_3,\texttt{s},\texttt{m}_\texttt{b}^2,\texttt{m}_\texttt{b}^2,\texttt{m}_\texttt{b}^2) &&\to\texttt{TRId4}(\texttt{s}_4,\texttt{s}_3,\texttt{s},\texttt{m}_\texttt{b}^2,\texttt{m}_\texttt{b}^2,\texttt{m}_\texttt{b}^2)&&=f(15)\\
f(20)&=\texttt{TRId4}(\texttt{u},\texttt{s}_3,\texttt{m}_\texttt{b}^2,\texttt{m}_\texttt{b}^2,\texttt{m}_\texttt{b}^2,\texttt{m}_\texttt{b}^2) &&\to\texttt{TRId4}(0,\texttt{s}_3,\texttt{t},\texttt{m}_\texttt{b}^2,\texttt{m}_\texttt{b}^2,\texttt{m}_\texttt{b}^2)&&=f(24)\\
f(21)&=\texttt{TRId4}(0,\texttt{s},0,\texttt{m}_\texttt{b}^2,\texttt{m}_\texttt{b}^2,\texttt{m}_\texttt{b}^2) &&\to\texttt{TRId4}(0,\texttt{s},0,\texttt{m}_\texttt{b}^2,\texttt{m}_\texttt{b}^2,\texttt{m}_\texttt{b}^2)&&=f(21)\\
f(22)&=\texttt{TRId4}(0,\texttt{s}_4,\texttt{u},\texttt{m}_\texttt{b}^2,\texttt{m}_\texttt{b}^2,\texttt{m}_\texttt{b}^2) &&\to\texttt{TRId4}(\texttt{t},\texttt{s}_4,0,\texttt{m}_\texttt{b}^2,\texttt{m}_\texttt{b}^2,\texttt{m}_\texttt{b}^2)&&=f(23)\\
f(23)&=\texttt{TRId4}(\texttt{t},\texttt{s}_4,0,\texttt{m}_\texttt{b}^2,\texttt{m}_\texttt{b}^2,\texttt{m}_\texttt{b}^2) &&\to\texttt{TRId4}(0,\texttt{s}_4,\texttt{u},\texttt{m}_\texttt{b}^2,\texttt{m}_\texttt{b}^2,\texttt{m}_\texttt{b}^2)&&=f(22)\\
f(24)&=\texttt{TRId4}(0,\texttt{s}_3,\texttt{t},\texttt{m}_\texttt{b}^2,\texttt{m}_\texttt{b}^2,\texttt{m}_\texttt{b}^2) &&\to\texttt{TRId4}(\texttt{u},\texttt{s}_3,\texttt{m}_\texttt{b}^2,\texttt{m}_\texttt{b}^2,\texttt{m}_\texttt{b}^2,\texttt{m}_\texttt{b}^2)&&=f(20)\\
f(25)&=\texttt{BUBd4}(\texttt{s},\texttt{m}_\texttt{b}^2,\texttt{m}_\texttt{b}^2) &&\to\texttt{BUBd4}(\texttt{s},\texttt{m}_\texttt{b}^2,\texttt{m}_\texttt{b}^2)&&=f(25)\\
f(26)&=\texttt{BUBd4}(\texttt{u},\texttt{m}_\texttt{b}^2,\texttt{m}_\texttt{b}^2) &&\to\texttt{BUBd4}(\texttt{u},\texttt{m}_\texttt{b}^2,\texttt{m}_\texttt{b}^2)&&=f(27)\\
f(27)&=\texttt{BUBd4}(\texttt{t},\texttt{m}_\texttt{b}^2,\texttt{m}_\texttt{b}^2) &&\to\texttt{BUBd4}(\texttt{t},\texttt{m}_\texttt{b}^2,\texttt{m}_\texttt{b}^2)&&=f(26)\\
f(28)&=\texttt{BUBd4}(\texttt{s}_3,\texttt{m}_\texttt{b}^2,\texttt{m}_\texttt{b}^2) &&\to\texttt{BUBd4}(\texttt{s}_3,\texttt{m}_\texttt{b}^2,\texttt{m}_\texttt{b}^2)&&=f(28)\\
f(29)&=\texttt{BUBd4}(\texttt{s}_4,\texttt{m}_\texttt{b}^2,\texttt{m}_\texttt{b}^2) &&\to\texttt{BUBd4}(\texttt{s}_4,\texttt{m}_\texttt{b}^2,\texttt{m}_\texttt{b}^2)&&=f(29)\\
f(30)&=\texttt{BUBd4}(0,0,\texttt{m}_\texttt{b}^2) &&\to\texttt{BUBd4}(0,0,\texttt{m}_\texttt{b}^2)&&=f(30)\\
f(31)&=\texttt{one} &&\to\texttt{one}&&=f(31)
\end{aligned}$$

One now expresses the amplitude in the transformed tensor structures and basis integrals, rearranges them in the tensor basis and integral basis and compares the coefficients:

$$C_1(s,t,u,s_3,s_4) = C_1(s,u,t,s_3,s_4) \tag{3.77}$$
$$C_2(s,t,u,s_3,s_4) = \frac{(t-s_3)(u-s_4)}{(u-s_3(t-s_4)}C_2(s,u,t,s_3,s_4) \tag{3.78}$$
$$C_3(s,t,u,s_3,s_4) = -\frac{(t-s_3)s}{(u-s_3)(t-s_4)}C_2(s,u,t,s_3,s_4) - \frac{t-s_3}{u-s_3}C_3(s,u,t,s_3,s_4) \tag{3.79}$$
$$C_4(s,t,u,s_3,s_4) = \frac{t-s_3}{u-s_3}C_4(s,u,t,s_3,s_4) \tag{3.80}$$
$$C_5(s,t,u,s_3,s_4) = \frac{s(u-s_4)}{(u-s_3)(t-s_4)}C_2(s,u,t,s_3,s_4) - \frac{u-s_4}{t-s_4}C_5(s,u,t,s_3,s_4) \tag{3.81}$$
$$\begin{aligned}C_6(s,t,u,s_3,s_4) = &-\frac{s^2}{(u-s_3)(t-s_4)}C_2(s,u,t,s_3,s_4) - \frac{s}{u-s_3}C_3(s,u,t,s_3,s_4)\\ &+\frac{s}{t-s_4}C_5(s,u,t,s_3,s_4) + C_6\end{aligned} \tag{3.82}$$

$$C_7(s,t,u,s_3,s_4) = \frac{ut - s_3 s_4}{u - s_3} C_4(s,u,t,s_3,s_4) - C_7(s,u,t,s_3,s_4) \tag{3.83}$$

$$C_8(s,t,u,s_3,s_4) = \frac{u - s_4}{t - s_4} C_8(s,u,t,s_3,s_4) \tag{3.84}$$

$$C_9(s,t,u,s_3,s_4) = \frac{s}{u - s_3} C_4(s,u,t,s_3,s_4) - \frac{s}{t - s_4} C_8(s,u,t,s_3,s_4) - C_9(s,u,t,s_3,s_4) \tag{3.85}$$

$$\tag{3.86}$$

As the coefficients are already at hand in Maple format it is easy to check these relations. I thereto wrote a program in Maple and found out that all these relations are fulfilled.

CP symmetry

The amplitude is not only invariant under Bose transformation of the gluons, reflecting in the interchange of p_1 and p_2, but, in the limit of massless leptons, also under CP transformation (cf. fig 3.9): The initial and the CP transformed state are identical since the flavors of the leptons cannot be distinguished in the massless limit.[2]

Since the CP transformation corresponds to an interchange of the momenta of the Z bosons, p_3 and p_4,

$$\mathcal{M}^{\lambda_1\lambda_2 J3J4}(p_1,p_2,p_3,p_4) = \mathcal{M}^{-\lambda_1\,-\lambda_2 J4J3}(p_1,p_2,p_4,p_3), \tag{3.88}$$

the amplitude must be also invariant under

$$t \leftrightarrow u, \tag{3.89}$$

$$s_3 \leftrightarrow s_4, \tag{3.90}$$

$$\tilde{p}_3 \leftrightarrow -\tilde{p}_3, \tag{3.91}$$

while s is again invariant.

The 9 tensor structures then transform under CP transformation as follows:

$$\begin{aligned}
J_3 \cdot J_4 &\to J_3 \cdot J_4 \\
p_1 \cdot J_3\; p_1 \cdot J_4 &\to p_1 \cdot J_3\; p_1 \cdot J_4 \\
p_1 \cdot J_3\; \tilde{p}_3 \cdot J_4 &\to -\tilde{p}_3 \cdot J_3\; p_1 \cdot J_4 \\
p_1 \cdot J_3\; \epsilon(p_1,p_2,\tilde{p}_3,J_4) &\to -p_1 \cdot J_4\; \epsilon(p_1,p_2,\tilde{p}_3,J_3) \\
\tilde{p}_3 \cdot J_3\; p_1 \cdot J_4 &\to -p_1 \cdot J_3\; \tilde{p}_3 \cdot J_4 \\
\tilde{p}_3 \cdot J_3\; \tilde{p}_3 \cdot J_4 &\to \tilde{p}_3 \cdot J_3\; \tilde{p}_3 \cdot J_4 \\
\epsilon(p_1,p_2,J_3,J_4) &\to -\epsilon(p_1,p_2,J_3,J_4) \\
p_1 \cdot J_4\; \epsilon(p_1,p_2,\tilde{p}_3,J_3) &\to -p_1 \cdot J_3\; \epsilon(p_1,p_2,\tilde{p}_3,J_4) \\
\tilde{p}_3 \cdot J_4\; \epsilon(p_1,p_2,\tilde{p}_3,J_3) &\to \tilde{p}_3 \cdot J_3\; \epsilon(p_1,p_2,\tilde{p}_3,J_4)
\end{aligned}$$

[2] Of course, it is also possible to consider the Bose symmetry of the Z bosons,

$$\mathcal{M}^{\lambda_1\lambda_2 J3J4}(p_1,p_2,p_3,p_4) = \mathcal{M}^{\lambda_1\lambda_2 J4J3}(p_1,p_2,p_4,p_3), \tag{3.87}$$

for checks of the amplitude.

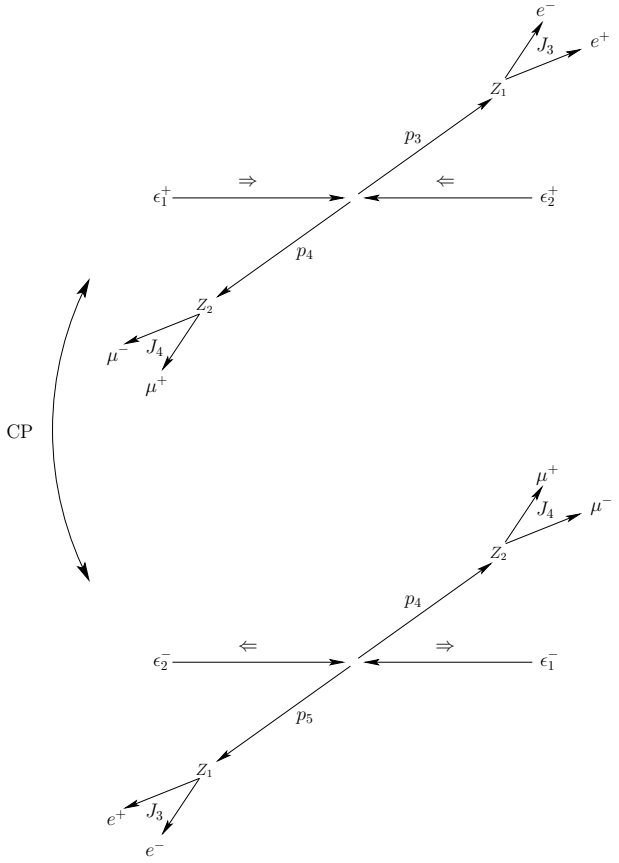

Figure 3.9.: Two kinematic configurations linked by a CP transformation

$$= \tilde{p}_3 \cdot J_4 \; \epsilon(p_1, p_2, \tilde{p}_3, J_3) - \frac{ut - s_3 s_4}{s} \epsilon(p_1, p_2, J_3, J_4)$$

The transformation properties of the basis functions can again be revealed quite easily:

$f(1)$=BOXd6(u, s, 0, s_4, s_3, 0, m_t^2, m_t^2, m_t^2, m_t^2)→BOXd6(t, s, 0, s_3, s_4, 0, m_t^2, m_t^2, m_t^2, m_t^2)=$f(2)$
$f(2)$=BOXd6(t, s, 0, s_3, s_4, 0, m_t^2, m_t^2, m_t^2, m_t^2)→BOXd6(u, s, 0, s_4, s_3, 0, m_t^2, m_t^2, m_t^2, m_t^2)=$f(1)$
$f(3)$=BOXd6(t, u, s_3, 0, s_4, 0, m_t^2, m_t^2, m_t^2, m_t^2)→BOXd6(t, u, s_3, 0, s_4, 0, m_t^2, m_t^2, m_t^2, m_t^2)=$f(3)$
$f(4)$=TRId4(s_4, s_3, s, m_t^2, m_t^2, m_t^2) →TRId4(s_4, s_3, s, m_t^2, m_t^2, m_t^2) =$f(4)$
$f(5)$=TRId4(u, s_3, 0, m_t^2, m_t^2, m_t^2) →TRId4(t, s_4, 0, m_t^2, m_t^2, m_t^2) =$f(8)$
$f(6)$=TRId4(0, s, 0, m_t^2, m_t^2, m_t^2) →TRId4(0, s, 0, m_t^2, m_t^2, m_t^2) =$f(6)$
$f(7)$=TRId4(0, s_4, u, m_t^2, m_t^2, m_t^2) →TRId4(0, s_3, t, m_t^2, m_t^2, m_t^2) =$f(9)$
$f(8)$=TRId4(t, s_4, 0, m_t^2, m_t^2, m_t^2) →TRId4(u, s_3, 0, m_t^2, m_t^2, m_t^2) =$f(5)$
$f(9)$=TRId4(0, s_3, t, m_t^2, m_t^2, m_t^2) →TRId4(0, s_4, u, m_t^2, m_t^2, m_t^2) =$f(7)$
$f(10)$=BUBd4(s, m_t^2, m_t^2) →BUBd4(s, m_t^2, m_t^2) =$f(10)$
$f(11)$=BUBd4(u, m_t^2, m_t^2) →BUBd4(t, m_t^2, m_t^2) =$f(12)$
$f(12)$=BUBd4(t, m_t^2, m_t^2) →BUBd4(u, m_t^2, m_t^2) =$f(11)$
$f(13)$=BUBd4(s_3, m_t^2, m_t^2) →BUBd4(s_4, m_t^2, m_t^2) =$f(13)$
$f(14)$=BUBd4(s_4, m_t^2, m_t^2) →BUBd4(s_3, m_t^2, m_t^2) =$f(14)$
$f(15)$=BUBd4(0, 0, m_t^2) →BUBd4(0, 0, m_t^2) =$f(15)$
$f(16)$=BOXd6(u, s, 0, s_4, s_3, 0, m_b^2, m_b^2, m_b^2, m_b^2)→BOXd6(t, s, 0, s_3, s_4, 0, m_b^2, m_b^2, m_b^2, m_b^2)=$f(17)$
$f(17)$=BOXd6(t, s, 0, s_3, s_4, 0, m_b^2, m_b^2, m_b^2, m_b^2)→BOXd6(u, s, 0, s_4, s_3, 0, m_b^2, m_b^2, m_b^2, m_b^2)=$f(16)$
$f(18)$=BOXd6(t, u, s_3, 0, s_4, 0, m_b^2, m_b^2, m_b^2, m_b^2)→BOXd6(t, u, s_3, 0, s_4, 0, m_b^2, m_b^2, m_b^2, m_b^2)=$f(18)$
$f(19)$=TRId4(s_4, s_3, s, m_b^2, m_b^2, m_b^2) →TRId4(s_4, s_3, s, m_b^2, m_b^2, m_b^2) =$f(19)$
$f(20)$=TRId4(u, s_3, 0, m_b^2, m_b^2, m_b^2) →TRId4(t, s_4, 0, m_b^2, m_b^2, m_b^2) =$f(23)$
$f(21)$=TRId4(0, s, 0, m_b^2, m_b^2, m_b^2) →TRId4(0, s, 0, m_b^2, m_b^2, m_b^2) =$f(21)$
$f(22)$=TRId4(0, s_4, u, m_b^2, m_b^2, m_b^2) →TRId4(0, s_3, t, m_b^2, m_b^2, m_b^2) =$f(24)$
$f(23)$=TRId4(t, s_4, 0, m_b^2, m_b^2, m_b^2) →TRId4(u, s_3, 0, m_b^2, m_b^2, m_b^2) =$f(20)$
$f(24)$=TRId4(0, s_3, t, m_b^2, m_b^2, m_b^2) →TRId4(0, s_4, u, m_b^2, m_b^2, m_b^2) =$f(22)$
$f(25)$=BUBd4(s, m_b^2, m_b^2) →BUBd4(s, m_b^2, m_b^2) =$f(25)$
$f(26)$=BUBd4(u, m_b^2, m_b^2) →BUBd4(t, m_b^2, m_b^2) =$f(27)$
$f(27)$=BUBd4(t, m_b^2, m_b^2) →BUBd4(u, m_b^2, m_b^2) =$f(26)$
$f(28)$=BUBd4(s_3, m_b^2, m_b^2) →BUBd4(s_4, m_b^2, m_b^2) =$f(29)$
$f(29)$=BUBd4(s_4, m_b^2, m_b^2) →BUBd4(s_3, m_b^2, m_b^2) =$f(28)$
$f(30)$=BUBd4(0, 0, m_b^2) →BUBd4(0, 0, m_b^2) =$f(30)$
$f(31)$=one →one =$f(31)$

One again expresses the amplitude in the transformed tensor structures and basis integrals, rearranges them in the tensor basis and integral basis and compares the coefficients:

$$C_1(s,t,u,s_3,s_4) = C_1(s,u,t,s_4,s_3) \tag{3.92}$$
$$C_2(s,t,u,s_3,s_4) = C_2(s,u,t,s_4,s_3) \tag{3.93}$$
$$C_3(s,t,u,s_3,s_4) = -C_5(s,u,t,s_4,s_3) \tag{3.94}$$
$$C_4(s,t,u,s_3,s_4) = -C_8(s,u,t,s_4,s_3) \tag{3.95}$$
$$C_5(s,t,u,s_3,s_4) = -C_3(s,u,t,s_4,s_3) \tag{3.96}$$
$$C_6(s,t,u,s_3,s_4) = C_6(s,u,t,s_4,s_3) \tag{3.97}$$
$$C_7(s,t,u,s_3,s_4) = -C_7(s,u,t,s_4,s_3) - \frac{ut-s_3s_4}{s} C_9(s,u,t,s_4,s_3) \tag{3.98}$$
$$C_8(s,t,u,s_3,s_4) = -C_4(s,u,t,s_4,s_3) \tag{3.99}$$
$$C_9(s,t,u,s_3,s_4) = C_9(s,u,t,s_4,s_3) \tag{3.100}$$
$$\tag{3.101}$$

I have checked these relations in a Maple program, too, and they are fulfilled.

3.3.4. Computation of the cross section

So far, only the Feynman amplitude $\mathcal{M}$ has been calculated as a function of the external momenta p_1, p_2, p_5, p_6, p_7 and p_8. To allow for experimental predictions, one must compute cross sections

$$d\sigma_{\text{hard}} = \frac{1}{2E_1 2E_1 |v_1 - v_2|} \underbrace{\left(\prod_f \frac{d^3 p_f}{(2\pi)^3} \frac{1}{2E_f} \right)}_{=:d\Phi} |\mathcal{M}(p_1, p_2 \to \{p_f\})|^2 (2\pi)^4 \delta^{(4)}(p_1 + p_2 - \sum_f p_f) \tag{3.102}$$

and, since pp collisions will be treated, convolve with the parton density function for the gluon $f_g(x, Q^2)$

$$d\sigma = dx_1 dx_2 d\sigma_{\text{hard}} f_g(x_1, Q^2) f_g(x_2, Q^2), \tag{3.103}$$

where x_1 and x_2 are the Bjorken variables of the gluons with momenta p_1 and p_2, respectively, and Q is the factorization scale.

As one cannot control the spins of the partons in a pp collision at the LHC and not does measure the spins of the final state particles, the amplitude is to be considered as spin averaged and spin summed, respectively.

To compute the total cross section σ or distributions $\frac{d\sigma}{dx}$ (where x can be every quantity of interest, for example rapidities of the particles in the interaction, angles between particles, invariant mass(es) of one or more particle etc.), an integration of $d\sigma$ must be performed. For this purpose the invariant phase space $d\Phi$ has to be parametrized conveniently. One then integrates over all degrees of freedom that are left after taking into account possible constraints like energy-momentum conservation or on-shell conditions for external particles, applying VEGAS-style Monte Carlo integration [40] with adaptive sampling.

This calculation is enclosed in a prêt-à-porter public program, named `GG2ZZ`, which will be explained in detail in the following subsections.

Kinematics

Before explaining the phase space parametrization, I will explain the kinematics and introduce the parametrization of four momenta p_j which is best adjusted to a LHC collider experiment.

First of all, one can distinguish two frames of reference: The first is the laboratory frame which coincides with the center of mass system (CMS) of the hadrons since the LHC is a colliding beams experiment. I will denote all quantities in this frame by plain letters. The second frame is the parton CMS defined by demanding the center of mass momentum of the two partons, gluons in this case, to be zero. This frame will be denoted by hatted quantities.

The momenta for the hadrons, in the case of the LHC protons, are p_a and p_b, respectively. Defining the coordinate system such as with the z-axis parallel to the beam line, the hadron momenta are

$$p_a = \frac{\sqrt{s}}{2}\begin{pmatrix}1\\0\\0\\1\end{pmatrix} \text{ and } p_b = \frac{\sqrt{s}}{2}\begin{pmatrix}1\\0\\0\\-1\end{pmatrix}, \tag{3.104}$$

where $\sqrt{s}$ is the hadron CMS energy. The momenta of the gluons in the hadron CMS are then given as fractions x_1 and x_2, called Bjorken variables, of the hadron momenta:

$$p_1 = x_1 p_a = x_1\frac{\sqrt{s}}{2}\begin{pmatrix}1\\0\\0\\1\end{pmatrix} \text{ and } \quad p_2 = x_2 p_b = x_2\frac{\sqrt{s}}{2}\begin{pmatrix}1\\0\\0\\-1\end{pmatrix}. \tag{3.105}$$

Taking into account the beam line as symmetry axis it is useful to split every 3 momentum $\vec{p}_j$ into a longitudinal momentum $\vec{p}_{Lj}$ and a transverse momentum $\vec{p}_{Tj}$:

$$\vec{p} = \vec{p}_{Lj} + \vec{p}_{Tj} \tag{3.106}$$

with $\vec{p}_{Tj}^{\,2} = \vec{p}_{jx}^{\,2} + \vec{p}_{jy}^{\,2}$, $\vec{p}_{Lj} = \vec{p}_{jz}$. One can define a transverse mass by

$$m_{Tj}^2 = m_j^2 + \vec{p}_{Tj}^{\,2}. \tag{3.107}$$

With the rapidity

$$y_j = \frac{1}{2}\log\frac{E_j + p_{Lj}}{E_j - p_{Lj}} \tag{3.108}$$

the energy is

$$E_j = m_{Tj}\cosh y_j \tag{3.109}$$

and the longitudinal momentum

$$p_{Lj} = m_{Tj}\cosh y_j. \tag{3.110}$$

For the transverse momentum there remains one degree of freedom that can be parametrized by the azimuthal angle ϕ_j:

$$p_{xj} = p_{Tj}\cos\phi_j; \quad p_{yj} = p_{Tj}\sin\phi_j. \tag{3.111}$$

The 4-momentum p_j^μ of a particle j of mass m is then given by

$$p_j^\mu = \begin{pmatrix} m_{Tj}\cosh y_j \\ p_{Tj}\cos\phi_j \\ p_{Tj}\sin\phi_j \\ m_{Tj}\sinh y_j \end{pmatrix}. \tag{3.112}$$

The advantage of this parametrization is that its behavior under Lorentz transformation along the z axis is quite simple since the transverse momentum, the transverse mass and the angle ϕ_j are invariant and the rapidity is additive under boosts along the z axis.

This parametrization is implemented in the C++ class `Fourmomentum` and all momenta, its components and the Bjorken variables in `Phasespace` which I adapted from [41].

Phase space parametrization

For the parametrization of a phase of n final state particles one needs $3n-2$ variables as two Bjorken variables are given and one can exploit the global momentum conservation and on-shell conditions for the final state particles:

n 4-momenta	$4n$
2 Bjorken variables x_1 and x_2	2
energy-momentum conservation	-4
n on-shell conditions for final state particles	n
degrees of freedom	$3n-2$

The phase space for $n = 4$ final state leptons is thus 10 dimensional. Since the integration is performed by a Monte Carlo algorithm, 10 independent random variables will be generated. Therefrom, the set of momenta for the calculation of the amplitude and the weight of the phase space point for the Monte Carlo integration are derived.

Decomposition of the phase space

Before calculating the momenta of the phase space, I will explain a possible decomposition of the phase space into three subspaces that makes the calculation more clearly. In general, every n-particle invariant phase space with one massive intermediate particle decaying into j particles $p_1 \dots p_j$ factorizes to

$$d\Phi_n(p_{in}; p_1 \dots p_n) = d\Phi_{n-j+1}(p_{in}; q, p_{j+1} \dots p_n)\frac{dq^2}{2\pi}d\Phi_j(q; p_1 \dots p_j) \tag{3.113}$$

with invariant mass of decay products

$$q^2 = \left(\sum_{i=1}^{j} E_i\right)^2 - |\sum_{i=1}^{j} \vec{p}_i|^2. \tag{3.114}$$

For a process with two massive intermediate particles, the phase space can be decomposed into

$$d\Phi_4(p_1,p_2;p_5,p_6,p_7,p_8) = d\Phi_2(p_1,p_2;p_3,p_4)\frac{dp_3^2}{2\pi}d\Phi_2(p_3;p_5,p_6)\frac{dp_4^2}{2\pi}d\Phi_2(p_4;p_7,p_8). \tag{3.115}$$

Moreover, the factors $\frac{1}{(p_i^2-m^2)^2+(m\Gamma)^2}, i = 3,4$ from the Z propagators have to be taken into account. Altogether, the Z resonances, $\left(\frac{dp_i^2}{2\pi}\frac{1}{(p_i^2-m^2)^2+(m\Gamma)^2}\right)$ and the phase space factors for the $gg \to Z^*Z^*$ process, $d\Phi_2(p_1,p_2;p_3,p_4)$, as well as for the decay of both Z bosons, $d\Phi_2(p_3;p_5,p_6)$ and $d\Phi_2(p_4;p_7,p_8)$ will be calculated below.

Z resonances

The first information that is needed for the generation of the $gg \to Z^*Z^*$ phase space and the $Z^* \to l\bar{l}$ decays are the invariant masses of the Z boson propagators. They are computed in the class `Zresonance`. For each boson its invariant mass q^2 is chosen randomly and its weight is set according to the Breit-Wigner distribution

$$\frac{1}{(q^2-m^2)^2+(m\Gamma)^2}. \tag{3.116}$$

For small widths, i.e. $\Gamma \ll m$, the Breit Wigner resonance in the propagator weight can hamper the quick convergence of the integrals and even lead to numerical instabilities. One therefore tries to avoid this resonance in q^2 by the following transformation:

$$x = m\Gamma \arctan\left(\frac{q^2-m^2}{m\Gamma}\right) \tag{3.117}$$

$$\Rightarrow dq^2 = \frac{(q^2-m)^2+m^2\Gamma^2}{m^2\Gamma^2}dx. \tag{3.118}$$

In practice, one restricts q^2 to a range $[0,s]$ corresponding to

$$x_{min} = m\Gamma \arctan\left(\frac{q_{min}^2-m^2}{m\Gamma}\right), \quad x_{max} = m\Gamma \arctan\left(\frac{q_{max}^2-m^2}{m\Gamma}\right). \tag{3.119}$$

With a linear mapping

$$x = (x_{max} - x_{min})r + x_{min} \text{ with } r \in [0,1] \tag{3.120}$$

the Jacobian becomes

$$dq^2 = \frac{(q^2 - m)^2 + m^2\Gamma^2}{m^2\Gamma^2} dr \tag{3.121}$$

and exactly cancels the Breit Wigner resonance thereby stabilizing the numerical behavior of the propagator.

gg → Z*Z*

Now that one knows the virtualities of the incoming and outgoing particles for the $gg \to Z^*Z^*$ process, its momenta p_1, p_2, p_3 and p_4 can be calculated. Here, a more general algorithm is presented allowing the generation of n outgoing particles (among $n-1$ jets and 1 residuum) from 2 ingoing particles. It is implemented in the class `TwoToJetsAndResiduum`.

In the CMS of the jets and the residuum, one can calculate its maximum energies:

$$\begin{aligned}
\hat{\vec{P}} &= \sum_{i=1}^{n} \hat{\vec{p}}_i = 0 \\
\hat{P} &= \sum_i \hat{p}_i = (\sum_{i=1}^{n} \hat{E}_i, 0)^T = (\sqrt{\hat{s}}, 0)^T \\
\Rightarrow \hat{P} \cdot \hat{p}_j &= \sqrt{\hat{s}} \hat{E}_j \\
\Rightarrow \hat{E}_j &= \frac{\hat{P} \cdot \hat{p}_j}{\sqrt{\hat{s}}} = \frac{\sum_i \hat{p}_i \cdot \hat{p}_j}{\sqrt{\hat{s}}} = \frac{\hat{p}_j^2 + \sum_{i \neq j} \hat{p}_i \cdot \hat{p}_j}{\sqrt{\hat{s}}} \\
&= \frac{\hat{p}_j^2 + \frac{1}{2}\sum_i (\hat{p}_i)^2 - \frac{1}{2}\sum_i \hat{p}_i^2}{\sqrt{\hat{s}}} = \frac{\hat{s} + m_j^2 - \sum_{i \neq j} m_i^2}{2\sqrt{\hat{s}}} \\
\Rightarrow \hat{E}_{j,max} &= \frac{\hat{s} + m_j^2}{2\sqrt{\hat{s}}}.
\end{aligned} \tag{3.122}$$

The momentum of each jet can now be calculated:

In the hadron CMS, i.e. the laboratory frame, in a loop over all jets:

1. The transverse mass m_{Tj} is hyperbolically distributed in $[m_j, E_{j,max}]$;
2. The rapidity y_j is equally distributed in $[-y_{max}, y_{max}]$ with the maximum rapidity $y_{max} = \operatorname{arcosh}\left(\frac{E_{j,max}}{m_{t,j}}\right)$;
3. The azimuthal angle ϕ_j between the jet and the beam line is equally distributed in $[0, 2\pi]$

4. Finally, p_j is derived from $m_{t,j}$, y_j and ϕ_j:

$$p_j = \begin{pmatrix} m_{Tj}\cosh y_j \\ \sqrt{m_{Tj}^2 - m^2}\cos\phi \\ \sqrt{m_{Tj}^2 - m^2}\sin\phi \\ m_{Tj}\sinh y_j \end{pmatrix}. \tag{3.123}$$

The momentum of the residuum is then $P_{res} = -P_{jets} = -\sum_j p_j$. As all momenta are fixed now, one can calculate the movement of the parton CMS with respect to the hadron CMS. Let y and $\hat{y}$ be the rapidity of the jets and the residuum in the hadron and parton CMS, respectively. As they are linked by a boost y_{cm}:

$$y = \hat{y} + y_{cm} \Rightarrow y_{cm} = y - \hat{y}. \tag{3.124}$$

One can show that

$$\hat{y}_{max} = \operatorname{arsinh}\sqrt{\frac{\frac{(s-(m_3+m_4)^2)(s-(m_3-m_4)^2)}{4s} - \vec{p}_T^2}{m^2 + \vec{p}_T^2}} \tag{3.125}$$

and distribute y equally in $[-\hat{y}_{max}, \hat{y}_{max}]$. To calculate $\hat{s}$, $\hat{E}_{jets}$ and $\hat{E}_{res}$ one Lorentz transforms to the parton CMS:

$$\begin{aligned} |\vec{\hat{p}}_{jets}|^2 &= \hat{p}_{t,jets}^2 - \hat{p}_{l,jets}^2 \\ &= p_{t,jets}^2 - \gamma^2(p_{l,jets} - \beta E_{jets})^2 \\ &= p_{t,jets}^2 - \gamma^2(p_{l,jets}\cosh y_{cm} - E_{jets}\sinh y_{cm})^2 \qquad (3.126) \\ \hat{E}_{jets} &= \sqrt{m_{jets}^2 + |\vec{\hat{p}}_{jets}|^2} \qquad (3.127) \\ \hat{E}_{res} &= \sqrt{m_{res}^2 + |\vec{\hat{p}}_{res}|^2} = \sqrt{m_{res}^2 + |\vec{\hat{p}}_{jets}|^2} \qquad (3.128) \\ \hat{s} &= \hat{E}_{pCMS} = \hat{E}_{res} + \hat{E}_{jets} \end{aligned}$$

The total momentum of partons in the hadron CMS is

$$p_{tot} := p_1 + p_2 = \begin{pmatrix} E_{pCMS}\cosh y_{cm} \\ 0 \\ 0 \\ E_{pCMS}\sinh y_j \end{pmatrix} \tag{3.129}$$

and can be calculated from $E_{pCMS} = \hat{E}_{pCMS}$ and y_{cm}.

One can now compute x_1 and x_2:

$$p_{tot} = \begin{pmatrix} p^0_{tot} \\ 0 \\ 0 \\ p^3_{tot} \end{pmatrix} = p_1 + p_2 = x_1 p_a + x_2 p_b = x_1 \frac{\sqrt{s}}{2} \begin{pmatrix} 1 \\ 0 \\ 0 \\ 1 \end{pmatrix} + x_2 \frac{\sqrt{s}}{2} \begin{pmatrix} 1 \\ 0 \\ 0 \\ -1 \end{pmatrix} \quad (3.130)$$

$$\Rightarrow \quad \begin{cases} \frac{2p^0_{tot}}{\sqrt{s}} = x_1 + x_2 \\ \frac{2p^3_{tot}}{\sqrt{s}} = x_1 - x_2 \end{cases} \Rightarrow \begin{cases} x_1 = \frac{p^0_{tot} + p^3_{tot}}{\sqrt{s}} \\ x_2 = \frac{p^0_{tot} - p^3_{tot}}{\sqrt{s}} \end{cases} \quad (3.131)$$

$$\Rightarrow \begin{cases} p_1 = x_1 p_a \\ p_2 = x_2 p_b \end{cases} . \quad (3.132)$$

Decays of the Z bosons

With the momentum of the Z boson p_3 having been calculated, the momenta of the decay products p_5 and p_6 will now be computed in the class `TwoBodyDecay`. In the CMS of the decaying Z boson:

$$p_3 = p_5 + p_6 = (E_5 + E_6, 0)^T = (\sqrt{s_3}, 0)^T \quad (3.133)$$

Therefrom, one derives E_5:

$$\begin{aligned} (p_5 + p_6) \cdot p_5 &= \sqrt{s_3} E_5 \\ \Rightarrow E_5 &= \frac{p_5^2 + p_5 \cdot p_6}{\sqrt{s}} \\ &= \frac{\frac{1}{2}s_3 + \frac{1}{2}m_5^2 - \frac{1}{2}m_6^2}{\sqrt{s}} \\ &= \frac{s_3 + m_5^2 - m_6^2}{2\sqrt{s}} \end{aligned} \quad (3.134)$$

with $s_3 = (p_5 + p_6)^2$ and E_6 analogously:

$$E_6 = \frac{s + m_5^2 - m_6^2}{2\sqrt{s}}. \quad (3.135)$$

For the 3 momenta one finds

$$|\vec{p}_5| = |\vec{p}_6| = \sqrt{E_1^2 - m_1^2} \quad (3.136)$$

$$= \frac{1}{2\sqrt{s}} \sqrt{s - (m_1 + m_2)^2)} \sqrt{s - (m_1 - m_2)^2)}. \quad (3.137)$$

For an isotropic distribution of the decay products, $\cos\theta_1$ and $\cos\theta_2$ as well as ϕ_1 and ϕ_2 are equally distributed. Finally, the momenta are boosted from the CMS of the decay products to the hadron CMS, i.e. the laboratory frame.

Monte Carlo integration

In the last subsection, I have shown how to parametrize the momenta p_j and hence the Feynman amplitude square $|\mathcal{M}|^2$ and the invariant phase space $d\Phi$ by a set of ten random variables $\{r_i\}_{i=1}^{10}$. As these variables are equally generated in $[0,1]$ it is possible to perform a Monte Carlo integration over a 10 dimensional hypercube. The integrand is composed of three factors,

$$d\sigma = \underbrace{|\mathcal{M}(p_1,p_2;p_5,p_6,p_7,p_8)|^2}_{\texttt{ampSqr}} \underbrace{(2\pi)^4 \left(\prod_f \frac{d^3p_f}{(2\pi)^3}\frac{1}{2E_f}\right)\frac{1}{2E_1E_2|v_1-v_2|}}_{\texttt{weight}} \underbrace{f_g(x_1,Q^2)f_g(x_2,Q^2)}_{\texttt{isp}}, \qquad (3.138)$$

where the δ function is implicit in the phase space parametrization.

The total cross section σ is obtained as integral over the hypercube while the distributions $\frac{d\sigma}{dx}$ are obtained as histograms of the quantity x (cf. A.4).

So far, the calculation has been performed in natural units with $\hbar = c = 1$, leading to cross sections with the dimension of an energy. To get cross sections with the dimension of an area, one finally multiplies with the factor

$$(\hbar c)^2 = 3.893796623 \cdot 10^8 \frac{\text{pb}}{\text{GeV}^2}. \qquad (3.139)$$

3.3.5. Checks II

Comparison with $gg \to WW$

For gluon-induced WW backgrounds, there exists a "pret-à-porter" program, `GG2WW` [42, 43] for the process $gg \to W^+W^- \to (l\bar{\nu})(\bar{l}'\nu')$. As the diagrams for $gg \to W^+W^-$ (cf. fig. 3.10) are topologically very similar to the $gg \to Z^*Z^*$ diagrams, the computation can be checked by compensating all remaining differences in the diagrams and then comparing the results, for example the total cross sections. They should be equal up to the accuracy of the Monte Carlo integration.

The necessary changes affect the $q\bar{q}Z$ couplings in the box amplitude,

$$-i\gamma^\mu(g_v - g_A\gamma_5), \qquad (3.140)$$

that are changed to $q\bar{q}'W$ couplings

$$-i\frac{g}{\sqrt{2}}\gamma^\mu\frac{1-\gamma_5}{2}. \qquad (3.141)$$

Furthermore, the same couplings appear in the leptonic currents

$$J_3^{\nu_3} = \frac{1}{2}\bar{v}(p_6)\gamma^{\mu_3}(g_V - g_A\gamma_5)u(p_5), \qquad (3.142)$$

$$J_4^{\nu_4} = \frac{1}{2}\bar{v}(p_8)\gamma^{\mu_4}(g_V - g_A\gamma_5)u(p_7) \qquad (3.143)$$

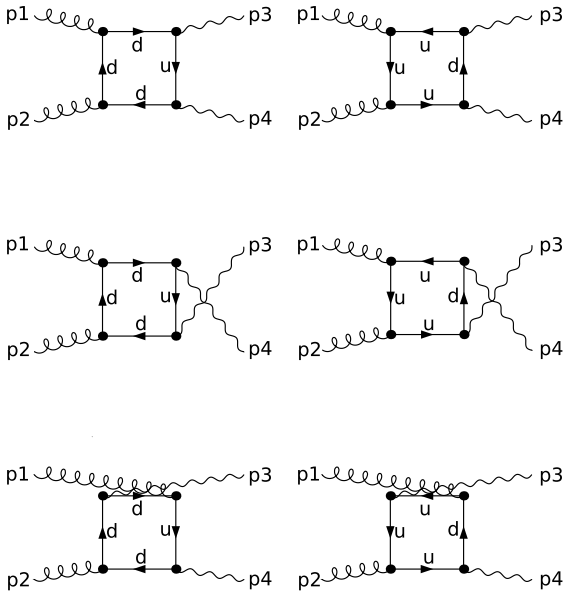

Figure 3.10.: For the process $gg \to W^{+*}W^{-*}$ there exist only 6 box diagrams; contributions from triangle diagrams vanish, cf. [42, 43]

that are changed to

$$J_3^{\nu_3} = \frac{1}{2}\bar{v}(p_6)\frac{g}{\sqrt{2}}\gamma^{\mu_3}\frac{1-\gamma_5}{2}u(p_5), \tag{3.144}$$

$$J_4^{\nu_4} = \frac{1}{2}\bar{v}(p_8)\frac{g}{\sqrt{2}}\gamma^{\mu_4}\frac{1-\gamma_5}{2}u(p_7) \tag{3.145}$$

The Z boson mass and width, appearing for example in the propagators for both Z bosons, are changed to W boson mass and width, respectively.

The diagrams are now formally equivalent, but in the $gg \to W^+W^-$ calculation there are only half as many diagrams (compare 3.10 with 3.3). Taking into account this factor of $\frac{1}{2}$ on the amplitude level and the factor for the Bose symmetry of the Zs, the total cross sections of both calculations for the massless case are in excellent agreement.

For the massive case, the $q\bar{q}'W$ couplings give rise to different flavors in the quark loop. But as the only distinction between the quarks of different flavors is the mass, since other quantum numbers have no effect in the $q\bar{q}'W$ couplings, it suffices to degenerate the bottom and top mass. Then, the agreement of the results of both computations is again excellent.

limit: massive → massless case

Another strong check is possible within our calculation. Consistency of the massless and massive case demand that the contributions for one quark generation agree in the

limit $m_q \to 0$. Since some of the basis functions occurring for the massive case are IR divergent when setting the masses to 0, one cannot just set $m_b = m_t = 0$. Instead, one can extrapolate the behavior for small masses to the limit $m_b = m_t \to 0$. The result from the massive case in this limit and the result from the massless case then agree.

3.4. Results

To show the potentials of my program, I will present some total cross sections and distributions of various observables. This chapter is not meant to present a comprehensive analysis, but to give an impression of the dynamics of the $gg \to Z^*Z^* \to (e^-e^+)(\mu^-\mu^+)$ background.

I therefore calculated the contributions of two massless and one massive generation of quarks with the bottom and top quark masses being 4.4 and 178 GeV, respectively. For the parton density functions I applied the CTEQ6M set from the Les Houches Accord Parton Density Functions (LHAPDF) [31]. The strong coupling α_s has been evaluated at the Z mass scale, also via the LHAPDF routines. As electroweak parameters, the Fermi coupling $G_F = 1.16639 \cdot 10^{-5}\,\mathrm{GeV}^{-2}$, the W mass $m_W = 80.419\,\mathrm{GeV}$ and the Z mass $m_Z = 91.188\,\mathrm{GeV}$ have been given as input. Therefrom, the weak mixing angle θ_W and the fine structure constant α have been derived as $\sin^2\theta_W = 1 - \left(\frac{m_W}{m_Z}\right)^2 \approx 0.222$ and $\alpha = \frac{\sqrt{2}}{\pi} G_F m_W \sin^2\theta_W \approx 1/132.507$, respectively. The mass of the Higgs boson has been set to 200 GeV to be above the threshold for Z production.

3.4.1. The total cross section

At first, I compare the contributions from three processes to the total cross sections:

- the gluon-induced Higgs signal;
- continuous ZZ production background from $q\bar{q}$ annihilation;
- continuous ZZ production background from gluon fusion;

As already stated in the previous chapter, the cancellation of as many Gram determinants as possible leads to such a numerically stable solution that a technical cut on the transverse Z momenta of $p_{TZ} > 4\,\mathrm{GeV}$ was sufficient. The contributions from the different processes can be found in table 3.1

$pp \to Z^*Z^* \to (l\bar{l})(l'\bar{l}')$ $[fb]$		
Higgs	gg	Higgs + gg
6.803	9.538	16.81

Table 3.1.: Total cross sections form the Higgs signal, the gg background, $q\bar{q}$ annihilation background in LO and NLO and from both, Higgs signal and gluon fusion background.

3.4.2. Distributions

Invariant mass distributions of 4 leptons

The most obvious observable for Higgs searches is the invariant mass of both Z bosons which is identical to the invariant mass of the four leptons in the final state. As the

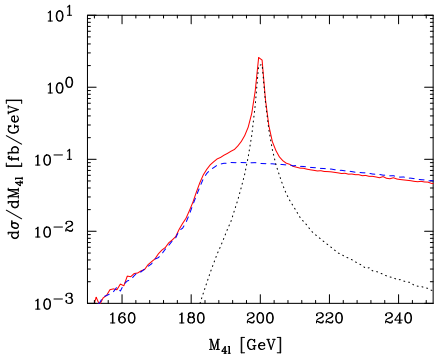

Figure 3.11.: Invariant mass distribution of all 4 leptons $\frac{d\sigma}{dm_{4l}}$ with a Higgs mass of $m_H = 200\text{GeV}/c^2$. signal: black (dotted), background from gluon fusion: blue (dashed), signal and gluon fusion background: red (solid)

electrons and positrons as well as the muons and antimuons can be detected, it is experimentally easily accessible. In figure 3.11, the mass peak of the Higgs boson can be clearly identified. The background increases already for invariant masses below $2m_Z$ due to the finite width of the Z bosons.

Distributions of intermediate Z bosons

The transverse momentum distribution of the Z bosons (fig. 3.12) shows an interesting feature, since the distributions for the signal and the background are peaked at different values. While the distribution of the Z bosons from the decay of the Higgs boson has a maximum at about 40 GeV, the distributions of the Z bosons produced in the quark box has a smaller maximum at about 10 GeV transverse momenta and is less sharply peaked.

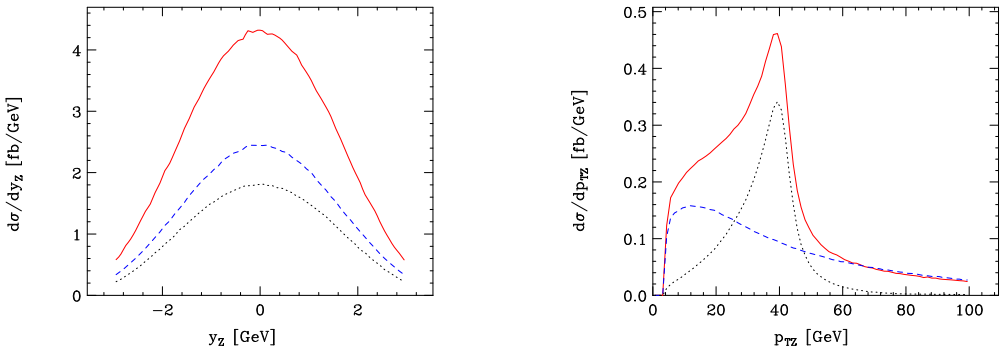

Figure 3.12.: Rapidity distribution $\frac{d\sigma}{dy_Z}$ (left) and transverse momentum distribution $\frac{d\sigma}{dp_{TZ}}$ of one Z boson. signal: black (dotted), background from gluon fusion: blue (dashed), signal and gluon fusion background: red (solid)

The invariant mass distribution (3.13) does not seem exceptional, one observes the Z

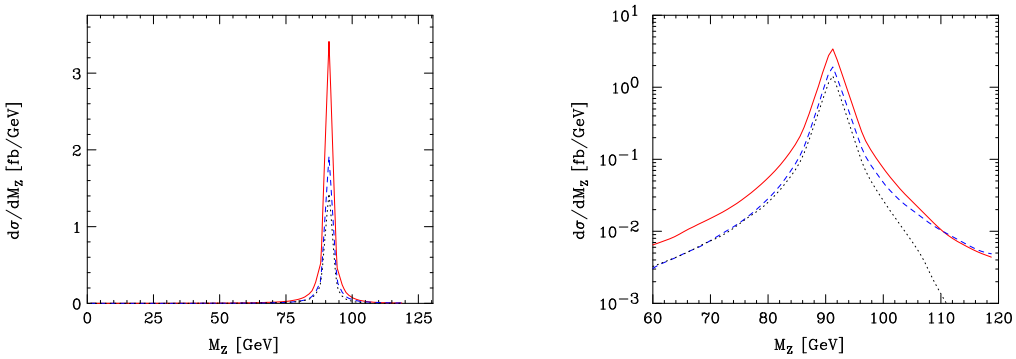

Figure 3.13.: Invariant mass distribution $\frac{d\sigma}{dm_Z}$ of one Z boson. signal: black (dotted), background from gluon fusion: blue (dashed), signal and gluon fusion background: red (solid)

mass peaks. In a logarithmic representation, one sees that the signal falls faster above the Z resonance than the background and the sum of both thus consists effectively only of the background.

Distributions of single leptons

The leptons both from the Higgs signal process and from the gluon-induced background are produced centrally in terms of pseudorapidity distribution (fig. 3.14) and less leptons are produced with higher transverse momenta (fig. 3.15). For the signal, the distribution almost vanishes for $p_{Tl} > 80\,\mathrm{GeV}/c^2$ while for the background there are also leptons with higher transverse momenta. This can be understood since already for the Z bosons the transverse momentum distribution extends to higher momenta (cf. 3.12).

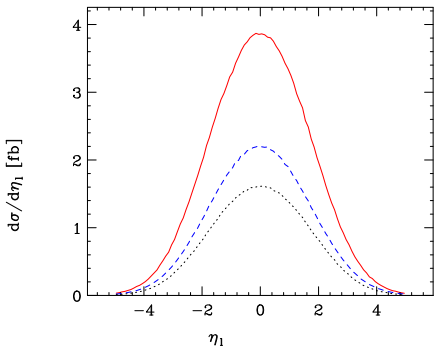

Figure 3.14.: Pseudorapidity distribution $\frac{d\sigma}{d\eta_l}$ of one final state lepton, assuming a Higgs mass of $m_H = 200\,\mathrm{GeV}/c^2$. signal: black (dotted), background from gluon fusion: blue (dashed), signal and gluon fusion background: red (solid)

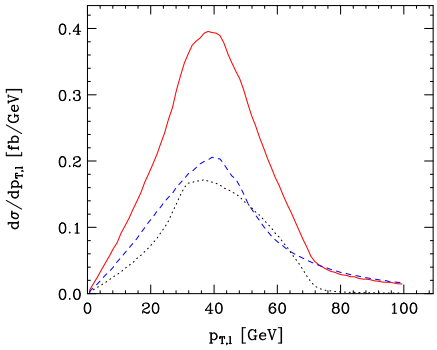

Figure 3.15.: Transverse momentum distribution $\frac{d\sigma}{dp_{Tl}}$ of one final state lepton, assuming a Higgs mass of $m_H = 200\text{GeV}/c^2$. signal: black (dotted), background from gluon fusion: blue (dashed), signal and gluon fusion background: red (solid)

Relative distributions of 2 leptons

I will now present some distributions for the relative orientation of two leptons which are emitted from the same Z boson. The production of leptons with smaller differences $\Delta\eta_{ll}$ in pseudorapidity (fig. 3.16 (left)) is more likely than with larger differences. The angle $\Delta\Phi_{ll}$ tends generally to larger values. The two leptons are thus most often produced nearly back to back since Z bosons that are boosted strongly with respect to the lab frame are very unlikely (cf. fig. 3.12).

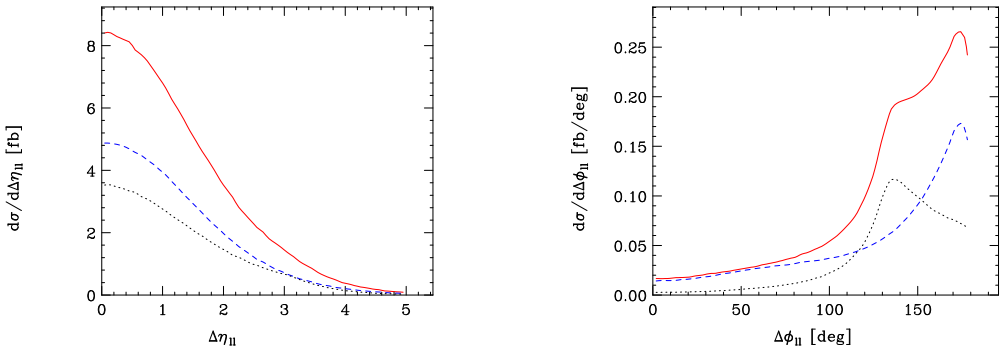

Figure 3.16.: Distribution of the difference in pseudorapidities $\Delta\eta$ (left) and of the azimuthal opening angle $\Delta\phi$ (right) of two leptons from the same Z, $\frac{d\sigma}{d\Delta\eta}$. signal: black (dotted), background from gluon fusion: blue (dashed), signal and gluon fusion background: red (solid)

For the distance ΔR_{ll} defined by

$$\Delta R_{ll} = \sqrt{(\Delta\eta)^2 + (\Delta\phi)^2} \tag{3.146}$$

this difference shows up again, since the Higgs signal again peaks at smaller distances

ΔR_{ll} than the gg background (fig 3.18).

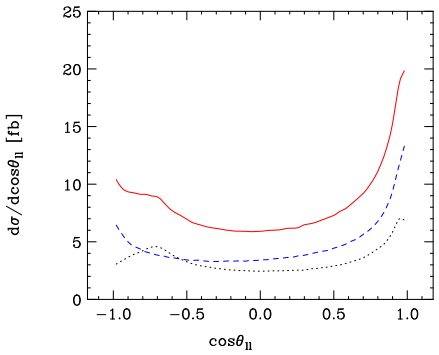

Figure 3.17.: Distribution of the polar angle θ_{ll} between two leptons from one Z boson, $\frac{d\sigma}{d\cos\theta}$. signal: black (dotted), background from gluon fusion: blue (dashed), signal and gluon fusion background: red (solid)

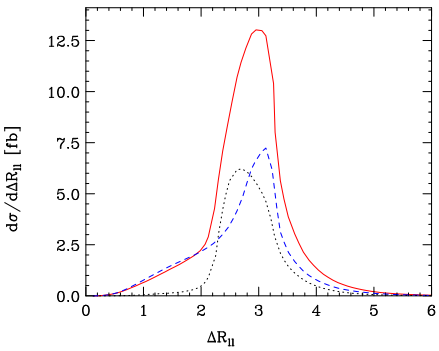

Figure 3.18.: Distribution of the distance ΔR, $\frac{d\sigma}{dR_{ll}}$ of two leptons from one Z. signal: black (dotted), background from gluon fusion: blue (dashed), signal and gluon fusion background: red (solid)

4. Summary

In this work, I calculate the loop-induced production of four charged leptons in gluon fusion via two off-shell Z bosons.

I started by reviewing the fundamentals of electroweak $SU(2)_L \times U(1)$ theory, with the lepton matter fields composed of a left-handed doublet and a right-handed singlet and the gauge fields introduced by postulating non-Abelian gauge invariance. Generating mass terms, both for gauge bosons and leptons, can be explained by a spontaneous breaking of gauge symmetry achieved by introduction of a doublet of complex scalar fields with non-vanishing vacuum expectation value. In the end, only one degree of freedom remains, the physical Higgs field. Demanding the known electric couplings leads to four gauge fields for electroweak interactions: Two charged ones, the W^+ and W^- bosons, as well as two neutral ones, the Z boson and the photon.

Afterwards, I briefly provided insight into Higgs boson searches at hadron colliders. After reviewing constraints on the Higgs mass, both from experimental results and from theoretical considerations, the fundamental production and decay modes were presented, finding that gluon fusion is the most important production channel for energies in the TeV range. I explained that for Higgs boson masses above 180 GeV, the decay $H \to Z^*Z^*$ is a favored channel since it allows for a reconstruction of the Higgs boson mass. I concluded this introductory chapter by presenting the main backgrounds to this signal process both at the Tevatron and the Large Hadron Collider. Here, I pointed out that besides the known quark-antiquark annihilation, $q\bar{q} \to Z^*Z^*$, the continuum Z production from gluon fusion is important.

After this phenomenological considerations, I calculated the contribution from quark-antiquark annihilation, $q\bar{q} \to ZZ$, in LO. Firstly, I introduced the parton model and presented some basic techniques. I showed a simple parametrization for two particle phase space and calculated both the differential and the total partonic cross section and finally obtained the total hadronic cross section.

Thereafter, I attended to the loop induced process $gg \to Z^*Z^*$ with off-shell Z bosons. Presenting all double-resonant box and triangle topologies, I showed that only the boxes survive. Single resonant diagrams were shown to vanish, too, mainly due to Furrys theorem and cancellations between the remaining diagrams.

In the following I dealt with contributions from double-resonant diagrams. The determination of the tensor structure started by decomposing the scattering tensor $\mathcal{M}^{\mu_1\mu_2\mu_3\mu_4}$ into Lorentz covariants. After contractions with the gluon polarization vectors and the leptonic currents from Z boson decay to charged leptons, I explicitly showed the gauge invariance of the Feynman amplitude. Then, I introduced helicity amplitudes thus achieving further simplifications to a linear combination of nine independent tensor structures.

I then cited a technique for reduction of tensor and scalar integrals. I could define a set of basis functions which remain when this scheme is applied to the amplitude. I showed by pinching of the diagrams that only $(n+2)$-dimensional scalar boxes, n dimensional scalar triangles and n-dimensional scalar bubbles are present in the amplitude.

Afterwards, I presented the implementation in detail. Since the computation is analytical as long as possible it can be modified easily to cover similar processes like $gg \to Z^*\gamma^*, \gamma^*\gamma^*$. I started with generating the amplitude for each diagram and performing manipulations separately for both independent helicity amplitudes. They were finally expressed in terms of tensor structures and scalar integrals. Their coefficients were then simplified and the contributions from all diagrams were added. I then performed a first check one the amplitude. From Bose and CP invariance of the amplitude I derived relations of the coefficients, which I checked with two programs. For calculating cross sections, I presented a phase space parametrization which is suitable for Monte Carlo integration. As a second kind of check, I tested the consistency of my program and its compatibility with another program for a similar process, and again found excellent agreement.

Finally, to show the ability of my program, I presented the total cross section for the $gg \to Z^*Z^* \to (l\bar{l})(l'\bar{l}')$ background process and compared it to the Higgs signal process $gg \to H \to Z^*Z^* \to (l\bar{l})(l'\bar{l}')$. Moreover, I showed a number of distributions of observables which can be of interest in Higgs searches.

A. Appendix

A.1. Spinor helicity formalism

Massless spinors

The massless spinors $u(p)$ and $v(p)$ satisfy the Dirac equation

$$\not{p}\, u(p) = \not{p}\, v(p) = \bar{u}(p)\, \not{p} = \bar{v}(p)\, \not{p} = 0. \tag{A.1}$$

The helicity parts can be obtained by projection:

$$u_\pm(p) := \frac{1 \pm \gamma_5}{2} u(p), \qquad \bar{u}_\pm(p) := \bar{u}(p) \frac{1 \mp \gamma_5}{2}, \tag{A.2}$$

$$v_\pm(p) := \frac{1 \mp \gamma_5}{2} v(p), \qquad \bar{v}_\pm(p) := \bar{v}(p) \frac{1 \pm \gamma_5}{2}, \tag{A.3}$$

so that different subspaces are orthogonal:

$$\frac{1 \mp \gamma_5}{2} u_\pm(p) = \frac{1 \pm \gamma_5}{2} v_\pm(p) = 0, \tag{A.4}$$

$$\bar{u}_\pm(p) \frac{1 \pm \gamma_5}{2} = \bar{v}_\pm(p) \frac{1 \mp \gamma_5}{2} = 0. \tag{A.5}$$

Following [33] and [44], one introduces the bra-ket notation:

$$|p_\pm\rangle := u_\pm(p) = v_\mp(p), \tag{A.6}$$

$$\langle p_\pm| := \bar{u}_\pm(p) = \bar{v}_\mp(p) \tag{A.7}$$

with the abbreviations

$$\langle pq\rangle := \langle p_-|q_+\rangle, \tag{A.8}$$

$$[pq] := \langle p_+|q_-\rangle. \tag{A.9}$$

$$\tag{A.10}$$

The spinors are normalized as usual:

$$\langle p_\pm|\gamma_\mu|p_\pm\rangle = 2p_\mu. \tag{A.11}$$

I will now cite some relations that will be of use calculating polarization vectors and leptonic currents:

$$\langle p_\pm|q_\pm\rangle = \left(\langle p_\pm|\frac{1\mp\gamma_5}{2}\right)|q_\pm\rangle = \langle p_\pm|\underbrace{\frac{1\mp\gamma_5}{2}|q_\pm\rangle}_{0} = 0, \tag{A.12}$$

$$|q+\rangle\langle p+| = \langle p+|\gamma^\mu|q+\rangle\gamma_\mu\frac{1}{4}(1-\gamma_5), \tag{A.13}$$

$$\Rightarrow |p_\pm\rangle\langle p_\pm| = \frac{1\pm\gamma_5}{2}\not{p}, \tag{A.14}$$

$$\langle p_-|p_+\rangle = \langle p_+|p_-\rangle = 0, \tag{A.15}$$

$$\langle p_-|q_+\rangle = -\langle q_-|p_+\rangle, \tag{A.16}$$

$$\langle p\pm|\gamma_{\mu_1}\dots\gamma_{\mu_{2n+1}}|q\pm\rangle = \langle q\mp|\gamma_{\mu_{2n+1}}\dots\gamma_{\mu_1}|p\mp\rangle, \tag{A.17}$$

$$\langle p+|\gamma_\mu|q+\rangle\langle r-|\gamma^\mu|s-\rangle = 2\,[ps]\,\langle qr\rangle, \tag{A.18}$$

$$|\langle pq\rangle|^2, = 2p\cdot q \tag{A.19}$$

$$\langle pq\rangle^* = \langle p_-|q_+\rangle^* = \langle q+|p-\rangle, \tag{A.20}$$

$$\langle pq\rangle = \langle p_-|q_+\rangle = -\langle q-|p+\rangle = -\langle qp\rangle, \tag{A.21}$$

$$[pq] = \langle p_+|q_-\rangle = -\langle pq\rangle^*. \tag{A.22}$$

Polarization vectors

One can introduce polarization vectors by referring to another momentum vector q ($q^2 = 0$):

$$\epsilon_\mu^+(p,q) := \frac{\langle q_-|\gamma_\mu|p_-\rangle}{\sqrt{2}\langle qp\rangle}, \tag{A.23}$$

$$\epsilon_\mu^-(p,q) := \frac{\langle q_+|\gamma_\mu|p_+\rangle}{\sqrt{2}\langle qp\rangle^*}. \tag{A.24}$$

This reference momentum can now be chosen freely without changing amplitude with this polarization vector. For proof, one shows that the difference between two polarization vectors for the same momentum k but different reference vectors q and p is proportional to the momentum k:

$$\begin{aligned}
\epsilon_\mu^+(k,q) - \epsilon_\mu^+(k,p) &= \frac{\langle q_-|\gamma_\mu|p_-\rangle}{\sqrt{2}\langle qk\rangle} - \frac{\langle p_-|\gamma_\mu|p_-\rangle}{\sqrt{2}\langle pk\rangle} \\
&= \frac{-\langle q_-|\gamma_\mu|p_-\rangle\langle p_-|p_+\rangle + \langle p_-|\gamma_\mu|p_-\rangle\langle p_-|q_+\rangle}{\sqrt{2}\langle pk\rangle\langle qk\rangle} \\
&= \frac{-\langle q_-|\gamma_\mu\frac{1-\gamma_5}{2}\not{k}|p_+\rangle + \langle p_-|\gamma_\mu\frac{1-\gamma_5}{2}\not{k}|q_+\rangle}{\sqrt{2}\langle pk\rangle\langle qk\rangle} \\
&= \frac{-\langle q_-|\frac{1+\gamma_5}{2}\gamma_\mu\not{k}|p_+\rangle + \langle p_-|\frac{1+\gamma_5}{2}\gamma_\mu\not{k}|q_+\rangle}{\sqrt{2}\langle pk\rangle\langle qk\rangle} \\
&= \frac{-\langle q_-|\gamma_\mu\not{k}|p_+\rangle + \langle p_-|\gamma_\mu\not{k}|q_+\rangle}{\sqrt{2}\langle pk\rangle\langle qk\rangle} \\
&= \frac{\sqrt{2}\langle p_-|k_\mu|q_+\rangle}{\langle pk\rangle\langle qk\rangle} \\
&= \frac{\sqrt{2}\langle pq\rangle}{\langle pk\rangle\langle qk\rangle}k_\mu \\
\Rightarrow \epsilon_\mu^+(k,q) &= \epsilon_\mu^+(k,p) + \frac{\sqrt{2}\langle pq\rangle}{\langle pk\rangle\langle qk\rangle}k_\mu.
\end{aligned} \tag{A.25}$$

Given gauge invariance and thus the Ward identity, the difference must vanish. As the reference momentum can thus be chosen freely, it will be suppressed as argument from now on. Then, in a somehow shorter notation:

$$\epsilon_\mu^+(p_1) := \frac{\langle 2_-|\mu|1_-\rangle}{\sqrt{2}\langle 2_-|1_+\rangle}, \tag{A.26}$$

$$\epsilon_\mu^-(p_1) := \frac{\langle 2_+|\mu|1_+\rangle}{\sqrt{2}\langle 2_+|1_-\rangle}, \tag{A.27}$$

$$\epsilon_\mu^+(p_2) := \frac{\langle 1_-|\mu|2_-\rangle}{\sqrt{2}\langle 1_-|2_+\rangle}, \tag{A.28}$$

$$\epsilon_\mu^-(p_2) := \frac{\langle 1_+|\mu|2_+\rangle}{\sqrt{2}\langle 1_+|2_-\rangle}. \tag{A.29}$$

For the $+-$ helicity amplitude, one calculates

$$\begin{aligned}
\epsilon_1^+ \cdot \epsilon_2^+ &= \epsilon^{+\mu}(p_1)\epsilon_\mu^+(p_2) \\
&= \frac{\langle 2_-|\mu|1_-\rangle}{\sqrt{2}\langle 2_-|1_+\rangle}\frac{\langle 1_-|\mu|2_-\rangle}{\sqrt{2}\langle 1_-|2_+\rangle} \\
&= \frac{1}{2\langle 21\rangle\langle 12\rangle}\frac{\langle 21\rangle^*}{\langle 21\rangle^*}\langle 2_-|\mu|1_-\rangle\langle 1_-|\mu|2_-\rangle \\
&= -\frac{1}{2s}\frac{[12]}{\langle 12\rangle}|2_-\rangle\langle 2_-|\gamma^\mu|1_-\rangle\langle 1_-|\gamma_\mu \\
&= -\frac{1}{2s}\frac{[12]}{\langle 12\rangle}\mathrm{tr}\left[\frac{1_-\gamma_5}{2}\not{p}_2\gamma^\mu\frac{1_-\gamma_5}{2}\not{p}_1\gamma_\mu\right] \\
&= -\frac{1}{2s}\frac{[12]}{\langle 12\rangle}\left(\frac{1}{2}\mathrm{tr}\left[\not{p}_2\gamma^\mu\not{p}_1\gamma_\mu\right] - \frac{1}{2}\mathrm{tr}\left[\gamma_5\not{p}_2\gamma^\mu\not{p}_1\gamma_\mu\right]\right) \\
&= -\frac{1}{2s}\frac{[12]}{\langle 12\rangle}\left(\underbrace{-\mathrm{tr}\left[\not{p}_2\not{p}_1\right]}_{-4p_1\cdot p_2=-2s} + \underbrace{\mathrm{tr}\left[\gamma_5\not{p}_2\not{p}_1\right]}_{=0}\right) \\
&= \frac{[12]}{\langle 12\rangle}
\end{aligned} \tag{A.30}$$

and

$$
\begin{aligned}
\epsilon^{+\mu}(p_1)\epsilon^{+\nu}(p_2) &= \frac{\langle 2_-|\mu|1_-\rangle}{\sqrt{2}\langle 2_-|1_+\rangle}\frac{\langle 1_-|\nu|2_-\rangle}{\sqrt{2}\langle 1_-|2_+\rangle} \\
&= \frac{1}{2}\frac{1}{\langle 12\rangle}\frac{\langle 21\rangle^*}{\langle 21\rangle\langle 21\rangle^*}\langle 2_-|\mu|1_-\rangle\langle 1_-|\nu|2_-\rangle \\
&= -\frac{1}{2s}\frac{[12]}{\langle 12\rangle}|2_-\rangle\langle 2_-|\gamma^\mu|1_-\rangle\langle 1_-|\gamma^\nu \\
&= -\frac{1}{2s}\frac{[12]}{\langle 12\rangle}\mathrm{tr}\left(\frac{1+\gamma_5}{2}\not{p}_2\gamma^\mu\frac{1+\gamma_5}{2}\not{p}_1\gamma^\nu\right) \\
&= -\frac{1}{4s}\frac{[12]}{\langle 12\rangle}\left(\mathrm{tr}\left(\not{p}_2\gamma^\mu\not{p}_1\gamma^\nu\right)+\mathrm{tr}\left(\gamma_5\not{p}_2\gamma^\mu\not{p}_1\gamma^\nu\right)\right) \\
&= -\frac{1}{s}\frac{[12]}{\langle 12\rangle}\left(p_1^\mu p_2^\nu + p_1^\nu p_2^\mu - p_1\cdot p_2 g^{\mu\nu} - \epsilon(p_1,\gamma^\nu,p_2,\gamma^\mu)\right), \quad \text{(A.31)}
\end{aligned}
$$

where $\frac{[12]}{\langle 12\rangle}$ is a pure phase factor. To substitute it in A.31, one contracts this relation with $p_{3\mu}p_{3\nu}$:

$$
\begin{aligned}
&\epsilon^{+\mu}(p_1)\epsilon^{+\nu}(p_2)p_{3\mu}p_{3\nu} \\
&= \epsilon_1^+\cdot p_3 \quad \epsilon_2^+\cdot p_3 \\
&= -\frac{1}{s}\frac{[12]}{\langle 12\rangle}\left(p_1\cdot p_3 \quad p_2\cdot p_3 + p_1\cdot p_3 \quad p_2\cdot p_3 - p_1\cdot p_2 p_3^2 - \underbrace{\epsilon(p_1,p_3,p_2,p_3)}_{=0}\right) \\
&= -\frac{1}{s}\frac{[12]}{\langle 12\rangle}\left(2\frac{u-s_3}{2}\frac{t-s_3}{2}-\frac{s}{2}s_3\right) \\
&= -\frac{1}{2s}\frac{[12]}{\langle 12\rangle}\left(ut-us_3-ts_3+s_3^2-ss_3\right) \\
&= -\frac{1}{2s}\frac{[12]}{\langle 12\rangle}\left(tu - s_3\underbrace{(u-t-s_3-s)}_{s_4}\right) \\
&= -\frac{1}{2s}\frac{[12]}{\langle 12\rangle}\left(tu-s_3s_4\right) \\
\Rightarrow \epsilon_1^+\cdot\epsilon_2^+ &= \frac{[12]}{\langle 12\rangle} = -\frac{2s}{tu-s_3s_4}\epsilon_1^+\cdot p_3 \quad \epsilon_2^+\cdot p_3. \qquad \text{(A.32)}
\end{aligned}
$$

For the $+-$ amplitude one finds

$$
\begin{aligned}
\epsilon_1^+ \cdot \epsilon_2^- &= \epsilon^{+\mu}(p_1)\epsilon_\mu^-(p_2) \\
&= \frac{\langle 2_-|\mu|1_-\rangle}{\sqrt{2}\langle 2_-|1_+\rangle}\frac{\langle 1_+|\mu|2_+\rangle}{\sqrt{2}\langle 1_+|2_-\rangle} \\
&= \frac{1}{2\langle 21\rangle\langle 21\rangle^*}\underbrace{\langle 2_-|\gamma^\mu|1_-\rangle\langle 1_+|\gamma_\mu|2_+\rangle}_{\overset{eq.\underline{A}.18}{=}2\underbrace{[11]}_{=0}\underbrace{\langle 22\rangle}_{=0}} \\
&= 0
\end{aligned}
\tag{A.33}
$$

and

$$
\begin{aligned}
&\epsilon^{+\mu}(p_1)\epsilon^{-\nu}(p_2) \\
&= \frac{\langle 2_-|\mu|1_-\rangle}{\sqrt{2}\langle 2_-|1_+\rangle}\frac{\langle 1_+|\nu|2_+\rangle}{\sqrt{2}\langle 1_+|2_-\rangle} \\
&= \frac{\langle 2_-|\mu|1_-\rangle}{\sqrt{2}\langle 2_-|1_+\rangle}\frac{\langle 2_-|\nu|1_-\rangle}{\sqrt{2}\langle 1_+|2_-\rangle} \\
&= \frac{1}{2}\frac{1}{\langle 21\rangle}\frac{1}{[12]}\langle 2_-|\mu|1_-\rangle\overbrace{\frac{\langle 1_-|\not{p}_3|2_-\rangle^2}{\langle 1_-|\not{p}_3|2_-\rangle^2}}^{1}\langle 2_-|\nu|1_-\rangle \\
&= \frac{1}{2s}\frac{1}{\langle 1_-|\not{p}_3|2_-\rangle^2}\underbrace{|2_-\rangle\langle 2_-|\gamma^\mu|1_-\rangle\langle 1_-|\not{p}_3}_{\mathrm{tr}\left[\frac{1-\gamma_5}{2}\not{p}_2\gamma^\mu\frac{1-\gamma_5}{2}\not{p}_1\not{p}_3\right]}\underbrace{|2_-\rangle\langle 2_-|\gamma^\nu|1_-\rangle\langle 1_-|\not{p}_3}_{\mathrm{tr}\left[\frac{1-\gamma_5}{2}\not{p}_2\gamma^\nu\frac{1-\gamma_5}{2}\not{p}_1\not{p}_3\right]} \\
&= \frac{1}{2s}\frac{1}{\langle 1_-|\not{p}_3|2_-\rangle^2}\frac{\langle 2_-|\not{p}_3|1_-\rangle}{\langle 2_-|\not{p}_3|1_-\rangle}\mathrm{tr}\left[\not{p}_1\not{p}_3\frac{1-\gamma_5}{2}\not{p}_2\gamma^\mu\frac{1-\gamma_5}{2}\right]\mathrm{tr}\left[\not{p}_1\not{p}_3\frac{1-\gamma_5}{2}\not{p}_2\gamma^\nu\frac{1-\gamma_5}{2}\right] \\
&= \frac{1}{2s}\underbrace{\frac{1}{\langle 1_-|\not{p}_3|2_-\rangle\langle 2_-|\not{p}_3|1_-\rangle}}_{=\frac{1}{ut-s_3s_4}}\frac{\langle 2_-|\not{p}_3|1_-\rangle}{\langle 1_-|\not{p}_3|2_-\rangle}\left(\frac{1}{2}\mathrm{tr}\left[\not{p}_1\not{p}_3\not{p}_2\gamma^\mu\right]-\frac{1}{2}\mathrm{tr}\left[\gamma_5\not{p}_1\not{p}_3\not{p}_2\gamma^\mu\right]\right) \\
&\quad\cdot\left(\frac{1}{2}\mathrm{tr}\left[\not{p}_1\not{p}_3\not{p}_2\gamma^\mu\right]-\frac{1}{2}\mathrm{tr}\left[\gamma_5\not{p}_1\not{p}_3\not{p}_2\gamma^\nu\right]\right) \\
&= \frac{\mathrm{tr}^-[\not{p}_1\not{p}_3\not{p}_2\gamma^\mu]\mathrm{tr}^-[\not{p}_1\not{p}_3\not{p}_2\gamma^\nu]}{2s(ut-s_3s_4)}\frac{\langle 2_-|\not{p}_3|1_-\rangle}{\langle 1_-|\not{p}_3|2_-\rangle}
\end{aligned}
\tag{A.34}
$$

with tr^- defined by

$$
\mathrm{tr}^-[\gamma^\mu\gamma^\nu\gamma^\rho\gamma^\sigma] := \frac{\mathrm{tr}\left[\gamma^\mu\gamma^\nu\gamma^\rho\gamma^\sigma\right]-\mathrm{tr}\left[\gamma_5\gamma^\mu\gamma^\nu\gamma^\rho\gamma^\sigma\right]}{2} \tag{A.35}
$$

and where it has been used that

$$
\begin{aligned}
\langle 1_-|\not{p}_3|2_-\rangle\langle 2_-|\not{p}_3|1_-\rangle &= \mathrm{tr}\left[\frac{1-\gamma_5}{2}\not{p}_1\not{p}_3\frac{1-\gamma_5}{2}\not{p}_2\not{p}_3\right] \\
&= \frac{1}{2}\mathrm{tr}\left[\not{p}_1\not{p}_3\not{p}_2\not{p}_3\right] - \frac{1}{2}\underbrace{\mathrm{tr}\left[\gamma_5\not{p}_1\not{p}_3\not{p}_2\not{p}_3\right]}_{\epsilon^{p_1p_3p_2p_3}=0} \\
&= 2\left(p_1\cdot p_3 \quad p_2\cdot p_3 - p_1\cdot p_2 \quad p_3\cdot p_3 + p_1\cdot p_3 \quad p_2\cdot p_3\right) \\
&= 2\left(2\frac{u-s_3}{2}\frac{t-s_3}{2} - \frac{s}{2}s_3\right) \\
&= ut - us_3 - ts_3 + s_3^2 - ss_3 \\
&= tu - s_3\underbrace{(u+t-s_3+s)}_{s_4} \\
&= ut - s_3s_4 \qquad \text{(A.36)} \\
& \qquad \text{(A.37)}
\end{aligned}
$$

with $\frac{\langle 2-|\not{p}_3|1-\rangle}{\langle 1-|\not{p}_3|2-\rangle}$ being a pure phase factor.

A.2. Leptonic currents

With the $f\bar{f}Z$ coupling

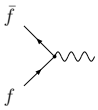

$$= -i\frac{e}{\cos\theta_W\sin\theta_W}\gamma^\mu\left(T_3^f\frac{1-\gamma_5}{2} - Q_f\sin^2\theta_W\right) \qquad \text{(A.38)}$$

the leptonic current $J_{3\mu}$ is

$$J_{3\mu} = \bar{v}(p_6)\gamma_\mu\left(-\frac{1}{2}\frac{1-\gamma_5}{2} + \sin^2\theta_W\right)u(p_5) \qquad \text{(A.39)}$$

when extracting the prefactor of $-i\frac{e}{\cos\theta_W\sin\theta_W}$. The first term in the bracket contributes with

$$
\begin{aligned}
\bar{v}(p_6)\gamma_\mu\frac{1-\gamma_5}{2}u(p_5) &= \bar{v}(p_6)\gamma_\mu\frac{1-\gamma_5}{2}u_-(p_5) \\
&= \bar{v}(p_6)\frac{1+\gamma_5}{2}\gamma_\mu u_-(p_5) \\
&= \bar{v}_+(p_6)\gamma_\mu u_-(p_5) \\
&= \langle 6-|\mu|5-\rangle. \qquad \text{(A.40)}
\end{aligned}
$$

It can be extended and then reads

$$\begin{aligned}
\langle 6-|\mu|5-\rangle &= \langle 6-|\mu|5-\rangle \frac{\langle 5-|2+\rangle\langle 2+|6-\rangle}{\langle 5-|2+\rangle\langle 2+|6-\rangle} \\
&= \frac{1}{\sqrt{s_{25}}\sqrt{s_{26}}}\mathrm{tr}\left[|5-\rangle\langle 5-|2+\rangle\langle 2+|6-\rangle\langle 6-|\mu\right] \\
&= \frac{1}{\sqrt{s_{25}}\sqrt{s_{26}}}\mathrm{tr}\left[\frac{1-\gamma_5}{2}\not{p}_5\frac{1+\gamma_5}{2}\not{p}_2\frac{1-\gamma_5}{2}\not{p}_6\gamma_\mu\right] \\
&= \frac{1}{\sqrt{s_{25}}\sqrt{s_{26}}}\mathrm{tr}\Bigg[\frac{1-\gamma_5}{2}\not{p}_5\underbrace{\left(\frac{1+\gamma_5}{2}\right)^2}_{=1}\not{p}_2\not{p}_6\gamma_\mu\Bigg] \\
&= \frac{1}{2\sqrt{s_{25}}\sqrt{s_{26}}}\left(\mathrm{tr}\left[\not{p}_5\not{p}_2\not{p}_6\gamma_\mu\right]-\mathrm{tr}\left[\gamma_5\not{p}_5\not{p}_2\not{p}_6\gamma_\mu\right]\right) \qquad \text{(A.41)}
\end{aligned}$$

up to a phase factor.

The second term in the bracket contributes with

$$\bar{v}(p_6)\gamma_\mu u(p_5) = \underbrace{\langle 6+|\mu|5+\rangle}_{\langle 5-|\mu|6-\rangle} + \langle 6-|\mu|5-\rangle, \qquad \text{(A.42)}$$

where

$$\begin{aligned}
\langle 5-|\mu|6-\rangle &= \frac{1}{2\sqrt{s_{25}}\sqrt{s_{26}}}\left(\mathrm{tr}\left[\not{p}_6\not{p}_2\not{p}_5\gamma_\mu\right]-\mathrm{tr}\left[\gamma_5\not{p}_6\not{p}_2\not{p}_5\gamma_\mu\right]\right) \qquad \text{(A.43)} \\
&= \frac{1}{2\sqrt{s_{25}}\sqrt{s_{26}}}\left(\mathrm{tr}\left[\not{p}_5\not{p}_2\not{p}_6\gamma_\mu\right]+\mathrm{tr}\left[\gamma_5\not{p}_5\not{p}_2\not{p}_6\gamma_\mu\right]\right) \qquad \text{(A.44)}
\end{aligned}$$

and thus

$$\bar{v}(p_6)\gamma_\mu u(p_5) = \frac{1}{\sqrt{s_{25}}\sqrt{s_{26}}}\mathrm{tr}\left[\not{p}_5\not{p}_2\not{p}_6\gamma_\mu\right]. \qquad \text{(A.45)}$$

Putting together the pieces gives

$$\begin{aligned}
J_{3\mu} &= -\frac{1}{2}\bar{v}(p_6)\gamma_\mu\frac{1-\gamma_5}{2}u(p_5) + \sin^2\theta_W\,\bar{v}(p_6)\gamma_\mu u(p_5) \\
&= -\frac{\mathrm{tr}\left[\not{p}_5\not{p}_2\not{p}_6\gamma_\mu\right]-\mathrm{tr}\left[\gamma_5\not{p}_5\not{p}_2\not{p}_6\gamma_\mu\right]}{4\sqrt{s_{25}}\sqrt{s_{26}}} + \sin^2\theta_W\frac{\mathrm{tr}\left[\not{p}_5\not{p}_2\not{p}_6\gamma_\mu\right]}{\sqrt{s_{25}}\sqrt{s_{26}}} \\
&= \frac{(4\sin^2\theta_W-1)\mathrm{tr}\left[\not{p}_5\not{p}_2\not{p}_6\gamma_\mu\right]+\mathrm{tr}\left[\gamma_5\not{p}_5\not{p}_2\not{p}_6\gamma_\mu\right]}{4\sqrt{s_{25}}\sqrt{s_{26}}} \qquad \text{(A.46)}
\end{aligned}$$

and analogously

$$J_{4\nu} = \frac{(4\sin^2\theta_W - 1)\mathrm{tr}\left[\not{p}_7\not{p}_1\not{p}_8\gamma_\nu\right] + \mathrm{tr}\left[\gamma_5\not{p}_7\not{p}_1\not{p}_8\gamma_\nu\right]}{4\sqrt{s_{17}}\sqrt{s_{18}}}. \tag{A.47}$$

A.3. Basis functions

`T2G1C1, T2G1C2, T2G1C3, T2G1C4`

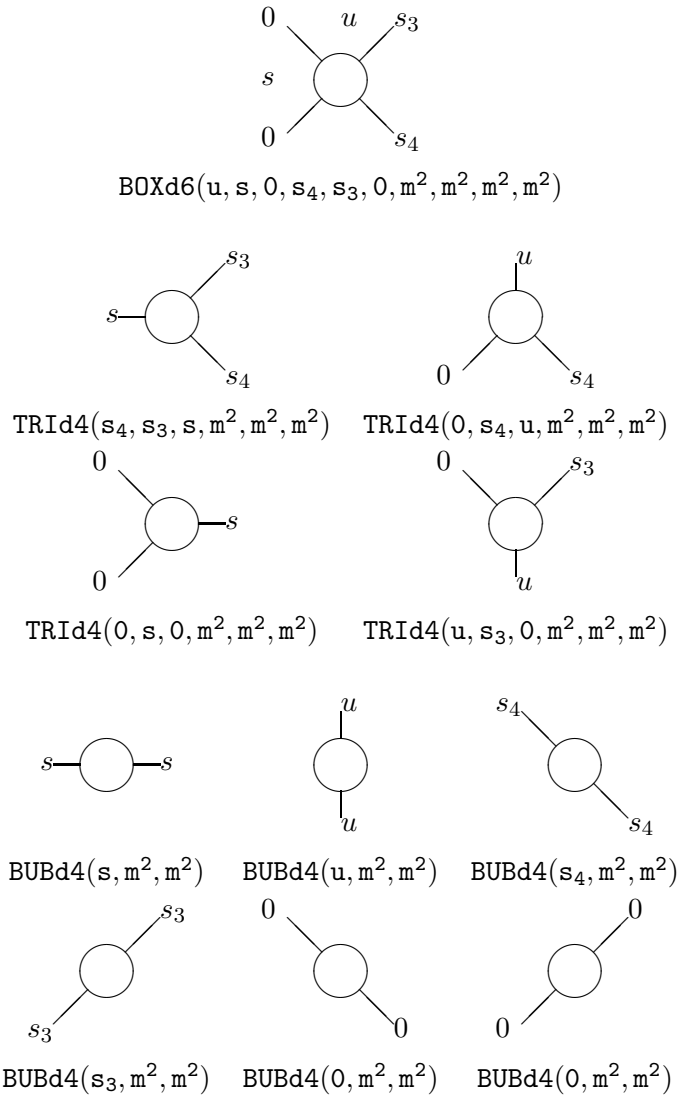

Figure A.1.: List of basis functions for the diagrams `T2G1C1`, `T2G1C2`, `T2G1C3` and `T2G1C4`. For the massive quark generation, set $m = m_t$ for `T2G1C1` and `T2G1C2` and $m = m_b$ for `T2G1C3` and `T2G1C4`. For the massless quark generations set $m = 0$

T3G1C1, T3G1C2, T3G1C3, T3G1C4

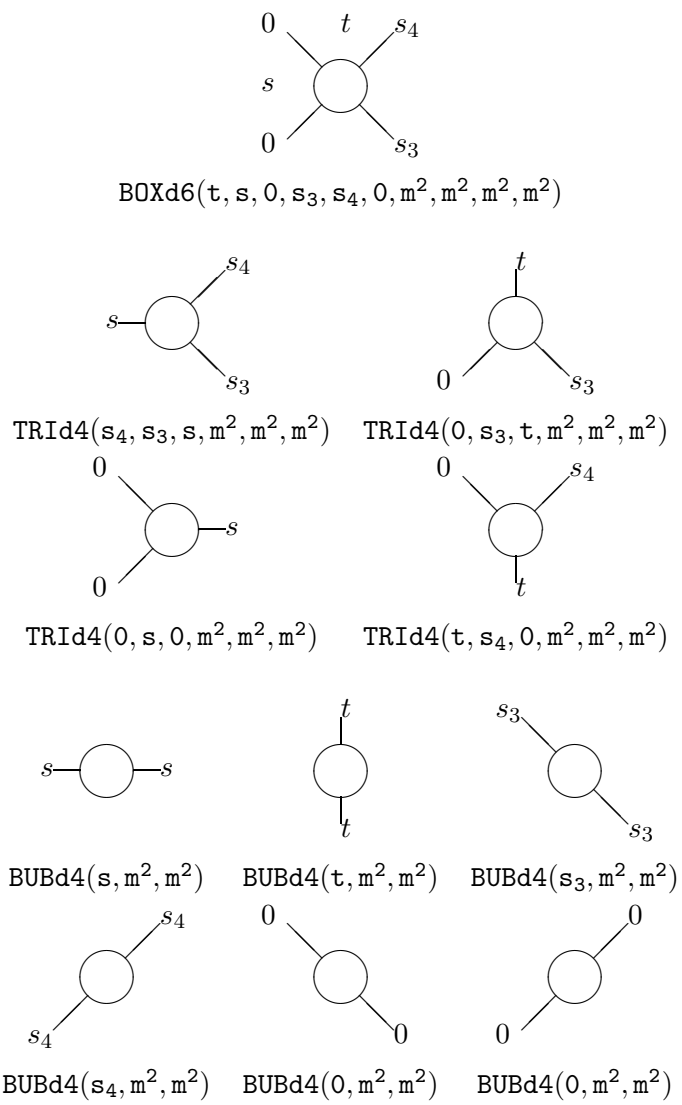

Figure A.2.: List of basis functions for the diagrams T3G1C1, T3G1C2, T3G1C3 and T3G1C4. For the massive quark generation, set $m = m_t$ for T3G1C1 and T3G1C2 and $m = m_b$ for T3G1C3 and T3G1C4. For the massless quark generations set $m = 0$

T4G1C1, T4G1C2, T4G1C3, T4G1C4

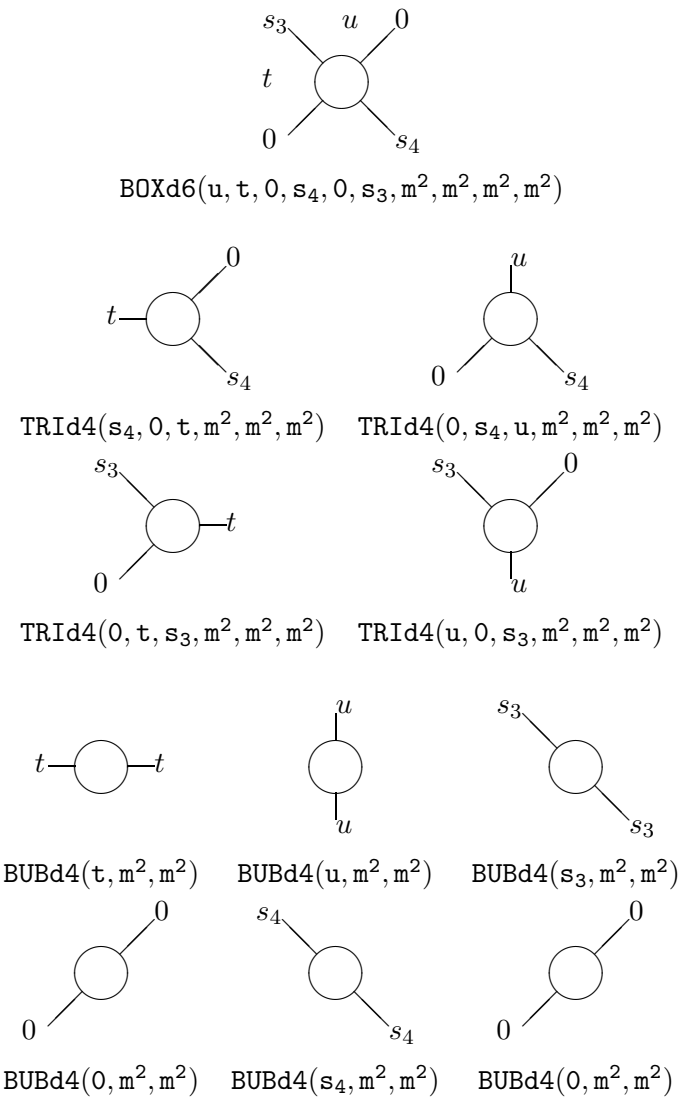

Figure A.3.: List of basis functions for the diagrams T4G1C1, T4G1C2, T4G1C3 and T4G1C4. For the massive quark generation, set $m = m_t$ for T4G1C1 and T4G1C2 and $m = m_b$ for T4G1C3 and T4G1C4. For the massless quark generations set $m = 0$

All functions for massive quark generation

$$
\begin{aligned}
f(1) &= \texttt{BOXd6}(\mathtt{u}, \mathtt{s}, 0, \mathtt{s}_4, \mathtt{s}_3, 0, \mathtt{m}_\mathtt{t}^2, \mathtt{m}_\mathtt{t}^2, \mathtt{m}_\mathtt{t}^2, \mathtt{m}_\mathtt{t}^2) \\
f(2) &= \texttt{BOXd6}(\mathtt{t}, \mathtt{s}, 0, \mathtt{s}_3, \mathtt{s}_4, \mathtt{m}_\mathtt{t}^2, \mathtt{m}_\mathtt{t}^2, \mathtt{m}_\mathtt{t}^2, \mathtt{m}_\mathtt{t}^2) \\
f(3) &= \texttt{BOXd6}(\mathtt{t}, \mathtt{u}, \mathtt{s}_3, 0, \mathtt{s}_4, 0, \mathtt{m}_\mathtt{t}^2, \mathtt{m}_\mathtt{t}^2, \mathtt{m}_\mathtt{t}^2, \mathtt{m}_\mathtt{t}^2) \\
f(4) &= \texttt{TRId4}(\mathtt{s}_4, \mathtt{s}_3, \mathtt{s}, \mathtt{m}_\mathtt{t}^2, \mathtt{m}_\mathtt{t}^2, \mathtt{m}_\mathtt{t}^2) \\
f(5) &= \texttt{TRId4}(\mathtt{u}, \mathtt{s}_3, 0, \mathtt{m}_\mathtt{t}^2, \mathtt{m}_\mathtt{t}^2, \mathtt{m}_\mathtt{t}^2) \\
f(6) &= \texttt{TRId4}(0, \mathtt{s}, 0, \mathtt{m}_\mathtt{t}^2, \mathtt{m}_\mathtt{t}^2, \mathtt{m}_\mathtt{t}^2) \\
f(7) &= \texttt{TRId4}(0, \mathtt{s}_4, \mathtt{u}, \mathtt{m}_\mathtt{t}^2, \mathtt{m}_\mathtt{t}^2, \mathtt{m}_\mathtt{t}^2) \\
f(8) &= \texttt{TRId4}(\mathtt{t}, \mathtt{s}_4, 0, \mathtt{m}_\mathtt{t}^2, \mathtt{m}_\mathtt{t}^2, \mathtt{m}_\mathtt{t}^2) \\
f(9) &= \texttt{TRId4}(0, \mathtt{s}_3, \mathtt{t}, \mathtt{m}_\mathtt{t}^2, \mathtt{m}_\mathtt{t}^2, \mathtt{m}_\mathtt{t}^2) \\
f(10) &= \texttt{BUBd4}(\mathtt{s}, \mathtt{m}_\mathtt{t}^2, \mathtt{m}_\mathtt{t}^2) \\
f(11) &= \texttt{BUBd4}(\mathtt{u}, \mathtt{m}_\mathtt{t}^2, \mathtt{m}_\mathtt{t}^2) \\
f(12) &= \texttt{BUBd4}(\mathtt{t}, \mathtt{m}_\mathtt{t}^2, \mathtt{m}_\mathtt{t}^2) \\
f(13) &= \texttt{BUBd4}(\mathtt{s}_3, \mathtt{m}_\mathtt{t}^2, \mathtt{m}_\mathtt{t}^2) \\
f(14) &= \texttt{BUBd4}(\mathtt{s}_4, \mathtt{m}_\mathtt{t}^2, \mathtt{m}_\mathtt{t}^2) \\
f(15) &= \texttt{BUBd4}(0, 0, \mathtt{m}_\mathtt{t}^2) \\
f(16) &= \texttt{BOXd6}(\mathtt{u}, \mathtt{s}, 0, \mathtt{s}_4, \mathtt{s}_3, 0, \mathtt{m}_\mathtt{b}^2, \mathtt{m}_\mathtt{b}^2, \mathtt{m}_\mathtt{b}^2, \mathtt{m}_\mathtt{b}^2) \\
f(17) &= \texttt{BOXd6}(\mathtt{t}, \mathtt{s}, 0, \mathtt{s}_3, \mathtt{s}_4, \mathtt{m}_\mathtt{b}^2, \mathtt{m}_\mathtt{b}^2, \mathtt{m}_\mathtt{b}^2, \mathtt{m}_\mathtt{b}^2) \\
f(18) &= \texttt{BOXd6}(\mathtt{t}, \mathtt{u}, \mathtt{s}_3, 0, \mathtt{s}_4, 0, \mathtt{m}_\mathtt{b}^2, \mathtt{m}_\mathtt{b}^2, \mathtt{m}_\mathtt{b}^2, \mathtt{m}_\mathtt{b}^2) \\
f(19) &= \texttt{TRId4}(\mathtt{s}_4, \mathtt{s}_3, \mathtt{s}, \mathtt{m}_\mathtt{b}^2, \mathtt{m}_\mathtt{b}^2, \mathtt{m}_\mathtt{b}^2) \\
f(20) &= \texttt{TRId4}(\mathtt{u}, \mathtt{s}_3, 0, \mathtt{m}_\mathtt{b}^2, \mathtt{m}_\mathtt{b}^2, \mathtt{m}_\mathtt{b}^2) \\
f(21) &= \texttt{TRId4}(0, \mathtt{s}, 0, \mathtt{m}_\mathtt{b}^2, \mathtt{m}_\mathtt{b}^2, \mathtt{m}_\mathtt{b}^2) \\
f(22) &= \texttt{TRId4}(0, \mathtt{s}_4, \mathtt{u}, \mathtt{m}_\mathtt{b}^2, \mathtt{m}_\mathtt{b}^2, \mathtt{m}_\mathtt{b}^2) \\
f(23) &= \texttt{TRId4}(\mathtt{t}, \mathtt{s}_4, 0, \mathtt{m}_\mathtt{b}^2, \mathtt{m}_\mathtt{b}^2, \mathtt{m}_\mathtt{b}^2) \\
f(24) &= \texttt{TRId4}(0, \mathtt{s}_3, \mathtt{t}, \mathtt{m}_\mathtt{b}^2, \mathtt{m}_\mathtt{b}^2, \mathtt{m}_\mathtt{b}^2) \\
f(25) &= \texttt{BUBd4}(\mathtt{s}, \mathtt{m}_\mathtt{b}^2, \mathtt{m}_\mathtt{b}^2) \\
f(26) &= \texttt{BUBd4}(\mathtt{u}, \mathtt{m}_\mathtt{b}^2, \mathtt{m}_\mathtt{b}^2) \\
f(27) &= \texttt{BUBd4}(\mathtt{t}, \mathtt{m}_\mathtt{b}^2, \mathtt{m}_\mathtt{b}^2) \\
f(28) &= \texttt{BUBd4}(\mathtt{s}_3, \mathtt{m}_\mathtt{b}^2, \mathtt{m}_\mathtt{b}^2) \\
f(29) &= \texttt{BUBd4}(\mathtt{s}_4, \mathtt{m}_\mathtt{b}^2, \mathtt{m}_\mathtt{b}^2) \\
f(30) &= \texttt{BUBd4}(0, 0, \mathtt{m}_\mathtt{b}^2) \\
f(31) &= \texttt{one}
\end{aligned}
$$

Table A.1.: List of all basis functions for the massive quark generation

All functions for massless quark generations

$f(1) =$	$\texttt{BOXd6}(\texttt{u}, \texttt{s}, 0, \texttt{s}_4, \texttt{s}_3, 0, 0, 0, 0, 0)$	
$f(2) =$	$\texttt{BOXd6}(\texttt{t}, \texttt{s}, 0, \texttt{s}_3, \texttt{s}_4, 0, 0, 0, 0, 0)$	
$f(3) =$	$\texttt{BOXd6}(\texttt{t}, \texttt{u}, \texttt{s}_3, 0, \texttt{s}_4, 0, 0, 0, 0, 0)$	
$f(4) =$	$\texttt{TRId4}(\texttt{s}_4, \texttt{s}_3, \texttt{s}, 0, 0, 0)$	
$f(5) =$	$\texttt{TRId4}(\texttt{u}, \texttt{s}_3, 0, 0, 0, 0)$	IR divergent
$f(6) =$	$\texttt{TRId4}(0, \texttt{s}, 0, 0, 0, 0)$	IR divergent
$f(7) =$	$\texttt{TRId4}(0, \texttt{s}_4, \texttt{u}, 0, 0, 0)$	IR divergent
$f(8) =$	$\texttt{TRId4}(\texttt{t}, \texttt{s}_4, 0, 0, 0, 0)$	IR divergent
$f(9) =$	$\texttt{TRId4}(0, \texttt{s}_3, \texttt{t}, 0, 0, 0)$	IR divergent
$f(10) =$	$\texttt{BUBd4}(\texttt{s}, 0, 0)$	
$f(11) =$	$\texttt{BUBd4}(\texttt{u}, 0, 0)$	
$f(12) =$	$\texttt{BUBd4}(\texttt{t}, 0, 0)$	
$f(13) =$	$\texttt{BUBd4}(\texttt{s}_3, 0, 0)$	
$f(14) =$	$\texttt{BUBd4}(\texttt{s}_4, 0, 0)$	
$f(14) =$	$\texttt{one}$	

Table A.2.: List of all basis functions for the massless quark generations

A.4. Monte Carlo integration

The integral of $f(\vec{x})$ over the n-dimensional hypercube is

$$z = \int dz = \int d^n x f(\vec{x}) = \int_0^1 dx_1 \int_0^1 dx_2 \dots \int_0^1 dx_n f(x_1, x_2, \dots x_n). \tag{A.48}$$

The average is then the integral itself

$$\bar{f} = \frac{\int d^n x f(\vec{x})}{\int d^n x} = \int d^n x f(\vec{x}) = z \tag{A.49}$$

and can be estimated as the average over a limited number of samples $f(\vec{x}_i)$:

$$z_{est} = \bar{f}_{est} = \lim_N \frac{\sum_{i=1}^N f(\vec{x}_i)}{N}. \tag{A.50}$$

Transforming the integration variable, one can cover arbitrary integration volumes:

$$z = \int dz = \int d^n q |\mathcal{J}| f(\vec{x}(\vec{q})) = \int d^n q |\mathcal{J}| g(\vec{q}) = \int dq_1 \int dq_2 \dots \int dq_n |\mathcal{J}| g(q_1, q_2, \dots q_n). \tag{A.51}$$

The average and the estimated integral are then

$$z = \bar{f} = \frac{\int d^n x f(\vec{x})}{\int d^n x} = \frac{\int d^n q |\mathcal{J}| g(\vec{q})}{\int d^n q |\mathcal{J}|} = \overline{|\mathcal{J}| g(\vec{q})}, \tag{A.52}$$

$$z_{est} = \bar{f}_{est} = \lim_N \frac{\sum_{i=1}^N |\mathcal{J}| g(\vec{q}_i)}{N}, \tag{A.53}$$

where $|\mathcal{J}| g(\vec{q}_i)$ is called the weight of the sample point $\vec{q}_i$.

Partial derivatives of the integral read

$$\begin{aligned} \frac{\partial z}{\partial x_l} &= \int_0^1 dx_1 \dots \int_0^1 dx_{l-1} \int_0^1 dx_{l+1} \dots \int_0^1 dx_n f(x_1, x_2, \dots x_n) \\ &= \int_0^1 dq_1 \dots \int_0^1 dq_{l-1} \int_0^1 dq_{l+1} \dots \int_0^1 dq_n |\mathcal{J}| g(q_1, q_2, \dots q_n). \end{aligned} \tag{A.54}$$

Choosing a set of random n-dimensional vectors $\{\vec{r}_1, \vec{r}_2 \dots \vec{r}_N\}$ one can define a histogram $h^l = \{h_1^l, \dots h_M^l\}$ of M bins h_j^l for the l-th dimension by

$$h_j^l = \sum_{\substack{i \\ \text{if } r_{i,l} \in [x_l^j, x_l^{j+1}]}} |\mathcal{J}| g(\vec{r}_i). \tag{A.55}$$

h^l is an estimate for $\frac{\partial z}{\partial x_l}$ since the summation of eq. A.55 corresponds to the integration of eq. A.54 over all dimensions but q_l.

Bibliography

[1] Steven Weinberg, Phys. Rev. Lett. 19 (1967) 1264.

[2] Abdus Salam, in N. Svartholm, editor, Elementary Particle Theory, Proc. VIII Nobel Symp. (Almquist and Wiksell Stockholm, 1968), (page 367).

[3] S. L. Glashow, J. Iliopoulos and L. Maiani, Phys. Rev. D2 (1970) 1285.

[4] Peter W. Higgs, Phys. Rev. Lett. 13 (1964) 508.

[5] T. W. B. Kibble, Phys. Rev. 155 (1967) 1554.

[6] R. Barate et al., Phys. Lett. B565 (2003) 61.

[7] LEP Collaboration, ALEPH Collaboration, DELPHI Collaboration, L3 Collaboration, OPAL Collaboration, LEP Electroweak Working Group, SLD Electroweak Group, SLD Heavy Flavor Group and OPAL Collaboration (2003).

[8] Benjamin W. Lee, C. Quigg and H. B. Thacker, Phys. Rev. Lett. 38 (1977) 883.

[9] M. Quiros, hep-ph/9703412 .

[10] Adrian Ghinculov and Thomas Binoth, Acta Phys. Polon. B30 (1999) 99.

[11] Guido Altarelli and G. Isidori, Phys. Lett. B337 (1994) 141.

[12] B. Grzadkowski and M. Lindner, Phys. Lett. 178B (1986) 81.

[13] Thomas Hambye and Kurt Riesselmann (1997).

[14] V. Buescher and K. Jakobs, International Journal of Modern Physics A 20 (2005) 2523.

[15] A. Djouadi, J. Kalinowski and M. Spira, Comput. Phys. Commun. 108 (1998) 56.

[16] ATLAS Collaboration, *Atlas technical design report*, http://atlas.web.cern.ch/Atlas/internal/tdr.html.

[17] CMS Collaboration, *Cms technical design report*, http://atlas.web.cern.ch/Atlas/internal/tdr.html.

[18] Frank Wilczek, Phys. Rev. Lett. 39 (1977) 1304.

[19] Thomas G. Rizzo, Phys. Rev. D 22 (1980) 178.

[20] A. Djouadi, M. Spira and P. M. Zerwas, Phys. Lett. B264 (1991) 440.

[21] S. Dawson and R. Kauffman, Phys. Rev. D49 (1994) 2298.

[22] R. W. Brown and K. O. Mikaelian, Phys. Rev. D19 (1979) 922.

[23] J. Ohnemus and J. F. Owens, Phys. Rev. D43 (1991) 3626.

[24] J. Ohnemus, Phys. Rev. D50 (1994) 1931.

[25] L. Dixon, Z. Kunszt and A. Signer, Nuclear Physics B 531 (1998) 3.

[26] Lance J. Dixon, Z. Kunszt and A. Signer, Phys. Rev. D60 (1999) 114037.

[27] Duane A. Dicus, Chung Kao and W. W. Repko, Phys. Rev. D36 (1987) 1570.

[28] E. W. N. Glover and J. J. van der Bij, Nucl. Phys. B321 (1989) 561.

[29] T. Matsuura and J. J. van der Bij, Z. Phys. C51 (1991) 259.

[30] C. Zecher, T. Matsuura and J. J. van der Bij, Z. Phys. C64 (1994) 219.

[31] http://hepforge.cedar.ac.uk/lhapdf/.

[32] W. M. Yao et al., J. Phys. G33 (2006) 1.

[33] Zhan Xu, Da-Hua Zhang and Lee Chang, Nucl. Phys. B291 (1987) 392.

[34] G. Passarino and M. J. G. Veltman, Nucl. Phys. B160 (1979) 151.

[35] T. Binoth, J. P. Guillet and G. Heinrich, Nucl. Phys. B572 (2000) 361.

[36] T. Binoth, J. Ph. Guillet, G. Heinrich, E. Pilon and C. Schubert, JHEP 10 (2005) 015.

[37] J. A. M. Vermaseren (2000).

[38] Thomas Hahn, Comput. Phys. Commun. 140 (2001) 418.

[39] M. J. G. Veltman, Nucl. Phys. B319 (1989) 253.

[40] N. Kauer, http://hepsource.sourceforge.net/dvegas/.

[41] T. Binoth and N. Kauer, http://hepsource.sourceforge.net/GG2WW/.

[42] T. Binoth, M. Ciccolini, N. Kauer and M. Kramer, JHEP 03 (2005) 065.

[43] T. Binoth, M. Ciccolini, N. Kauer and M. Kramer (2006).

[44] Michelangelo L. Mangano and Stephen J. Parke, Phys. Rept. 200 (1991) 301.

Danksagung

An dieser Stelle möchte ich allen danken, die mich während meiner Diplomarbeit unterstützt haben und ohne die diese Arbeit nicht zustande gekommen wäre: Dr. Nikolas Kauer für die engagierte Betreuung und geduldige Unterstützung; Dr. Thomas Binoth für die vielen Erklärungen und die kontinuierliche Motivation; meinen zahlreichen Zimmerkollegen für die freundliche und entspannte Atmosphäre; Professor Dr. Rückl für die Möglichkeit, an seinem Lehstuhl eine großartige Ausbildung zu genießen; schließlich meinen Eltern für den verlässlichen Rückhalt.

Erklärung

Hiermit erkläre ich, dass ich die vorliegende Arbeit selbständig verfasst und keine anderen als die angegebenen Hilfsmittel verwendet habe.

Würzburg, 28.11.2006